creative commons

Namensnennung-Keine kommerzielle Nutzung-Keine Bearbeitung 2.5 Schweiz

---

Sie dürfen:

das Werk vervielfältigen, verbreiten und öffentlich zugänglich machen

Zu den folgenden Bedingungen:

Namensnennung. Sie müssen den Namen des Autors/Rechteinhabers in der von ihm festgelegten Weise nennen (wodurch aber nicht der Eindruck entstehen darf, Sie oder die Nutzung des Werkes durch Sie würden entlohnt).

Keine kommerzielle Nutzung. Dieses Werk darf nicht für kommerzielle Zwecke verwendet werden.

Keine Bearbeitung. Dieses Werk darf nicht bearbeitet oder in anderer Weise verändert werden.

- Im Falle einer Verbreitung müssen Sie anderen die Lizenzbedingungen, unter welche dieses Werk fällt, mitteilen. Am Einfachsten ist es, einen Link auf diese Seite einzubinden.
- Jede der vorgenannten Bedingungen kann aufgehoben werden, sofern Sie die Einwilligung des Rechteinhabers dazu erhalten.
- Diese Lizenz lässt die Urheberpersönlichkeitsrechte unberührt.

Quelle: http://creativecommons.org/licenses/by-nc-nd/2.5/ch/ Datum: 3.4.2009

The organization of the microtubule cytoskeleton and its role on nuclear dynamics in the multinucleate hyphae of *Ashbya gossypii* revealed by live cell imaging and electron microscopy

Inauguraldissertation

zur
Erlangung der Würde eines Doktors der Philosophie
vorgelegt der
Philosophisch-Naturwissenschaftlichen Fakultät
der Universität Basel

von

Claudia Birrer-Lang

aus Binningen, Basel-Land

Basel, 2009

Genehmigt von der Philosophisch-Naturwissenschaftlichen Fakultät auf Antrag von

Prof. Dr. Peter Philippsen und Dr. Sue Jaspersen

Basel, den 17. Februar 2009

Prof. Dr. Eberhard Parlow

Dekan

Table of contents

Table of contents

Summary

Summary

Nuclear migration is important for normal growth and development of all eukaryotes including filamentous fungi. Among those, *Ashbya gossypii,* which is evolutionarily related to the budding yeast *Saccharomyces cerevisiae*, is a particularly attractive organism to study nuclear migration in multi-nucleated, elongated cells (hyphae). Upon hyphal extension, nuclei move toward the growing tip, showing not only long-range migration and asynchronous division, but also extensive non-synchronized oscillations and occasional bypassing. However, little is known how these processes are coordinated.

This thesis is structured in three parts that all share the common purpose to increase our understanding how the particular nuclear dynamics of *A. gossypii* are controlled with a gene set very similar to the mono-nucleate budding yeast *S. cerevisiae*.

In part I a detailed characterization of the *A. gossypii* microtubule cytoskeleton is presented. By combining high-resolution electron microscopy analysis of *A. gossypii* MTOCs and associated microtubules with live cell imaging of GFP-Tub1 labeled microtubules, we found distinct differences to the *S. cerevisiae* SPBs and a plausible answer to the question how nuclei can behave independently in the continuous cytoplasm of *A. gossypii*.
Part II describes the functional analysis of several *A. gossypii* MTOC components. Unexpected deletion phenotypes reveal that even though the *A. gossypii* genome encodes orthologs for all presently known *S. cerevisiae* SPB genes, their cellular function show distinctive differences to the *S. cerevisiae* homologs. Our data also suggests that an evolved SPB outer plaque and the cytoplasmic microtubules that it nucleates account for the complexity of nuclear dynamics in *A. gossypii*.
Part III of this thesis deals with the role of the *A. gossypii* ortholog of Kar9, a protein that is required for the establishment of spindle asymmetry in *S. cerevisiae*. The presented data indicate that spindle asymmetry and orientation prior to mitosis is not critical in the continuous cytoplasm of *A. gossypii*.

Part I (Manuscript by C. Birrer, T. van den Hoorn, R. Trimble, P. Philippsen and S. L. Jaspersen under review at Molecular Biology of the Cell)

Ashbya gossypii is a multinucleate filamentous fungus that shares a common ancestor with the unicellular budding yeast *Saccharomyces cerevisiae*. To better understand how non-synchronous nuclear oscillations, spindle orientation and bypassing of nuclei are achieved in its contiguous cytoplasm using cytoskeletal proteins homologous to those of *S. cerevisiae*, we examined *A. gossypii* spindle pole bodies (SPBs) and microtubules by live cell imaging and electron microscopy. We show that multilayered SPBs embedded in the nuclear envelope are the sole sites of microtubule nucleation. The SPB inner plaque forms over 25 nuclear microtubules even though *A. gossypii* nuclei contain only seven chromosomes. Two types of cytoplasmic microtubules are nucleated at the SPB outer plaque: perpendicular microtubules like in budding yeast, and in addition tangentially associated microtubules. Perpendicular microtubules are short and often contact the cell cortex. Tangential microtubules extend along the growth axis beyond adjacent nuclei but do not align with microtubules emanating from other SPBs. Thus, our results indicate that an independent cytoskeletal subdomain forms for each nucleus. We propose that this unique microtubule arrangement accounts for the specific nuclear dynamics in *A. gossypii* hyphae. Our studies illustrate how the microtubule cytoskeleton may have adapted during evolution of unicellular and multinucleated fungi.

Part II (Manuscript prepared for submission)

Ashbya gossypii is a multinucleated filamentous fungus that shares a common ancestor with the mono-nucleate budding yeast *Saccharomyces cerevisiae*. Here, we examined components of the *A. gossypii* microtubule cytoskeleton to investigate how the distinct nuclear dynamics are regulated with proteins homologous to those of *S. cerevisiae*. We provide evidence that the SPB outer plaque is required for formation of these cytoplasmic microtubules by characterization of deletion mutants in *AgSPC72*, *AgCNM67* and *AgNUD1*. In *Agspc72*Δ, detachment of

cytoplasmic microtubules from the SPB results in severe defects in nuclear oscillations, bypassing and nuclear spacing control. Deletion of either *AgCNM67* or *AgNUD1* results in loss of the SPB outer plaque. In contrast to wild-type, we observe cytoplasmic microtubules emanating from the bridge in these mutants. Alternative nucleation of cytoplasmic microtubules form the bridge is most likely a rescue mechanism in the absence of a functional outer plaque and thus the reason why *Agcnm67*Δ and *Agnud1*Δ mutants display only mild defects in nuclear dynamics. Together, our data suggests that the SPB outer plaque and the cytoplasmic microtubules that it nucleates account for the complexity of nuclear dynamics in *A. gossypii*. Furthermore this study demonstrates that even though the *A. gossypii* genome encodes homologs for all presently known *S. cerevisiae* SPB genes, their cellular role cannot be predicted. The unexpected differences we observe between deletion phenotypes of *A. gossypii* and *S. cerevisiae* SPB homologs indicate that additional components might be involved in microtubule nucleation in *A. gossypii*.

Part III

In *S. cerevisiae* Kar9 is a key player in the correct spindle positioning prior to mitosis. Its asymmetric loading to the bud-proximal SPB and cytoplasmic microtubules emanating form it, ensures proper alignment of the mitotic spindle (Liakopoulos *et al.*, 2003). *ScKAR9* has a syntenic homolog *in A. gossypii.* The identity between the two protein sequences is only 22.7% but sequence comparison revealed that the two serines involved in establishment of the asymmetry are conserved in *A. gossypii*.

By live cell imaging we could show that AgKar9 localizes to spindle pole bodies and filaments emanating from them. Treatment of *A. gossypii* cells with either nocodazole or latrunculin A revealed that this localization depends on an intact microtubule- but not actin cytoskeleton. However, we could find no evidence that AgKar9 localizes asymmetrically to SPBs or microtubules emanating from them.

Deletion of AgKar9 leads to a slight decrease in the average distance between nuclei. Oscillations, bypassing of nuclei and long-range nuclear transport do not seem to be affected drastically within the resolution of our measurements. Thus, our results indicate that the spatial orientation of the spindle is not crucial in the contiguous cytoplasm of *A. gossypii* and that the AgKar9 function may has adapted to a life-style lacking cell division during evolution.

Note:

The movies referred to in Part I to III are stored on a CD located at the end of this manuscript. The movies are available in uncompressed AVI and in compressed QuickTime format.

Background

Background

The filamentous fungus *Ashbya gossypii*

The filamentous fungus *Ashbya gossypii* was first isolated more than 80 years ago from cotton plants by Ashby and Nowell (Ashby and Nowell, 1926). During the last century, *A. gossypii* was mainly known as a plant pathogen (Batra, 1973) and a natural overproducer of riboflavin (vitamin B_2) (Stahmann *et al.*, 2000).

Nowadays, *A. gossypii* has become recognized as an attractive model organism to study sustained polar growth and nuclear dynamics of multinucleated fungal cells. The *A. gossypii* genome is completely sequenced and annotated (Dietrich *et al.*, 2004), expression data of most protein-coding loci are available (Gattiker *et al.*, 2007) and powerful molecular tools (e.g. PCR-based gene targeting, recombinant plasmid technology, fluorescent dyes to stain the actin cytoskeleton, cell wall, ER and mitochondria) can be applied (Wright and Philippsen, 1991; Steiner and Philippsen, 1994; Wach *et al.*, 1994; Steiner *et al.*, 1995; Altmann-Johl and Philippsen, 1996; Wach *et al.*, 1997; Wendland *et al.*, 2000).

Surprisingly, the annotation of the *A. gossypii* genome revealed a gene set very similar to that of the budding yeast *Saccharomyces cerevisiae*. About 95% of all *A. gossypii* genes are orthologs of *S. cerevisiae* genes and 90% map within blocks of synteny (conserved gene order) (Dietrich *et al.*, 2004). These findings allowed the reconstruction of the evolutionary history of the two organisms (reviewed in (Philippsen *et al.*, 2005)). It is believed that *A. gossypii* and *S. cerevisiae* originate from a common ancestor that lived 100 million years ago and carried about 5000 genes. Since then, both organisms evolved by several genome rearrangements, a few million base pair changes and a limited number of gene deletions, duplications and additions. Additionally, the *S. cerevisiae* genome underwent a whole-genome duplication. As a result of those events, *S. cerevisiae* carries 12 million base pairs and 5800 protein coding genes on 16 chromosomes, while the genome of *A. gossypii* contains only 9 million base pairs and 4700 protein coding genes on seven chromosomes.

Nuclear migration and division in *A. gossypii*

Despite the similar set of genes, lifestyle and morphogenesis of both organisms are significantly different. In *S. cerevisiae* mitosis is linked to cell division, leading to small, mono-nucleate cells. In contrast, these two processes are uncoupled in *A. gossypii* resulting in the formation of long and branched cells (hypha) that contain multiple nuclei in a contiguous cytoplasm.

A colony of *A. gossypii* develops from a needle-shaped asexual spore that contains a single, haploid nucleus (Figure 1A). Upon germination, the nucleus undergoes several rounds of division within the developing germ bubble. Germ bubbles containing three nuclei indicate, that nuclear division is already asynchronous at this life cycle stage (Figure 1B). After the formation of a small germ tube, nuclei start to migrate towards the growing tip to populate the newly formed hypha (Figure 1C). Subsequently, a second germ tube is established opposite of the first one (Figure 1D) (Ayad-Durieux *et al.*, 2000; Knechtle *et al.*, 2003). Hyphal growth combined with further lateral branching results in the formation of a small mycelium (Figure 1E). In mature mycelia, hyphal elongation rates can reach 3.5 µm/min (Knechtle *et al.*, 2003). At this stage, new hyphal tips are generated by tip splitting (Figure 1F). During the whole development, nuclei are fairly evenly distributed within the cell, implying that nuclei have to divide within the elongating hyphae and to migrate towards the tips to maintain this high nuclear density.

Monitoring of histone H4-GFP-marked nuclei revealed that nuclear movement in *A. gossypii* includes not only long-range migration and asynchronous division but also extensive, non-synchronized oscillations and occasional bypassing of nuclei (Alberti-Segui et al., 2001; Gladfelter et al., 2006). Nuclear oscillations are abolished by addition of nocodazole, a microtubule-destabilizing drug, indicating the dependence of these movements on an intact microtubule network (Alberti-Segui *et al.*, 2001). However, so far little is known about the arrangement of the *A. gossypii* microtubule cytoskeleton and how it drives the particular nuclear dynamics of this filamentous fungus.

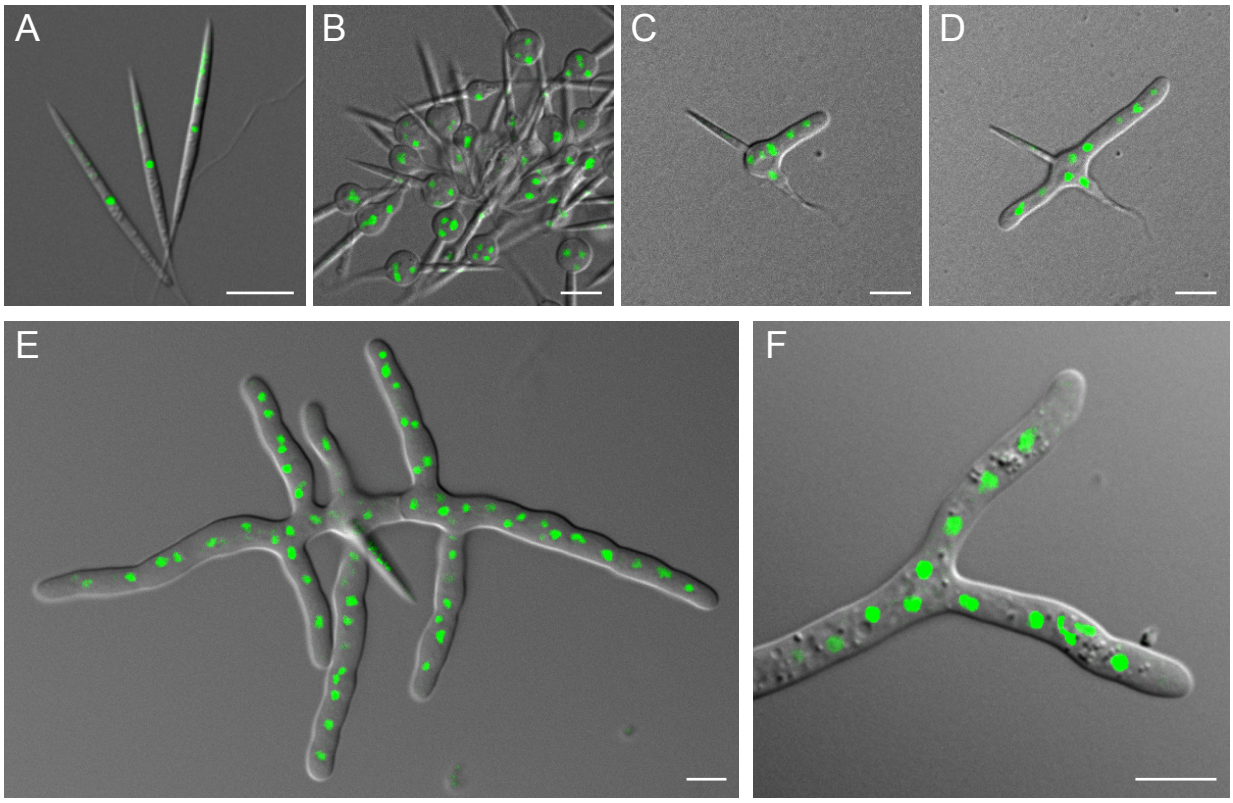

Figure 1. Nuclear distribution during the *A. gossypii* development.
(A) Spores prior to incubation. (B) Germ bubbles, after ~ 5 h of incubation at 30°C. (C) Germling with one germ tube, after ~ 7 h of incubation at 30°C. (D) Germling with two germ tubes, after ~ 8 h of incubation at 30°C. (E) Young mycelium after ~ 14 h of incubation at 30°C. (F) Tip splitting of a hypha, after ~ 20 h of incubation at 30°C. Bars, 10 µm.

Microtubules and their organizing centers (MTOCs)

Microtubules are conserved cytoskeletal elements that play key roles in nuclear division, directional transport of proteins, cell shape, polarity and motility. They are assembled by a head-to-tail-polymerization of α/β–heterodimer tubulin subunits, forming cylindrical polymers. This leads to a defined polarity and different polymerization/depolymerization kinetics at the individual ends. The rapidly growing end is referred to as the plus end, the slower growing end as the minus end (reviewed in (Wiese and Zheng, 2006). The possibility to switch from states of growing to shrinking (catastrophe) and from shrinking to growing (rescue) makes microtubules highly dynamic structures and appears to be crucial for the function of microtubules (Carminati and Stearns, 1997; Wiese and Zheng, 2006; Li and Gundersen, 2008). *In vitro*, microtubules can self-assemble of high concentrations of α/β-tubulin subunits. However, inside cells, the α/β-tubulin concentration is below the level required for spontaneous microtubule nucleation. *In vivo*, γ-tubulin together with additional proteins, forms a conserved complex, which serves as nucleation template for the formation of microtubules (Wiese and Zheng, 2006; Li and Gundersen, 2008). Thus, microtubules are anchored with their minus end to a distinct organelle family – the microtubule organizing centers (MTOCs).

MTOCs are structures found in all eukaryotes. Despite being a morphologically diverse group of organelles, MTOC function in nucleating and anchoring microtubules is highly conserved. Well-established and researched examples are the centrosome of animal cells and the spindle pole body (SPB) of yeast (reviewed in Jaspersen and Winey, 2004; Luders and Stearns, 2007).

At the beginning of the last century, R. A. Harper described "… a conspicuous, well-differentiated, disk-shaped granule… lying close on the surface of the nuclear membrane…" he observed by light microscopy in several fungi (Harper, 1905). This "central body", as Harper called it, seemed to set up the meiotic spindles in those fungi (Harper, 1905) (Harper, 1895). The term "spindle pole body" was first introduced by J. R. Aist 1971 as an

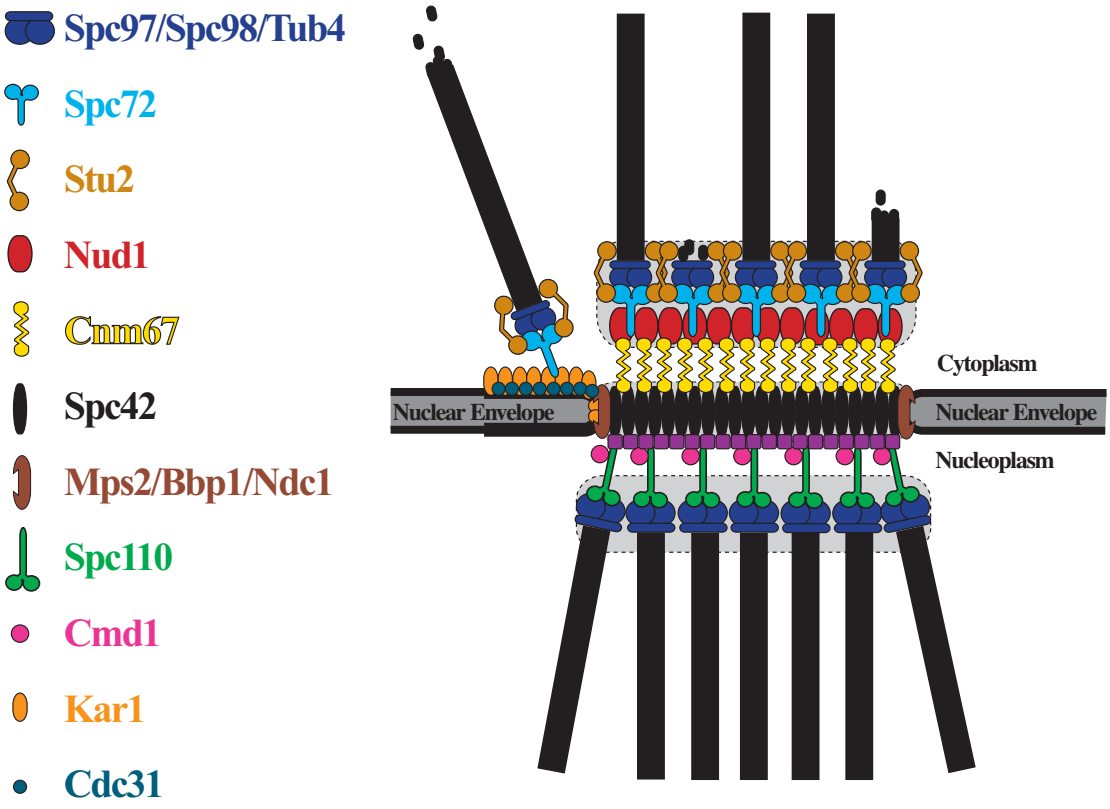

Figure 2. Model of the *S. cerevisiae* SPB (adapted from Dominic Hoepfner).
Microtubules are shown in black, SPB components are indicated on the left side. A description of the components can be found in Table 3 in Part I of this thesis.

English translation of "Spindelpolkörperchen" used by Harper in 1895 (Aist and Williams, 1972). In a discussion session on terminology, the scientific field agreed on this name as it "… is a more acceptable term, because, among other reasons, it is neutral with respect to morphology and function." (Aist and Williams, 1972).

Meanwhile, the application of new technologies such as electron microscopy (EM) and visualization of fluorescent labeled proteins have let to tremendous increase of knowledge about these organelles. Probably the best-characterized MTOC is the SPB of *S. cerevisiae* (Figure 2). Detailed analysis of its structure and composition has helped to elucidate the key roles it plays in spindle formation, chromosome segregation, sporulation and nuclear migration (reviewed in (Jaspersen and Winey, 2004)).

Unlike in animal cells, the nuclear envelope of fungal cells does not break down during mitosis. This physical barrier creates two classes of microtubules, nuclear and cytoplasmic. In *S. cerevisiae*, three SPB substructures are directly involved in the binding of microtubules (Figure 2). Nuclear microtubules, that are involved in the assembly of a bipolar spindle and in segregation of the chromosomes, are organized by the SPB inner plaque throughout the cell cycle. Cytoplasmic microtubules are nucleated by the outer plaque during the whole cell cycle and in addition also from the half-bridge or bridge during G1 and until SPB separation. They are essential for spindle orientation and nuclear migration during mitosis and mating (reviewed in (Jaspersen and Winey, 2004)).

Microtubule organization in filamentous fungi

Among filamentous fungi, the organization of the microtubule cytoskeleton appears to be quite distinct. In *Ustilago maydis*, a fungus that can switch between yeast-like and hyphal growth, four different classes of microtubules could be detected

in the yeast-like cells. Beside the SPB-bound spindle- and cytoplasmic microtubules, two types of SPB-independent microtubules were observed during interphase: short, motile ones, and long ones that are part of a microtubule bundle. In hyphae, however, the microtubule organization remains to be elucidated (reviewed by (Steinberg and Fuchs, 2004)).

In contrast to *U. maydis*, *Neurospora crassa* , *Aspergillus nidulans* and *Magnaporthe grisea* show only filamentous growth. Cytoplasmic microtubules of those filamentous fungi are predominantly arranged along the longitudinal axis of the hyphae (Minke *et al.*, 1999; Czymmek *et al.*, 2005; Horio and Oakley, 2005; Konzack *et al.*, 2005; Mourino-Perez *et al.*, 2006). In *A. nidulans*, it has been shown, that during interphase, cytoplasmic microtubules are not only nucleated by the SPBs, but also form non-nuclear MTOCs at septa and in the cytoplasm (Konzack *et al.*, 2005) leading to a bi-directional organization of cytoplasmic microtubules.

Two classes of cytoplasmic microtubules could be observed in *N. crassa*. One that connects adjacent nuclei and a second type that has no obvious association with nuclei (Minke *et al.*,

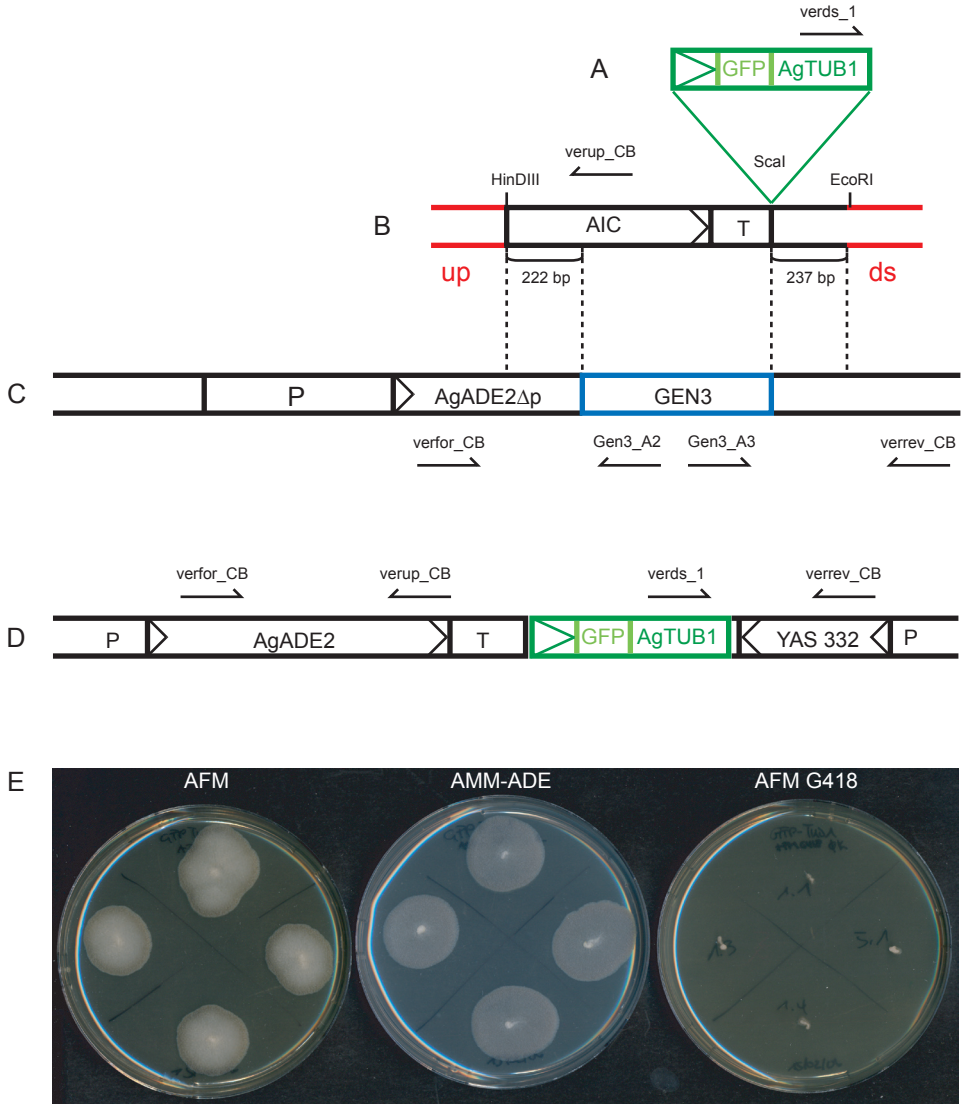

Figure 3. Construction of an *A gossypii* α-tubulin label.
(A) *AgTUB1-promotor – GFP – AgTUB1* cassette that was obtained by digestion of pTH38 (Van den Hoorn, 2004) with HindIII and BamH1. Blunt ends were generated using the 3'–5' exonuclease activity of T4 polymerase. (B) pAIC integration module. The *AgTUB1-promotor – GFP – AgTUB1* fragment was cloned into the indicated ScaI site. Lengths of homology to the truncated *AgADE2* locus in *Agade2Δ1* ((C)) are 222 and 237 bp, respectively. (C) *Agade2Δ1* with truncated *AgADE2* locus. The regions of homology between the chromosomal *AgADE2Δp* locus and pAIC are indicated with dashed lines. The *AgTUB1-promotor – GFP – AgTUB1* containing pAIC ((B)) was digested with EcoRI/HindIII and transformed into *Agade2Δ1*. (D) The new *GFP-AgTUB1* strain. GEN3 is replaced by *AgTUB1-promotor – GFP – AgTUB1*, and the AgADE2 locus restored. (E) Four homokaryon *GFP-AgTUB1* strains were grown for 3 days on AFM, AMM-ADE and AFM+G418 agar plates.

1999). The cytoplasmic microtubules of *N. crassa* show a distinct helical curvature and a tendency to intertwine with one another to form a network throughout the cytoplasm (Mourino-Perez *et al.*, 2006). Upon hyphal elongation, the microtubule cytoskeleton advances as a unit. Nuclei, that seem to be trapped in that microtubule network, are thereby carried forward (Mourino-Perez *et al.*, 2006). It is assumed that in addition to the SPBs, extra nuclear MTOCs at hyphal tips are involved in the formation of this dense microtubule network (Minke *et al.*, 1999; Mourino-Perez *et al.*, 2006). Non-nuclear MTOCs are also suspected to be involved in the organization of the microtubule cytoskeleton in *M. grisea* (Czymmek *et al.*, 2005).

In *A. gossypii*, *in vivo* fluorescent labeling of microtubules has proved to be very difficult, most likely due to disturbing effects of GFP for the assembly of long cytoplasmic microtubules. After many unsuccessful attempts to visualize *A. gossypii* microtubules *in vivo*, a functional *GFP-AgTUB1* strain has been constructed recently, providing preliminary data about the *A. gossypii* microtubule cytoskeleton (Van den Hoorn, 2004; Philippsen *et al.*, 2005). As it was an aim of this thesis to further develop this tool and carefully analyze the microtubule cytoskeleton, we first constructed a new GFP-AgTub1 strain that carries a *GFP-AgTUB1* fusion that is stable integrated in the genome.

To generate the new *GFP-AgTUB1* strain, a fragment containing an N-terminal fusion of GFP to *AgTUB1* under the control of the *AgTUB1*-promotor (Figure 3A) was subcloned into a the plasmid pAIC ((Knechtle, 2002), Figure 3B) that contains homologies to the truncated *AgADE2* locus of the *Agade2∆1* strain ((Knechtle, 2002), Figure 3C). The new plasmid (Figure 3B) was digested with EcoRI and HindIII, and the fragment transformed into *Agade2∆1*, thereby restoring the *AgADE2* locus and replacing *GEN3* by the *prom-GFP-TUB1* fragment (Figure 3D). Thus, transformants were sensitive to G418 and could grow on medium lacking adenine (Figure 3E). Even though the GFP signal of the new GFP-AgTUB1 strain was still week, the fusion was stabile integrated in the genome and expressed in all hyphae.

Aim of this thesis

Aim of this thesis

Nuclear motility seems to be required for the proper growth and development of essentially all eukaryotes. *A. gossypii* is a particularly attractive model system to study nuclear dynamics and long range nuclear migration since its hyphae contain many nuclei in one contiguous cytoplasm. Moreover, annotation of the *A. gossypii* genome revealed a high level of synteny (gene order conservation) with the well-studied budding yeast *S. cerevisiae.*

As nuclear migration in general depends on the action of microtubules, the elucidation of the microtubule cytoskeleton is a crucial premise to better understand the coordination of nuclear migration in *A. gossypii*, but may also give insight into common mechanisms shared by other elongated cells like neurons or muscle fibres.

The purpose of **Part I** of this thesis was a detailed characterization of the microtubule cytoskeleton to provide the indispensable foundation for further work and understanding how nuclear migration is achieved in *A. gossypii*. In a first step we focused on *A. gossypii* MTOCs in wild-type cells. By determining their localization, ultra structure and association with microtubules we aimed to gain insight how the *A. gossypii* microtubule network is organized and whether differences to the well-characterized budding yeast might account for the additional complexity of nuclear dynamics in *A. gossypii*. Additionally, we constructed an *in vivo* α-tubulin label to refine our knowledge about the cytoplasmic microtubule network and integrate this data with the electron microscopy analysis of MTOCs.

In **Part II** of my thesis we addressed the question whether diverged cellular functions of *A. gossypii* homologs to *S. cerevisiae* SPB components could possibly account for the higher complexity of the *A. gossypii* microtubule cytoskeleton and its distinct nuclear dynamics. Therefore, we analyzed several MTOC components and their deletion phenotypes by live cell imaging and electron microscopy. We were particularly interested in Spc72 and Cnm67 since in *S. cerevisiae*, these are the only two non-essential mitotic SPB components and deletion of either gene leads to impaired nuclear migration due to changes of the cytoplasmic microtubule cytoskeleton.

In **Part III** of this thesis we examine the role of the *A. gossypii* ortholog of Kar9, a protein that is required for the establishment of spindle asymmetry in *S. cerevisiae*. By tagging AgKar9 with fluorophores we aimed to determine the localization of this protein and investigate whether AgKar9 might localizes asymmetrically to SPBs. To gain insight in possible roles of AgKar9 in nuclear dynamics of *A. gossypii*, we also analyzed various parameters in *AgKAR9*-deletion mutants.

Part I

Nuclear dynamics and organization of microtubules in multinucleate hyphae of *Ashbya gossypii*

Introduction

Nuclear migration is important for normal growth and development of basically all eukaryotes (reviewed in (Morris, 2000). In many cells controlled nuclear positioning and migration depend on microtubules and their organizing centers (MTOCs). Despite being a morphologically diverse group of organelles, MTOC function in nucleating and anchoring microtubules is highly conserved throughout all eukaryotes. Well-established and researched examples of MTOCs are the centrosome of animal cells and the spindle pole body (SPB) of budding yeast (reviewed in (Jaspersen and Winey, 2004; Luders and Stearns, 2007)). A defining feature of all MTOCs is the presence of γ-tubulin, a phylogenetically conserved protein responsible for microtubule nucleation *in vivo*. Based on the ability of γ-tubulin and its associated proteins to form a ring-shaped complex with an approximate diameter of a microtubule cylinder, it probably templates assembly of α/β-tubulin heterodimers and serves as a cap to stabilize the microtubule minus end (reviewed in (Wiese and Zheng, 2006; Luders and Stearns, 2007)).

In *S. cerevisiae*, the SPB is the sole site of microtubule nucleation. SPB structure has been analyzed extensively by electron microscopy (EM). It appears as a multi-layered structure permanently embedded in the nuclear envelope (Robinow and Marak, 1966; Moens and Rapport, 1971; Byers and Goetsch, 1974). Three main layers can be distinguished: the outer plaque (OP) faces the cytoplasm and associates with cytoplasmic microtubules, the central plaque (CP) lies in the plane of the nuclear membrane and the inner plaque (IP) faces the nucleoplasm and associates with nuclear microtubules (Moens and Rapport, 1971; Byers and Goetsch, 1974; Rout and Kilmartin, 1990). On one side of the CP is the half-bridge. During SPB duplication, a full bridge is formed from this structure, resulting in two SPBs attached by its ends (Moens and Rapport, 1971; Byers and Goetsch, 1974, 1975a; Adams and Kilmartin, 1999; Li *et al.*, 2006). In addition to SPB sub-structures originally observed, cryo-EM and electron tomography allowed detection of two additional SPB layers termed intermediate layer 1 and 2 (IL1 and IL2), which are located between the CP and OP (Bullitt *et al.*, 1997; O'Toole *et al.*, 1999).

The filamentous fungus *A. gossypii* is closely related to *S. cerevisiae* on the genomic level. The *A. gossypii* genome project revealed that more than 90% of the *A. gossypii* genes show both homology and synteny with *S. cerevisiae* (Dietrich *et al.*, 2004). Despite the very similar set of genes, the morphogenesis of both organisms is completely different. In contrast to mono-nucleated *S. cerevisiae* cells, hyphae of *A. gossypii* contain many nuclei in the same cytoplasm, making it an excellent model organism to study the basis of nuclear migration and positioning in multinucleate cells (Figure 1, A and B). Upon hyphal extension, nuclei migrate toward the growing tip, showing not only long-range migration but also extensive oscillations and occasional bypassing of one another (Alberti-Segui *et al.*, 2001). The nuclei also undergo asynchronous divisions within the hypha (Gladfelter *et al.*, 2006). Nuclear division, bypassing, oscillation and tip-directed movement, collectively termed nuclear dynamics, are all involved in maintaining an approximately equidistant distribution of nuclei along the hypha (Figure 1A) (Alberti-Segui *et al.*, 2001; Gladfelter *et al.*, 2006). Nuclear oscillations are abolished by addition of nocodazole, a microtubule-destabilizing drug, indicating the dependence of these movements on an intact microtubule network (Alberti-Segui *et al.*, 2001). However, little is known about the arrangement of the *A. gossypii* microtubule cytoskeleton that drives its nuclear dynamics.

Based on the similarity between the *A. gossypii* and *S. cerevisiae* genomes, *A. gossypii* may solely use nuclear-associated SPBs to form both nuclear and cytoplasmic microtubules to regulate chromosome segregation and nuclear dynamics. This scenario raises the interesting question of how the distinct lifestyles of *A. gossypii* and *S. cerevisiae* are controlled by similar cytoskeletal components. Alternatively, *A. gossypii* might contain multiple MTOCs. In other fungi, including *Schizosaccharomyces pombe*, *Aspergillus nidulans*

and *Ustilago maydis*, the γ-tubulin complex localizes not only to nuclear-associated SPBs but also to other sites, such as tips, septa and cytoplasmic MTOCs (Heitz *et al.*, 2001; Straube *et al.*, 2003; Konzack *et al.*, 2005; Sawin and Tran, 2006). Often, use of non-nuclear MTOCs is cell cycle regulated, and they are important for nucleation of cytoplasmic microtubules that control nuclear dynamics. Non-nuclear MTOCs have the ability to give rise to different populations of cytoplasmic microtubules, including overlapping anti-parallel microtubules that interconnect with each other to regulate spatial positioning of organelles within the cytoplasm.

To better understand the *A. gossypii* microtubule cytoskeleton and its role in nuclear dynamics, we first identified the localization of MTOCs in hyphal tip compartments carrying many actively dividing nuclei. Using transmission EM we then focused on SPBs of *A. gossypii* to see if they are embedded in the nuclear membrane at all stages of the nuclear cycle and compared its SPB structure to the well characterized SPB of *S. cerevisiae*. Finally, we examined the number and arrangement of nuclear and cytoplasmic microtubules emanating from the inner and outer sides of the *A. gossypii* SPB using both EM and live cell imaging with GFP-α-tubulin. Based on these studies, we hypothesize that the ability of *A. gossypii* SPBs to nucleate two distinct classes of cytoplasmic microtubules is essential for the complex dynamics of multiple nuclei in a common cytoplasm.

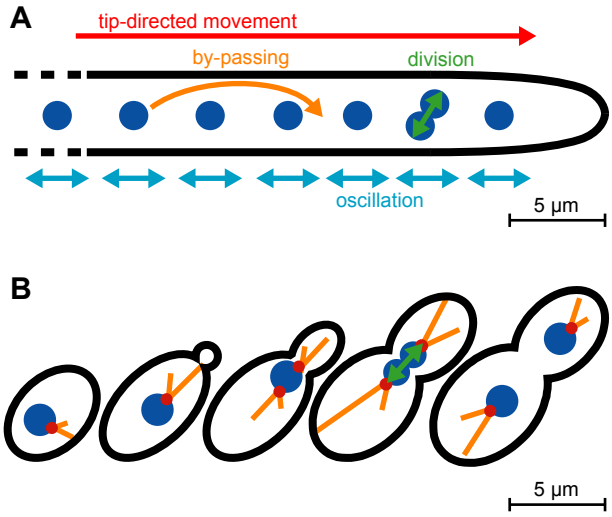

Figure 1. Model of nuclear dynamics in *A. gossypii* and *S. cerevisiae*.
(A) Tip compartment of an *A. gossypii* hypha with multiple nuclei. Nuclear dynamics includes an overall tip-directed movement, non-synchronous oscillation of nuclei with amplitudes up to 3 µm/min, occasional bypassing, nuclear division, and rotational orientation of dividing nuclei along the growth axis. (B) Cell cycle stages of a *S. cerevisiae* cell. Nuclear dynamics is restricted to positioning of the S-phase nucleus to the bud neck, orientation of the spindle along the mother-bud axis, and pulling of one daughter nucleus into the bud. These processes are accomplished by forces acting on the nucleus via cytoplasmic (orange) and nuclear (green) microtubules emanating from the SPB (red) (reviewed by Hildebrandt and Hoyt, 2000).

Materials and Methods

A. gossypii media and growth conditions

A. gossypii media and culturing are described in (Ayad-Durieux *et al.*, 2000; Wendland *et al.*, 2000) and strains are listed in Table 1. To depolymerize microtubules, spores were grown for 16 hours at 30°C in liquid AFM before nocodazole (Sigma-Aldrich) was added to a final concentration of 15 µg/ml. After 1 hour of incubation at 30°C under shaking conditions, cells were washed 5 times in AFM and incubated in AFM for 1 hour at 30°C to allow microtubule re-polymerization. Samples were taken at all steps and immediately fixed for immuno-fluorescence staining.

Plasmid and strain construction

Plasmids generated and used in this study are described below. All DNA manipulations were carried out according to (Sambrook, 2001) with *E. coli* DH5αF' as host (Hanahan, 1983). PCR amplification was performed using standard methods with Taq DNA polymerase, Expand High Fidelity PCR system or the Expand Long Template PCR system (Roche Diagnostics). Oligonucleotides are listed in Table 2 and were synthesized by Microsynth. For recombination of plasmids and PCR products, both were co-transformed into the budding yeast host strain DY3 (*MATα his3Δ200 trp1Δ63 leu2Δ1 ura3-52Δ*) according to (Gietz *et al.*, 1995). Plasmids were isolated from yeast using the High Pure Plasmid Purification Kit (Roche Diagnostics) with a modified protocol as previously described (Schmitz *et al.*, 2006).

To generate the *GFP-AgTUB1* strain, the plasmid pCB2 was constructed as follows: The *prom GFP-AgTUB1* fusion (764 bp upstream *TUB1*-ORF, *GFP*-ORF without stop codon, 1347 bp *TUB1*-ORF plus downstream sequences) was isolated as BamHI/HindIII fragment from pFS197 (kindly provided by Florian Schaerer). Blunt ends were generated using the 3'–5' exonuclease activity

Table 1. *A. gossypii* strains used in this study

Strain	Genotype	Reference
ΔIΔt *(referred to as wild-type)*	*Agleu2Δ Agthr4Δ*	(1)
Agade2Δ1	*Agade2(310-566)Δ::GEN3, Agleu2Δ, Agthr4Δ*	(2)
AgTUB4-YFP	*AgTUB4-YFP-LEU2 Agleu2Δ Agthr4Δ*	this study
GFP-AgTUB1	*Agade2::AgADE2-GFP-AgTUB1 Agleu2Δ Agthr4Δ*	this study

(1) (Altmann-Johl and Philippsen, 1996)
(2) (Knechtle, 2002)

Table 2. Olignucleotide primers used in this study

Name	Sequence[a] 5' – 3'
AgTUB4_F1	TGGGTGGAGATGCTGAGATGATCGATATTGAAAGTAACGACGACATCATAAaaacga cggccagtgaattcg
AgTUB4_F2	AGGTCCCGTTTCTAGTATCTACTAATGATGAAGCCAATGGTTACTAGCCTATTTACG CGAaccatgattacgccaagcttgc
L3	aactggtgatttaggtggttcc
Green2.2	tgtagttcccgtcatctttg
AgTUB4_A3	cgttatattcaaacgcggtgcc
AgTUB4_A4	gtccatttgcatctccaccccc
Agade2verfor_CB	gcgggttgctgactcaatcc
Agade2_verup_CB	atgcccatcctcttccaaac
Agade2verrev_CB	ctacgtggtgccacagtatgc
Agade2_verds_1	gggcagggatttattcggcg

[a] Lowercase letters are regions of homology to the cassette containing a selectable marker.

of T4 polymerase, and the 3923-bp fragment was subcloned into pAIC opened at the ScaI site (Knechtle, 2002). pCB2 was digested with EcoRI and HindIII, and transformed into the partially deleted *AgADE2* locus of the *Agade2Δ1* strain (Knechtle, 2002). Transformants were obtained on minimal medium lacking adenine and verified by PCR analysis with primer pairs Agade2verfor_ CB/ Agade2_verup_CB and Agade2verrev_CB/ Agade2_verds_1.

pAGT123 (kindly provided by Andreas Kaufmann) was used as a template to amplify *YFP-LEU2* using oligonucleotides TUB4_F1/F2. The resulting PCR product was co-transformed into yeast cells with pAG10748 to generate *pAgTUB4-YFP-LEU2*. *pAgTUB4-LEU2* was digested with AvaI and SacII to tag the endogenous *TUB4* gene with YFP in the wild-type strain. Integration was verified with oligonucleotides pairs AgTUB4_A3/green2.2 and L3/AgTUB4-A4.

Fluorescence microscopy and image processing

Chitin (calcofluor white), DNA (Hoechst) and immuno-fluorescence stainings were performed as previously described (Ayad-Durieux *et al.*, 2000; Gladfelter *et al.*, 2006). Rat anti-α-tubulin (YOL1/34, Serotec, UK) was used at a 1:25 dilution and Alexa Fluor 568 goat-anti-rat IgG (Molecular Probes, USA) at a 1:200 dilution.

An Axioplan2 microscope equipped with the objectives Plan-Apochromat 100x/1.40 NA Oil DIC and Plan-Apochromat 63x/1.40 NA Oil DIC (Carl Zeiss AG, Feldbach, Switzerland) and appropriate filters (Zeiss and Chroma Technology,

Brattleboro, VT) was used for microscopy. The light source for fluorescence microscopy was either a 75 W XBO lamp (OSRAM GmbH, Augsburg, Germany), controlled by a MAC2000 shutter and filter wheel system (Ludl Electronics, Hawthorne, NY) or a Polychrome V monochromator (TILL Photonics GmbH, Gräfelfing, Germany). Images were acquired at room temperature using a cooled charge-coupled device camera CoolSNAP HQ (Photometrics, Tucson, AZ) with MetaMorph 6.2r5 software (Molecular Devices Corp., Downingtown, PA). Out-of-focus shading references were used for DIC image acquisitions. For fluorescence images, multiple planes with a distance between 0.3 and 1 µm in the Z-axis were taken.

Image processing was performed with MetaMorph 6.2r5 software. Z-stacks were deconvolved with Nearest Neighbor and compressed by maximum or average projection with Stack Arithmetic. Brightness and contrast were adjusted using Scale Image. Images were colored and overlaid by using Overlay Images and exported from MetaMorph as 8-bit grayscale or RGB TIFF files. Z-Stacks were converted to QuickTime H.264 movies with QuickTime Player Pro (Apple Inc., Cupertino, CA).

Transmission electron microscopy

Spores were grown for 10 - 14 hours in liquid AFM to give rise to small mycelia containing no more than 100 nuclei. Samples were frozen on the Leica EM-Pact (Welzlar, Germany) at ~ 2050 bar, then transferred under liquid nitrogen into 2% osmium tetroxide/0.1% uranyl acetate/acetone and transferred to the Leica AFS (Welzlar, Germany). The freeze substitution protocol was as follows: -90°C for 16 hours, up 4°C an hour for 7 hours, -60°C for 19 hours, up 4°C an hour for 10 hours, -20°C for 20 hours. Samples were removed from the AFS and placed in the refrigerator for 4 hours, then allowed to incubate at room temperature for 1 hour. Samples went through 3 changes of acetone over 1 hour and were removed from the planchettes. Then, they were embedded in acetone/Epon mixtures to final 100% Epon over several days in a stepwise procedure as described (McDonald, 1999). 60 nm serial thin sections were cut on a Leica UC6 (Welzlar, Germany), stained with uranyl acetate and Sato's lead and imaged on a FEI Technai Spirit (Hillsboro, OR). Serial section images were aligned using AutoAligner (Bitplane AG, Zurich, Switzerland).

Bioinformatic analysis

Protein alignments were performed with sequences retrieved from the *Ashbya* Genome Database (AGD,http://agd.vital-it.ch/) (Gattiker *et al.*, 2007) and the *Saccharomyces* Genome Database (SGD, http://www.yeastgenome.org/) using the EMBOSS Pairwise Alignment Algorithms (Blosum62 Matrix, gap open 10, gap extend 0.5).

Results

The SPB is the sole site of microtubule nucleation in *A. gossypii*

We first wanted to determine if SPBs are the only site of microtubule nucleation in *A. gossypii* as they are in budding yeast or if other non-nuclear MTOCs also exist. To investigate the sites of microtubule nucleation, we fused the *A. gossypii* homolog of γ-tubulin with YFP since labeling of Tub4 with fluorophores has been used to visualize both nuclear and non-nuclear MTOCs in various fungi (Oakley *et al.*, 1990; Horio *et al.*, 1991; Stearns *et al.*, 1991; Sobel and Snyder, 1995; Marschall *et al.*, 1996; Spang *et al.*, 1996; Heitz *et al.*, 2001). AgTub4-YFP appeared as small foci fairly evenly distributed along the length of the hypha and co-labeling of nuclei with Hoechst revealed that AgTub4-YFP localizes exclusively to one or two spots at the nuclear periphery (Figure 1, A and B). It was never observed at other locations such as hyphal tips, septa or the cytoplasm (Figure 1, A-C).

We also analyzed the sites of microtubule re-growth in *A. gossypii* following microtubule depolymerization using nocodazole. Newly formed microtubules that emerged after wash-out of nocodazole were associated with nuclei and were not seen at other sites (Figure 1D). Taken together, these results strongly suggest that similar to *S. cerevisiae*, perinuclear SPBs are the sole site of microtubule nucleation in *A. gossypii*. Thus, only microtubules nucleated at SPBs participate in the complex dynamics of *A. gossypii* nuclei.

SPB components in *A. gossypii*

To better understand the composition of *A. gossypii* SPBs, we searched the *A. gossypii* genome for homologs of genes that encode

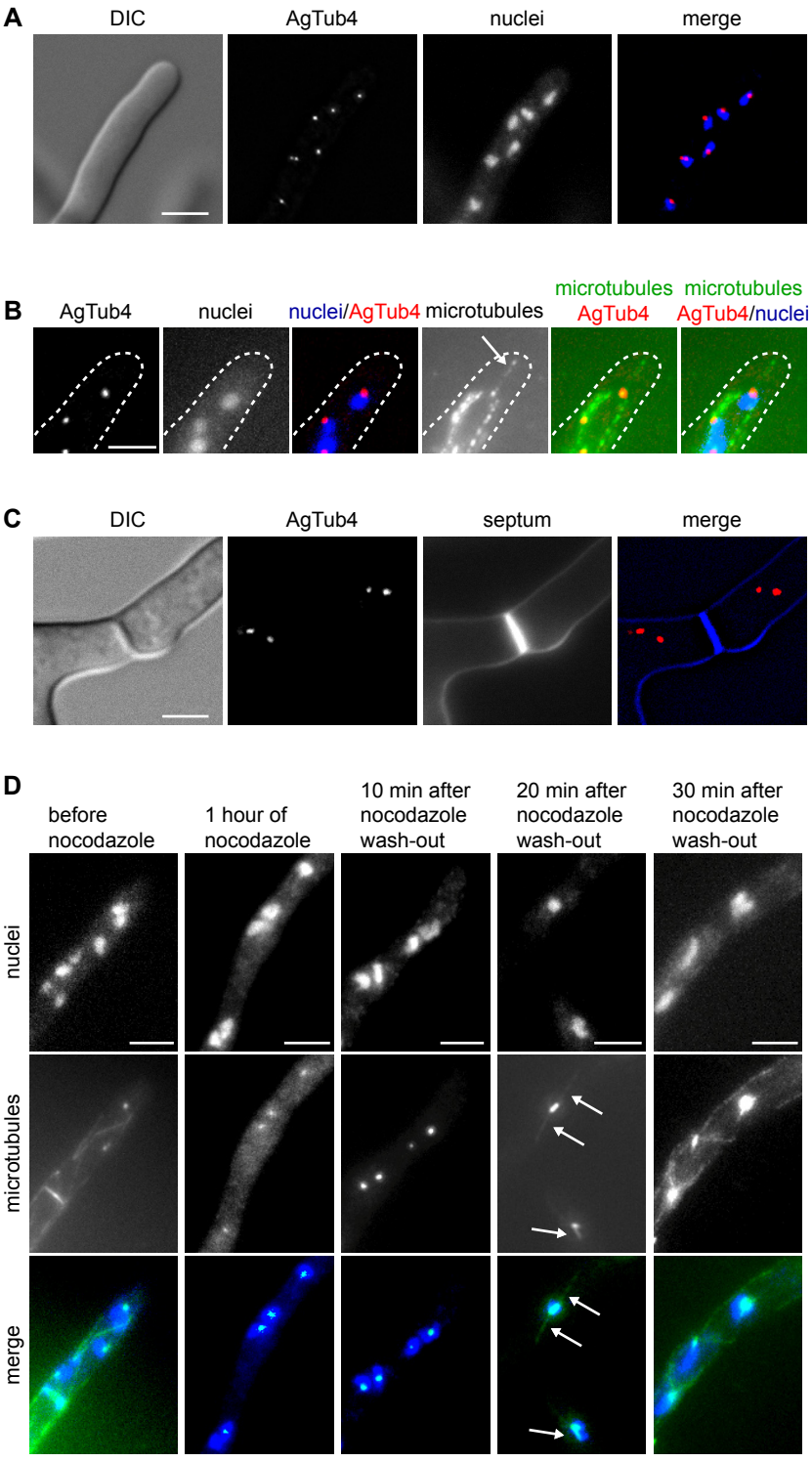

Figure 2. Localization of MTOCs in *A. gossypii*.
(A) Images of a tip compartment expressing *AgTUB4-YFP* to localize MTOCs and stained with Hoechst to visualize nuclei. (B) Images of a hyphal tip showing YFP-marked MTOCs, Hoechst stained nuclei, and microtubules labeled with anti-α-tubulin antibodies. Although microtubules can be detected at the tip (arrow), AgTub4-YFP signal is associated only with the nuclei. (C) Images of a hyphal compartment with a calcofluor stained septum and YFP-marked MTOCs. No YFP fluorescence can be seen at the septum. (D) Images of *A. gossypii* hyphae prior to and after incubation with 15 µg/ml nocodazole for one hour, and different times after wash-out of the drug. Nuclei are stained with Hoechst and microtubules are labeled with anti-α-tubulin antibodies. The untreated hypha shows cytoplasmic microtubules, one metaphase spindle prior to orientation along the growth axis, and fluorescent foci representing SPBs. After nocodazole treatment only SPB foci are detectable with anti-α-tubulin antibodies. 20 minutes after nocodazole wash-out faintly stained short cytoplasmic microtubules reemerged at the nuclear SPBs (arrows). By 30 minutes, the microtubules appeared similar to untreated cells. Bars in panels A-D, 5 µm.

components of the evolutionary related budding yeast SPB. SPB components were defined as proteins required to maintain the structural integrity of the organelle (Jaspersen and Winey, 2004). Since we are interested in nuclear dynamics in mitotically dividing cells, we focused on the mitotic SPB proteins.

Sequence analysis revealed that the *A. gossypii* genome encodes syntenic homologs for all 18 mitotic *S. cerevisiae* SPB components as well as the microtubule subunits, α- and β-tubulin (Table 3). Although α- and β-tubulin are highly conserved between both organisms (≥ 88% identical), most SPB components share only 20-40% identity along their entire length. Notable exceptions are the

Table 3. Amino acid sequence comparison of SPB components and microtubule subunits from *S. cerevisiae* and *A. gossypii*

***S. cerevisiae* SPB component**[a]	***S. cerevisiae* SPB localization**	**Role in SPB function *S. cerevisiae***	***A. gossypii* ortholog**	**Protein length in amino acids (*S.c./A.g.*)**[b]	**% Identity**[b]
Tub4	γ-tubulin complex	Microtubule nucleation	AgTub4	473/470	56
Spc97	γ-tubulin complex	Microtubule nucleation	AgSpc97	823/836	30
Spc98	γ-tubulin complex	Microtubule nucleation	AgSpc98	846/845	41
Spc72	OP, HB	γ-tubulin complex binding protein	AgSpc72	622/795	22
Nud1	OP	MEN signaling[c]	AgNud1	851/757	26
Cnm67	IL1, OP	Spacer, anchors OP to CP	AgCnm67	581/862	18
Spc42	CP, IL2	Structural SPB core	AgSpc42	363/314	28
Spc29	CP	Structural SPB core	AgSpc29	253/293	20
Cmd1	CP	Spc110 binding protein	AgCmd1	147/147	95
Spc110	CP to IP	γ-tubulin complex binding protein	AgSpc110	944/852	26
Mps2	SPB periphery	SPB insertion	AgMps2	387/338	19
Ndc1	SPB periphery	SPB insertion	AgNdc1	655/591	36
Bbp1	SPB periphery	SPB core to HB membrane linker	AgBbp1	385/353	26
Nbp1	SPB periphery	SPB core to HB membrane linker	AgNbp1	319/328	28
Cdc31	HB	SPB duplication	AgCdc31	161/172	71
Sfi1	HB	SPB duplication	AgSfi1	946/991	24
Kar1	HB	SPB duplication	AgKar1	433/330	23
Mps3	HB	SPB duplication	AgMps3	682/616	35
***S. cerevisiae* MT component**	***S. cerevisiae* MT composition**	**Localization in *S. cerevisiae***	***A. gossypii* ortholog**	**Protein length in amino acids (*S.c./A.g.*)**[b]	**% Identity**[b]
Tub1	major α-tubulin	nMTs and cMTs[e]	AgTub1	447/448	91
Tub2	β-tubulin	nMTs and cMTs[e]	AgTub2	457/449	91
Tub3	minor α-tubulin	nMTs and cMTs[e]	AgTub1[d]	445/448	88

[a] SPB components are defined as proteins required to maintain the structural integrity of the organelle (Jaspersen and Winey, 2004)
[b] Based on gene information in the *Saccharomyces cerevisiae* and *Ashbya* gossypii databases (SGD,http://www.yeastgenome.org/ and AGD, http://agd.vital-it.ch/). Percent identity was determined along the entire length as described in Materials and Methods
[c] MEN, mitotic exit network
[d] *TUB1* and *TUB3* both code for α-tubulin in *S. cerevisiae* . In *A. gossypii* only one gene (named *AgTUB1*) exists that codes for α-tubulin.
[e] nMT, nuclear microtubule; cMT, cytoplasmic microtubule

small calcium-binding proteins Cmd1 (calmodulin) and Cdc31, the ortholog of human centrin, which are 95% and 71% identical, respectively. Both of these proteins are conserved components of many MTOCs, including SPBs and centrosomes (Jaspersen and Winey, 2004). γ-tubulin is 56% identical between *A. gossypii* and *S. cerevisiae* but its associated proteins, Spc97 and Spc98, are not as highly conserved.

The *A. gossypii* SPB is embedded in the nuclear membrane

Next, we examined the architecture of the *A. gossypii* SPB to determine if it shares a similar morphology to that of *S. cerevisiae*. EM has provided valuable insights not only into SPB structure and assembly but also into microtubule organization in a variety of organisms, including budding and fission yeast. Here we report the first EM study of nuclei in multinucleate hyphae of *A. gossypii*. To ensure that all nuclei analyzed by EM were actively dividing, we prepared young mycelium that had no more than 10 growing tips and contained no more than 100 nuclei (Figure 3A). These samples were fast-frozen and then freeze-substituted to preserve the structural integrity of the SPBs and microtubules, and serial thin sections (~60 nm) of nuclei were examined.

We found that the nuclear envelope is continuous throughout the nuclear cycle (Figure 3, B-E), indicating that *A. gossypii* undergoes a closed mitosis. Single SPBs (Figure 3B) or duplicated SPBs (Figure 3, C and D) were embedded in the nuclear envelope like in budding yeast. Interestingly, we observed a relatively high number of nuclei (11 of 39) containing SPBs in the duplicated side-by-side configuration (Figure 3C). The nuclear division cycle of *A. gossypii* most likely pauses at this stage of SPB duplication, which could correspond to G2 phase of the cell division cycle.

Because *A. gossypii* undergoes a closed mitosis, organization of its nuclear and cytoplasmic microtubules is spatially separated. A structural analysis of this organization based on high-resolution images will be presented below. The low magnification cross sections of whole nuclei presented in Figure 3 show microtubules emanating from *A. gossypii* SPBs during multiple stages of the mitotic division cycle, suggesting that the ability of SPBs to nucleate microtubules is not altered during the cell cycle (Figure 3, B-D). This is similar to microtubule nucleation regulation in *S. cerevisiae* but differs from that of fungi carrying multiple MTOCs, where formation of microtubules is tightly controlled during different stages of the cell cycle (Moens and Rapport, 1971; Byers and Goetsch, 1974; Ding *et al.*, 1997; Straube *et al.*, 2003; Konzack *et al.*, 2005; Sawin and Tran, 2006). Multiple nuclear microtubules on the duplicated side-by-side SPBs interdigitate to form cross-bridges required to drive SPBs apart (Figure 3C), leading to a short bipolar spindle (Figure 3D). At the end of mitosis, long microtubules extend through the nuclear midzone (Figure 3E), suggesting that there is a tight coordination between spindle disassembly and karyokinesis.

The *A. gossypii* SPB is a multi-layered structure

Detailed ultrastructural analysis revealed that *A. gossypii* SPBs are laminar structures (Figure 4A), which is similar to the SPB of *S. cerevisiae* (Byers and Goetsch, 1974; Bullitt *et al.*, 1997; Adams and Kilmartin, 1999; O'Toole *et al.*, 1999). An electron dense central plaque (CP) appears to anchor the SPB in the nuclear membrane via hook-like appendages. The inner plaque (IP) at the nuclear side of the budding yeast SPB lacks a distinctive staining pattern, and this is what we also observe in the region below the CP of *A. gossypii* SPBs. This ill-defined IP serves as the site of nuclear microtubule formation (Figure 4A). Directly above the CP are two sharply staining plaques that correspond to intermediate layers IL1 and IL2 of the budding yeast SPB. A region of amorphous material follows, from which cytoplasmic microtubules emanate (Figure 4 A-C), indicating it is the outer plaque (OP). Two types of cytoplasmic microtubules emerge from the OP, one in a perpendicular fashion and a second in a tangential direction. Perpendicular and tangential microtubules were observed emanating from unduplicated, duplicated and separated SPBs, indicating that their formation is not regulated during the mitotic division cycle (Figure 4 A-D). Two types of OP microtubules can explain the arrangement of cytoplasmic microtubules observed by *in vivo* imaging (see below).

A structure equivalent to the *S. cerevisiae* half-bridge was found in only two of more than 50 analyzed SPBs. This structure may be present only during a short period of the nuclear cycle and/or may not be detected easily by EM in *A. gossypii*. However, since we observed duplicated SPBs connected by a bridge (Figures 3C and 4C), it seems likely that *A. gossypii* uses the half-bridge mechanism for SPB duplication. The bridge is associated with the nuclear envelope and appears as three distinct layers throughout its length (Figure 4C). This is similar, but not identical,

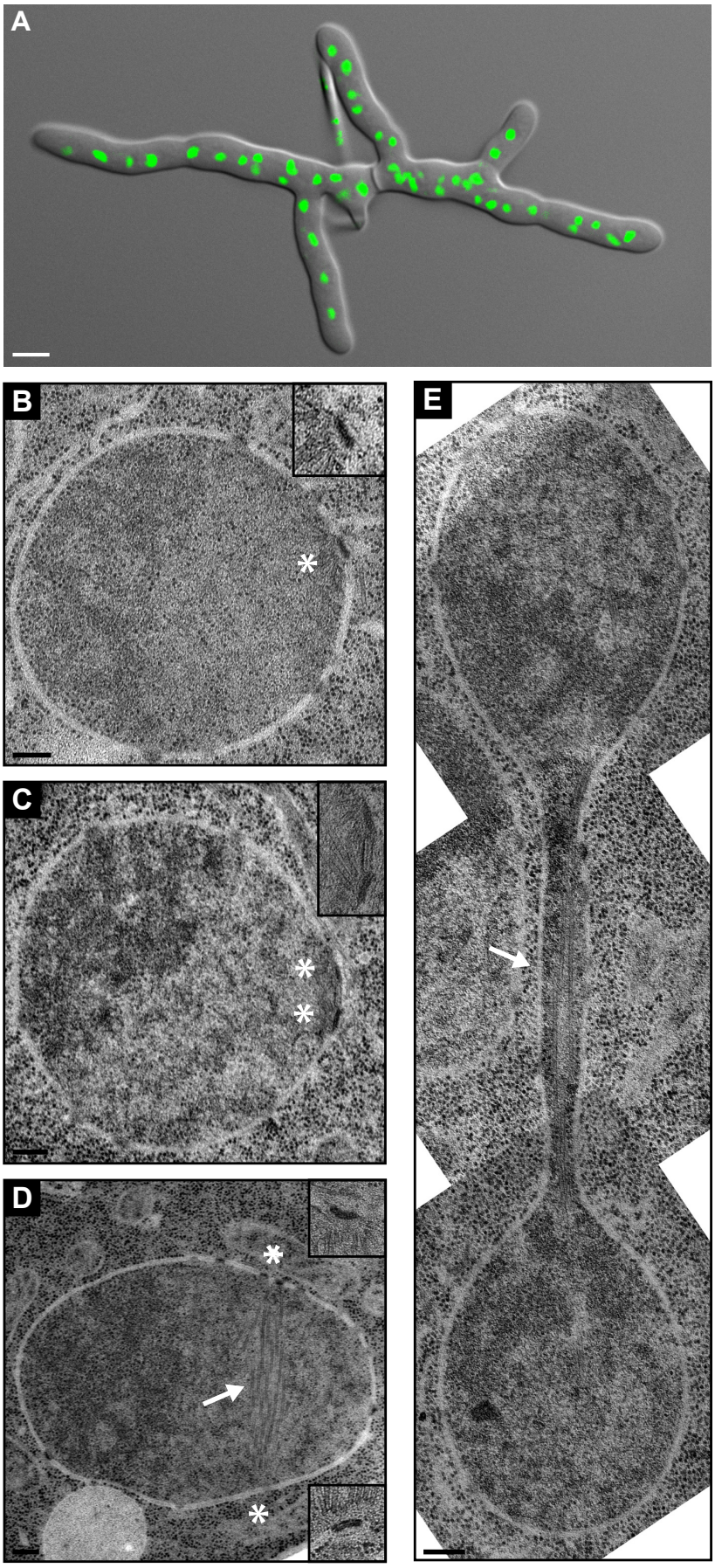

Figure 3. EM analysis of nuclei in multinucleated hyphae.
(A) Overlay of a DIC and a fluorescence image of a young *A. gossypii* mycelium that was stained with Hoechst to visualize nuclei. Such mycelia with 5 to 10 tips and 50 to 100 nuclei were prepared for thin section EM analysis as described in Materials and Methods. Bar, 5 µm. (B-E) EM of nuclei in different nuclear cycle stages. The continuous nuclear membrane and nuclear pore complexes within the nuclear envelope can be seen in all images. Bars, 200 nm. (B) A single SPB (asterisk) is embedded in the nuclear envelope. A higher magnification is shown in the top right corner. (C) Duplicated SPBs (asterisks) connected by a bridge are embedded in the nuclear envelope. A higher magnification is presented in the top right corner. (D) A nucleus with spindle microtubules (arrow) and continuous nuclear membrane. The two SPBs were observed in the adjacent sections at positions marked by the asterisks. Magifications are shown in the top and bottom right corners. (E) Montage of three EM images showing a nucleus in anaphase. The continuous nuclear envelope and spindle microtubules (arrow) are visible. The SPBs are in other sections.

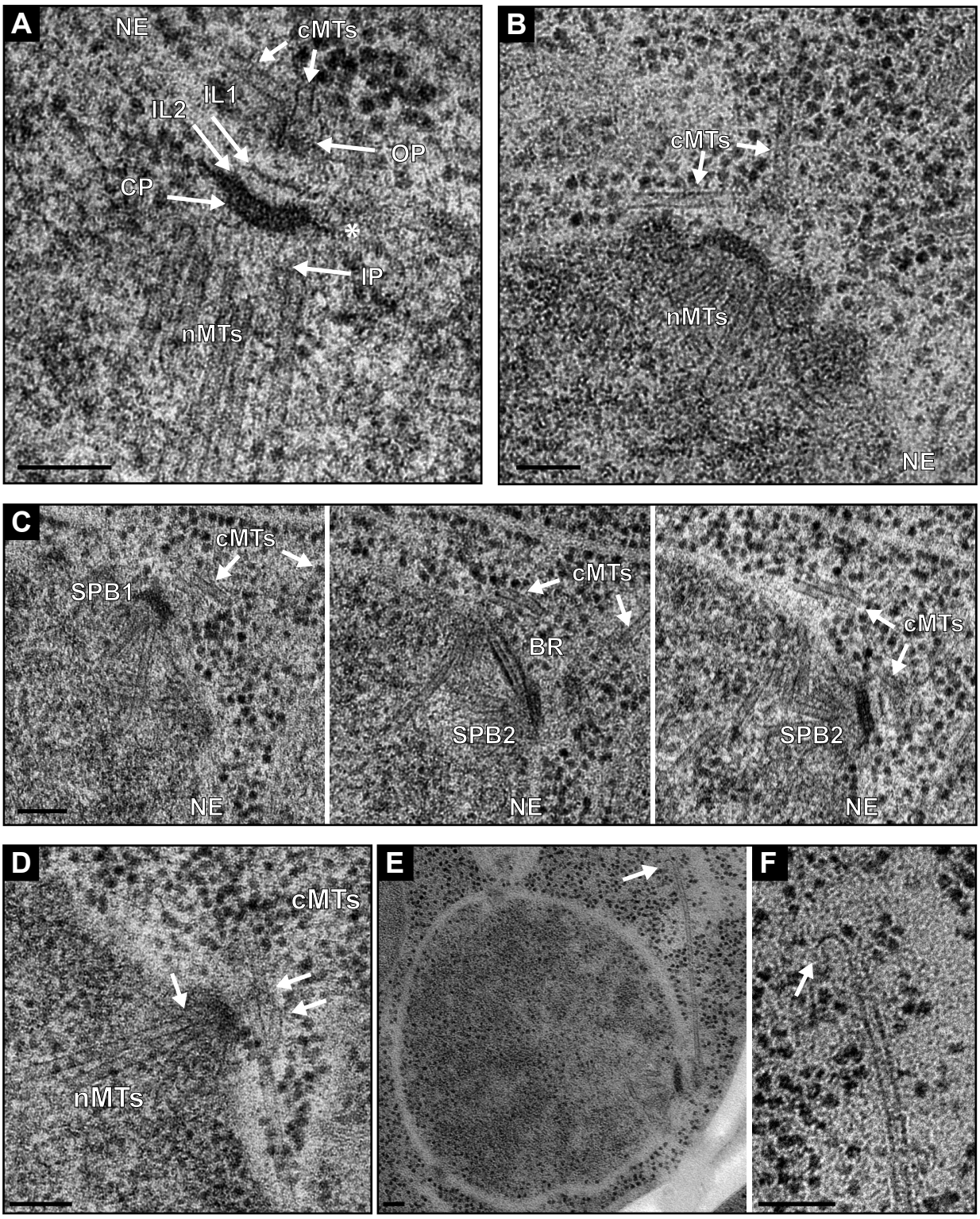

Figure 4. High resolution EM analysis of *A. gossypii* SPBs and microtubules.
(A) Electron micrograph showing five discrete SPB layers: the inner plaque (IP), central plaque (CP), intermediate layer 2 (IL2), intermediate layer 1 (IL1) and outer plaque (OP). Hook-like appendages (asterisk) extending from the CP anchor the SPB in the nuclear envelope (NE). Nuclear microtubules (nMTs) emanate from the IP and cytoplasmic microtubules (cMTs) from the OP. (B) Two types of cytoplasmic microtubules, one extending from the OP in a perpendicular direction and the other in a tangential direction. (C) Three serial sections of a duplicated SPB (SPB1 and SPB2) connected by a bridge (BR). Again, perpendicular and tangential cytoplasmic microtubules nucleate at OPs. (D) SPB with capped nuclear and cytoplasmic microtubules (arrows). The rounded caps at the microtubule ends are associated with electron dense material. (E) Low and (F) high magnification image of a cytoplasmic microtubule that ends in a distinct flare at its plus end (arrow). Bars in panels A – F, 100 nm.

to the bridge of *S. cerevisiae* (Byers and Goetsch, 1974; O'Toole *et al.*, 1999).

Dimensions of *A. gossypii* SPBs

Even though the general structure of the *A. gossypii* SPB is similar to that of *S. cerevisiae*, careful analysis of the size and spacing between *A.gossypii* SPB layers revealed distinct differences compared to budding yeast SPBs. One of the most notable features of *A. gossypii* SPBs is the distance between the OP and IL2, which is approximately 25 nm greater than it is in *S. cerevisiae*. There is also a slight increase in the spacing between IL2 and IL1, whereas the distance between the remaining plaques is equivalent (Figure 5). A second major distinction of the *A. gossypii* SPB lies in the OP, which is significantly smaller than the *S. cerevisiae* OP. In *A. gossypii*, the OP does not form a distinctive plaque but rather appears as an amorphous sphere with a diameter significantly reduced compared to the other layers of the SPB (Figure 5). These features result in a considerable degree of variability in the height measurement of the *A. gossypii* SPB (Table S1, Supplementary Material).

The average diameter of the *A gossypii* SPB based on the width of the CP was 119±21 nm (n = 46) (Figure 5; Table S1, Supplementary Material). This finding has interesting implications in terms of the number of microtubules *A. gossypii* SPBs are capable of nucleating (see below). In budding yeast, the diameter of the CP grows from 80 nm in G1 to 110 nm in mitosis (Byers and Goetsch, 1974. When we considered the stage of nuclear cycle, based on the number and arrangement of SPBs (single SPB, duplicated side-by-side SPBs and two separated SPBs per nucleus), the average diameter of CP in single SPBs, most likely representing G1 nuclei, was slightly larger than the CP of duplicated or separated SPBs, most likely representing G2 or mitotic nuclei (Table S1, Supplementary Material). Thus, mitotic regulation of SPB size and possibly exchange of SPB components may differ between *A. gossypii* and *S. cerevisiae*.

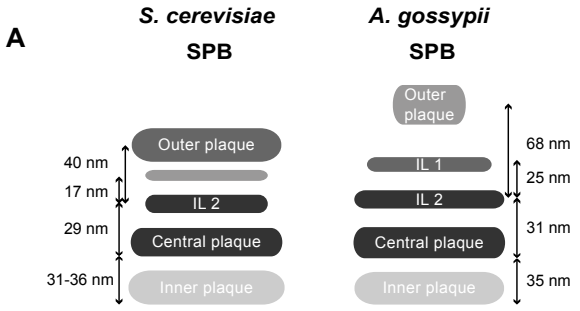

B

	S. cerevisiae	*A. gossypii*		
	mean (nm)	mean (nm)	SD	n
IP - CP	31 - 36	35.2	6.1	40
CP - IL2	29	31.3	3.2	41
IL2 - IL1	17	24.8	5.3	30
IL2 - OP	40	67.6	9.9	28
CP width	80 - 110 (1n) 160 (2n)	118.5	20.6	46

Figure 5. Comparison of *A. gossypii* and *S. cerevisiae* SPB structure based on EM analysis. (A) Schematic depicting the *S. cerevisiae* and *A. gossypii* SPB layers and distances between SPB layers. While the CP and IL2 are similar in size and structure in *A. gossypii* and *S. cerevisiae*, the IL1 and OP of *A. gossypii* are considerably smaller and the spacing between those layers is increased compared to budding yeast. The *A. gossypii* OP appears amorphous rather than electron-dense like in *S. cerevisiae*. (B) Quantitation of distances between *A. gossypii* SPB layers with standard deviation and number of plaques used for the measurements. The data for *S. cerevisiae* SPB plaques were compiled from published work (Byers and Goetsch, 1974; Bullitt *et al.*, 1997; O'Toole *et al.*, 1999; Schaerer *et al.*, 2001).

Structure of the ends of microtubules

The microtubule minus ends formed at the IP and OP appeared rounded and often associated with electron dense material (Figure 4D). Based on the similarity to capped microtubules previously described in *S. cerevisiae* (Byers *et al.*, 1978; Rout and Kilmartin, 1990; Bullitt *et al.*, 1997; O'Toole *et al.*, 1999), these probably are the closed ends of nuclear and cytoplasmic microtubules formed at the SPB by the γ-tubulin complex. No difference between the minus ends of nuclear and cytoplasmic microtubules was observed.

In some cases where a distinct microtubule plus end could be visualized in the cytoplasm, we observed a flaring of its tip: one side of the microtubule end extended and curved outward (Figure 4, E and F). Flared microtubule plus ends

Figure 6. (next page) Cross-sections of *A. gossypii* spindle microtubules.Nine adjacent planes of serial section EM images through a mitotic spindle. Section 1 and 9 are close to the SPB and the central region of the nucleus, respectively and are also shown in low magnification (1* and 9*). The observable rotation of the nucleus is due to the arrangement of the sections on the grid. Sections 7 – 9 were aligned using AutoAligner to create the merged cross-sectional view of microtubules shown in the schematic. Red circles mark microtubules seen in image A, the blue circle marks an additional microtubule seen in image B and the green circles mark two additional microtubules seen in image C. Altogether, 27 nuclear microtubules were observed. Bars, 200 nm.

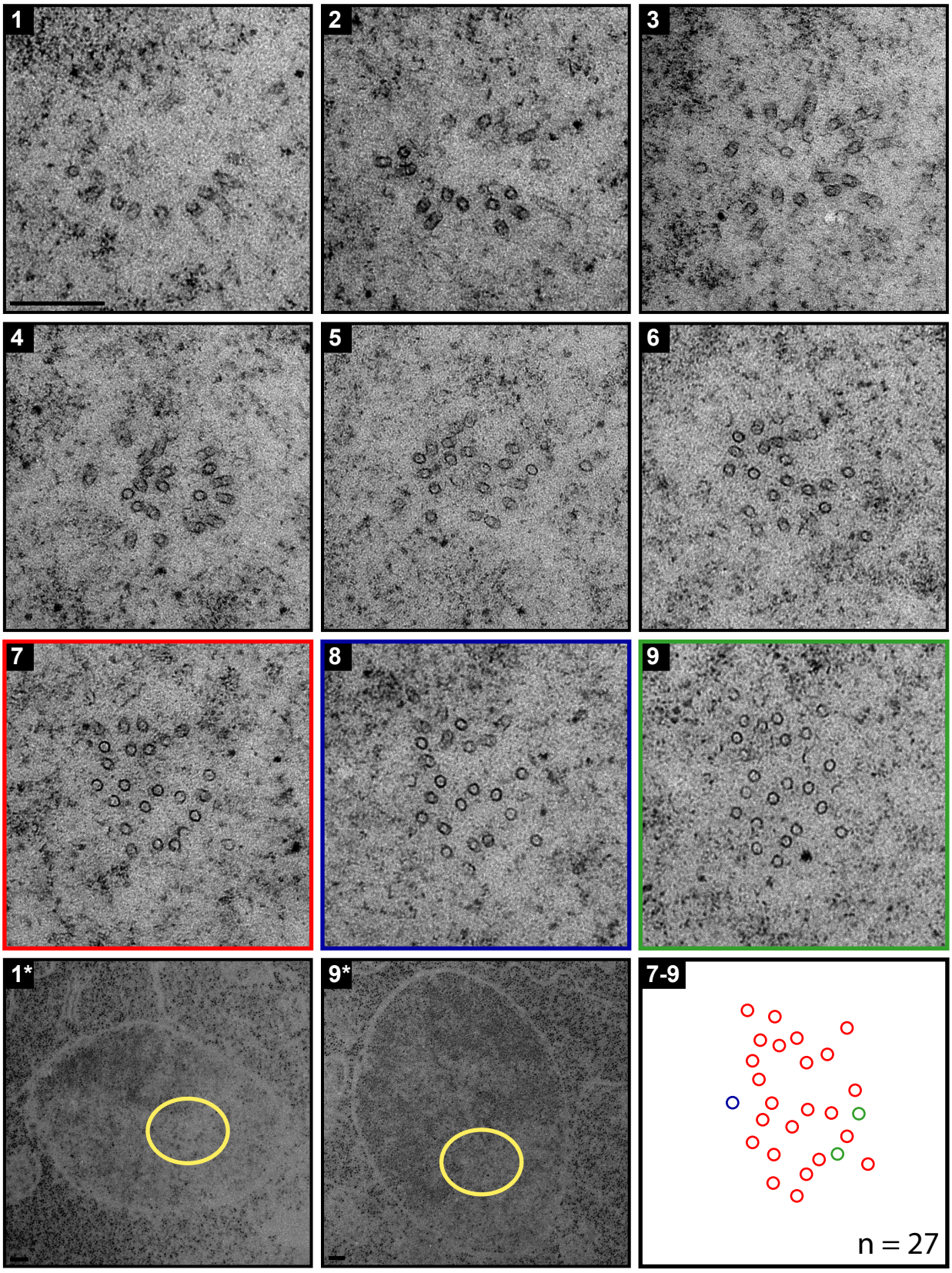
1
2
3
4
5
6
7
8
9
1*
9*
7-9
n = 27

were seen on nuclear as well as cytoplasmic microtubules, suggesting that this is an intrinsic property of the microtubule itself (O'Toole *et al.*, 1999).

Types of *A. gossypii* microtubules

Nuclear microtubules that form the mitotic spindle are nucleated at the SPB IP. Both longitudinal and cross-sectional views of nuclear microtubules revealed that the *A. gossypii* SPB nucleates a surprisingly large number of spindle microtubules (Figures 3C and 6; Figure S1, Supplementary Material). Greater than 25 nuclear microtubules can be seen in cross-section in the central region of the *A. gossypii* spindle even though there are only seven chromosomes per haploid genome. In this and other images of nuclei containing short spindles, we were unable to distinguish the different functional classes of nuclear microtubules previously described (Winey *et al.*, 1995). However, EM analysis of anaphase spindles (Figure 3E) suggests that *A. gossypii* likely has two types of spindle microtubules: microtubules that attach to kinetochores, which have depolymerized during

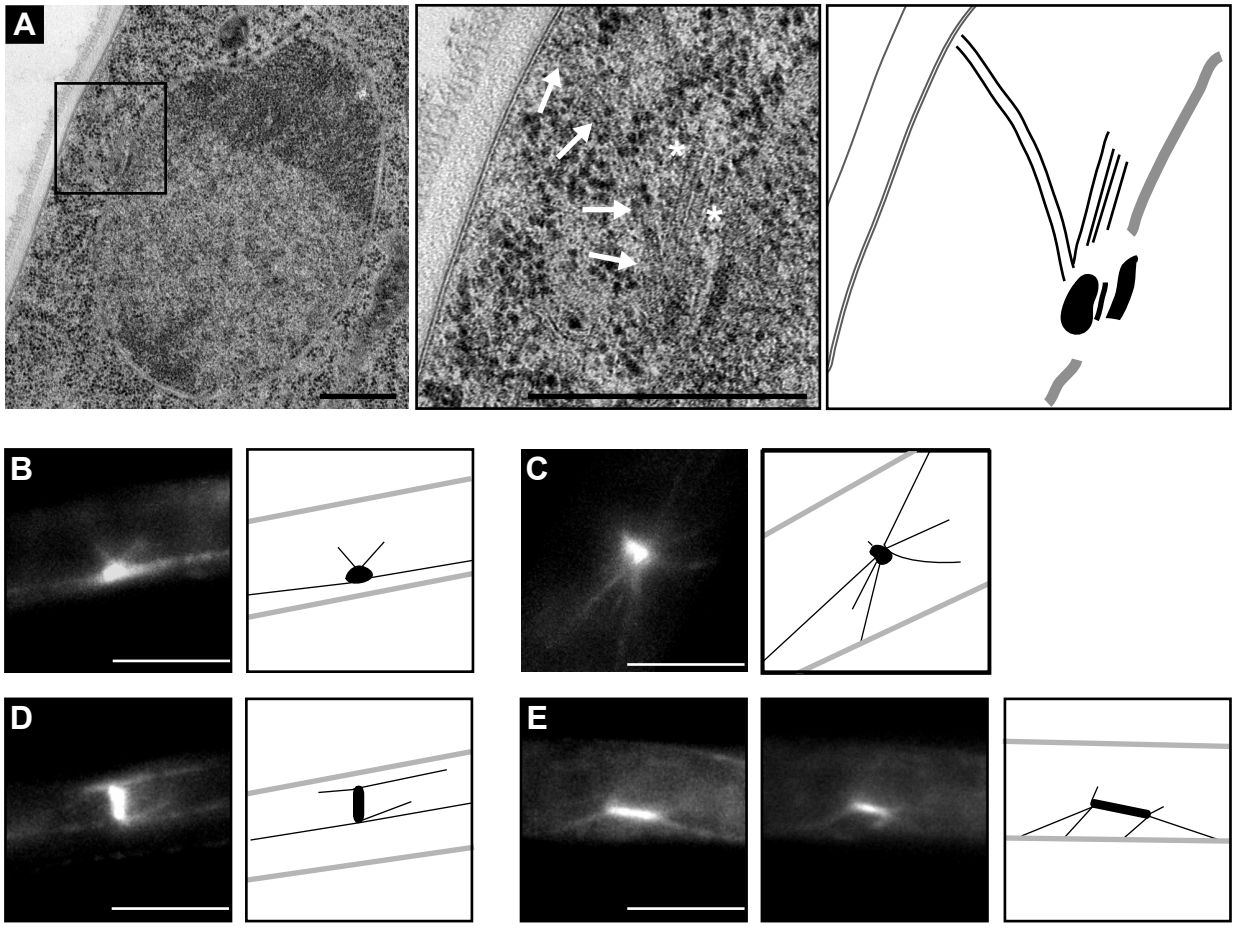

Figure 7. Two types of cytoplasmic microtubules in *A. gossypii*.
(A) EM micrograph of a hyphal thin section showing a nucleus with its SPB near the cell cortex (left panel). Magnified view of the cortex region with a perpendicular cytoplasmic microtubule (arrows) ending at the cell cortex and two cytoplasmic microtubules (asterisks) tangential to the nucleus and parallel to the hyphal axis (center panel). Graphic presentation of the SPB and the emanating cytoplasmic microtubules shown in the center panel (right panel). Bars, 500 nm. (B to E) Fluorescent live cell images of SPBs and microtubules in different nuclear cycle stages. Hyphae expressing GFP-AgTub1 were used to visualize microtubules and SPBs. Graphic representations are shown at the right side of the fluorescent images. Bars, 5 µm. (B) One fluorescent focus (representing the SPB) nucleating two short and two long microtubules. The short microtubules radiate into the cytoplasm, the long microtubules are aligned in the same direction as the hyphal growth axis. (C) Seven microtubules radiate from a brighter and larger focus (possibly representing a duplicated SPB). The two long microtubules very likely represent tangential microtubules. (D) Cytoplasmic microtubules emanate form both ends of a metaphase spindle. The two microtubules attached to the cortex-proximal SPB are most likely tangential microtubules, which attach to the cortex. The two long microtubules emanating from the other SPB are very likely also nucleated in a tangential direction at the OP and run along the longitudinal axis of the hypha. (E) Images of two Z-planes of the same anaphase spindle. The spindle is aligned along the growth axis of the hypha and both poles nucleate three cytoplasmic microtubules, two of which make contact with the cortex.

anaphase, and microtubules that form the central spindle, which interdigitate with microtubules from both half-spindles to drive spindle elongation.

EM tomography of *S. cerevisiae* SPBs and three-dimensional reconstruction of spindles has clearly demonstrated that budding yeast nucleates two distinct types of nuclear microtubules and only a single type of cytoplasmic microtubule (Winey *et al.*, 1995; O'Toole *et al.*, 1999). Our EM analysis indicates that *A. gossypii* has two classes of cytoplasmic microtubules (Figure 4 A-C; Figure 7A). We observed cytoplasmic microtubules that are nucleated perpendicularly to the SPB OP. At least some of these perpendicular cytoplasmic microtubules could be tracked to a region near the cell cortex (Figure 7A). We also observed tangential microtubules extending into the hyphal cytoplasm parallel to the growth axis (Figure 7A). This later

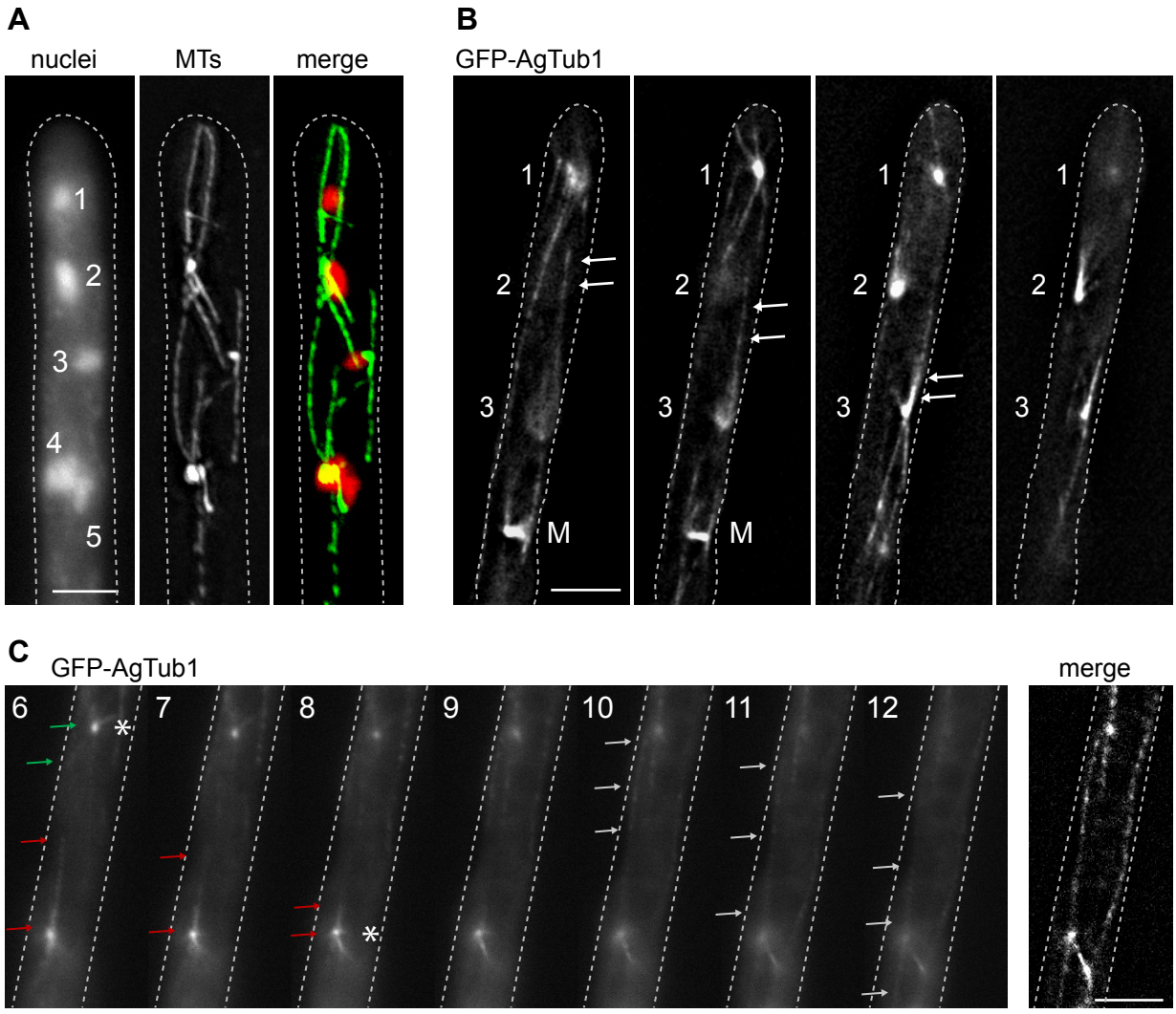

Figure 8. Long and short microtubules in the hyphae of *A. gossypii*.
(A) Immuno-labeling of microtubules. Hyphae were stained with Hoechst to visualize nuclei and with anti-α-tubulin antibodies to detect microtubules. Long and short microtubules are attached to bright foci that represent SPBs. One long microtubule seems to interconnect nucleus 2 with nucleus 4. (B) Deconvolved images of a Z-stack of a hypha expressing GFP-AgTub1. The complete stack is compiled as Movie 8B. Short and long cytoplasmic microtubules emanate from both sides of a mitotic spindle (M) and from bright foci representing SPBs (1-3). Short cytoplasmic microtubules frequently point toward the cell cortex; long cytoplasmic microtubules run along the longitudinal axis of the hyphae and can often be followed over several focal planes (arrows). They either terminate in the cytoplasm or seem to glide along the cell cortex. The SPB from nucleus 1 is connected to the cell cortex of the tip region by three short cytoplasmic microtubules while at least three longer cytoplasmic microtubules run toward the distal part of the hypha. (C) Merged, deconvolved image and its six single live images from a hypha expressing GFP-AgTub1. The single images are frames 6 to 12 of the Z-stack compiled as Movie 8C. The upper SPB is in focus in frame 6, the lower SPB in frame 8 (asterisks). They both nucleate several microtubules, one of each pointing toward but never touching each other (red and green arrows). In planes 10 to 12 one long microtubule can be followed that is located on top of the two SPBs (grey arrows). The merged image gives the impression that the two SPBs are directly connected although our microtubule tracking data shows this is not the case. Bars, 5 µm.

class of microtubules has not been observed in *S. cerevisiae* and might account for some of the differences in nuclear dynamics and cytoskeletal organization between the two organisms.

Examination of GFP-labeled microtubules by live cell imaging of nuclei containing unduplicated, duplicated and separated SPBs confirmed the existence of two types of cytoplasmic microtubules (Figure 7 B-E). Short microtubules radiating in random directions from the SPBs and long microtubules that always run along the growth axis of the hypha could be visualized. Short and long microtubules likely correspond to the perpendicular and tangential microtubules we observed by EM. Two classes of cytoplasmic microtubules were also observed in hyphae stained with anti-α-tubulin antibodies (Figure 8A). In these *in situ* images, long cytoplasmic microtubules seem to connect SPBs from different nuclei. Such an arrangement is intriguing since it leads to the prediction that most nuclei in multinucleate hyphae are interconnected by a complex system of cytoplasmic microtubules.

In vivo imaging of GFP-labeled microtubules

In order to test the hypothesis that most nuclei are connected to each other by cytoplasmic microtubules, we employed three dimensional *in vivo* imaging with an *A. gossypii* strain expressing an N-terminal GFP fusion of α-tubulin in addition to the wildtype α-tubulin, both under control of the native promoter. We tracked microtubules and SPBs through Z-stacks of 20 focal planes with 300 nm distances for 10 apical hyphal compartments each carrying 5 to 7 nuclei. Representative images from Z-stacks of two hyphae documenting this analysis are shown (Figure 8, B and C). Arrays of short or long cytoplasmic microtubules were observed emanating from bright SPB foci (single or side-by-side SPBs) and from the ends of bright bars, which correspond to metaphase or anaphase spindles. However, we were unable to confirm that long microtubules emanating from different SPBs align. In no case could we track two overlapping microtubules through three dimensional space. Thus, it is highly unlikely that a large array of anti-parallel microtubules formed throughout the mycelium controls the dynamic behavior of nuclei. Rather, our results suggest that both long and short microtubules form a regional microtubule network to influence nuclear positioning, oscillations and bypassing.

Discussion

We have shown that SPBs are the only MTOCs in the multinucleate hyphae of *A. gossypii*. SPBs of this filamentous fungus assemble into a multi-layered organelle that is permanently embedded in the nuclear membrane, similar to *S. cerevisiae* SPBs. Even though all mitotic SPB components are conserved between the two organisms, the *A. gossypii* SPB is structurally distinct, particularly on the cytoplasmic side. In our EM images, the OP of *A. gossypii* appears as an amorphous sphere rather than an electron-dense plaque like in *S. cerevisiae*. Also, the distance between IL2 and the OP is increased. In budding yeast, Cnm67 controls the spacing between these layers: decreasing or increasing its size by removal or addition of 270 amino acids of protein-internal sequences decreases or increases the IL2-OP distance by about 20 nm, respectively (Schaerer *et al.*, 2001). Interestingly, AgCnm67 is 281 amino acids longer than ScCnm67 whereas most other pairs of SPB orthologs have similar sizes. Why would the size of this spacer protein and thus, the distance between IL2 and the OP, which nucleates cytoplasmic microtubules, have evolved so differently?

One striking difference between *S. cerevisiae* and *A. gossypii* is the types of cytoplasmic microtubules that form at the SPB OP (Figure 9A). In *A. gossypii* we found both perpendicular and tangential cytoplasmic microtubules emanating from the SPB OP. Perhaps an increased distance between IL2 and the OP correlates with the ability to nucleate perpendicular as well as tangential cytoplasmic microtubules.

EM analysis of *S. pombe* showed cytoplasmic microtubules that were oblique with respect to the SPB, similar to the tangential microtubules we observed in *A. gossypii*. Often the oblique microtubules were not attached to the SPB and may have originated at one of fission yeast's non-nuclear MTOCs (Ding *et al.*, 1997). *Neurospora crassa* also has two classes of cytoplasmic microtubules, one of which is reported to connect adjacent nuclei. The second type of cytoplasmic microtubule has no obvious association with the nucleus and is probably not nucleated by its SPB (Minke *et al.*, 1999). In contrast to these organisms, the ability to nucleate multiple classes of cytoplasmic microtubules must be intrinsic to the SPB in *A. gossypii* as it is the only MTOC in this organism.

Images obtained with anti-α-tubulin antibody staining in fixed *A. gossypii* hyphae show cytoplasmic microtubules connecting different nuclei. This would predict an anti-parallel alignment

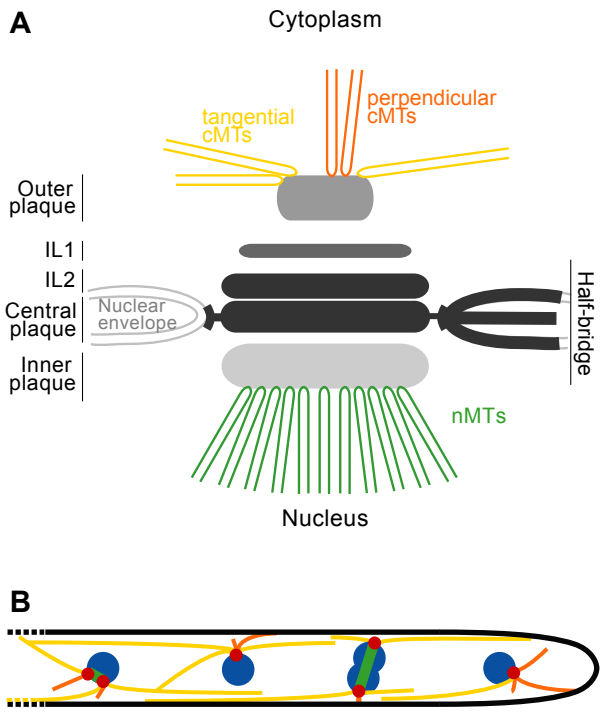

Figure 9. Model of *A. gossypii* SPB and microtubule cytoskeleton.
(A) Schematic representation of an *A. gossypii* SPB and associated microtubules (see text for details). (B) Schematic representation of a hyphal tip compartment with 4 nuclei in different nuclear cycle stages. SPBs in each stage of duplication are shown. Our studies suggest that the perpendicular microtubules seen in EM images correspond to the short cytoplasmic microtubules observed by *in vivo* fluorescence microscopy while the tangential microtubules extend along the growth axis of the hyphae, thereby often bypassing adjacent SPBs without, or only very rarely, aligning with long cytoplasmic microtubules emanating from other SPBs. The apparent lack of interconnected cytoplasmic microtubules emanating from different SPBs explains the observed independent oscillations of adjacent nuclei. The ability of the long microtubules to reach far beyond neighbouring nuclei to make distant cortical contacts can explain the observed bypassing of adjacent nuclei. Both long tangential (yellow) and short perpendicular (orange) cytoplasmic microtubules were seen throughout the nuclear cycle.

of cytoplasmic microtubules is formed throughout the hyphae. However, by tracing single long GFP-marked microtubules by live cell imaging, we found no evidence for such connections. Previous data suggesting that long cytoplasmic microtubules align with each other is perhaps an artifact of the fixation process and/or of processing three dimensional images (e.g. Figure 8A). By EM, we also found no evidence for interacting anti-parallel microtubules in the cytoplasm.

Our data suggest that each SPB in growing *A. gossypii* hyphae forms its own cytoskeletal subdomain consisting of short perpendicular and long tangential cytoplasmic microtubules, the short ones often reaching the cortex and the long ones frequently growing far beyond adjacent nuclei (Figure 9B). Interactions between adjacent microtubules are, if anything, transient. Such cytoskeletal subdomains allow nuclei in multinucleate hyphae to undergo dynamic behavior, which is independent from the dynamics of adjacent nuclei, permit non-synchronized oscillatory movements and facilitate orientation of the spindle axis and nuclear bypassing. If we assume that tangential microtubules are important for nuclear dynamics along a hypha, the different growth-mode of budding yeast could explain why the ability to nucleate this class of microtubules may have disappeared in the 100 million years between the divergence of *A. gossypii* and *S. cerevisiae*.

An alternative explanation for the existence of two sets of cytoplasmic microtubules in *A. gossypii* is that they play a necessary role in the regulation of microtubule dynamics in the absence of distinct α-tubulin isoforms. Microtubules assembled *in vitro* using Tub1, the major α-tubulin in budding yeast, were more dynamic than those assembled with Tub3, the non-essential isoform (Bode *et al.*, 2003). This suggests that a balance of α-tubulin proteins is important for regulation of microtubule dynamics. Because *A. gossypii* contains only a single α-tubulin gene, it might utilize two distinct modes of nucleation to regulate cytoplasmic microtubule stability.

Not only did EM reveal unexpected differences in cytoplasmic microtubule organization between *S. cerevisiae* and *A. gossypii*, but also in the structure of the *A. gossypii* spindle. The area of the haploid *S. cerevisiae* SPB allows it to nucleate roughly 19-20 nuclear microtubules: 1 per each of its 16 chromosomes and 3-4 microtubules to interdigitate with microtubules from the other half-spindle (Byers and Goetsch, 1974; Winey *et al.*, 1995). The diameter and microtubule nucleation capacity of SPBs in diploid and tetraploid yeast is doubled or quadrupled, respectively (Byers and Goetsch, 1975b; Bullitt *et al.*, 1997). Hence, we expected the SPB would be small and form 10-12 spindle microtubules since *A. gossypii* has only seven chromosomes (Dietrich *et al.*, 2004). What we observed were SPBs with an average diameter of 119±21 nm that were able to form 25-30 nuclear microtubules. *A. gossypii* spindles may contain

a greater number of central spindle microtubules and/or chromosomes could attach to more than one kinetochore microtubule. From serial section images of nuclei in metaphase or anaphase showing nuclear microtubules that cross the center of the nucleus, we predict that approximately 10-14 nuclear microtubules are part of the central spindle. However, because *A. gossypii* have ~180 bp point centromeres, rather than the ~125 bp centromere repeats of *S. cerevisiae*, it may form two centromeric nucleosomes (Meraldi *et al.*, 2006). If this corresponds to formation of a kinetochore with two microtubule attachment sites (Joglekar *et al.*, 2008), the *A. gossypii* spindle should have 14 kinetochore microtubules. Higher numbers of interdigitating and kinetochore microtubules could both be accommodated by the *A. gossypii* SPBs we observed and might be necessary for accurate chromosome segregation in a multinucleate organism. Due to the fact that nuclei within the *A. gossypii* mycelium are highly dynamic during nuclear division (Alberti-Segui *et al.*, 2001), the spindle must withstand additional forces not observed in the unicellular organisms like budding yeast.

In conclusion, the multinucleate growth mode of *A. gossypii* results in unique requirements for microtubule nucleation. It assembles a SPB able to nucleate cytoplasmic and nuclear microtubule arrays distinct from those of budding yeast, as well as unique from other multinucleate fungi. The timing of SPB duplication/microtubule nucleation is also different in *A. gossypii* due to the fact that DNA synthesis likely starts immediately after nuclear division; there is no need to pause for growth or mating during G1 like in *S. cerevisiae*. This explains why the half-bridge structure that is normally observed in budding yeast during G1 was hardly ever detected in *A. gossypii* and why we observed a large percentage of SPBs in the duplicated side-by-side configuration. Through our analysis of the *A. gossypii* microtubule cytoskeleton and comparison to that of *S. cerevisiae*, we can better understand the adaptive properties of the cytoskeleton involved in growth and development of many eukaryotic cells. Our studies provide the groundwork for future analysis of nuclear dynamics in the genetically tractable *A. gossypii* system and illustrate the importance of high-resolution EM and live cell image analysis.

Acknowledgements

We are grateful to Dominic Hoepfner for guidance in the early stage of this project and Mark Winey and Tom Giddings for advice and suggestions at later stages. We also thank Jenny Friederichs, Teri Johnson and Fengli Guo for assistance with EM and Katie Perko for help with AutoAligner. This work was supported by a grant from the Swiss National Science Foundation to P.P. (No. 3100A0 – 112688). S.L.J. is supported by a March of Dimes Basil O'Connor Award and the Stowers Institute for Medical Research.

Part II

Components of the spindle pole body outer plaque are required for nuclear dynamics in the multinucleate filamentous fungus *Ashbya gossypii*

Introduction

Microtubule organizing centers (MTOCs) are organelles that assemble and organize microtubules in all eukaryotes (reviewed in (Jaspersen and Winey, 2004; Luders and Stearns, 2007). One of the best-characterized MTOC is the spindle pole body (SPB) of *Saccharomyces cerevisiae*. It appears as a multi-layered structure permanently embedded in the nuclear envelope, with a so-called half bridge attached to one side (Robinow and Marak, 1966; Moens and Rapport, 1971; Byers and Goetsch, 1974; Bullitt *et al.*, 1997; O'Toole *et al.*, 1999). After SPB duplication the side-by-side SPBs are connected by the bridge (Moens and Rapport, 1971; Byers and Goetsch, 1974, 1975a; Adams and Kilmartin, 1999).

Three SPB substructures are involved in the nucleation and binding of microtubules. Intranuclear microtubules, which form the spindle and attach to kinetochores, are organized by the SPB inner plaque (IP) throughout the cell cycle. Cytoplasmic microtubules are nucleated and maintained by the outer plaque (OP) during the whole cell cycle. In addition they are also formed at the half-bridge or bridge during G1 and until SPB separation (Byers and Goetsch, 1975a; Brachat *et al.*, 1998; Adams and Kilmartin, 1999). Components of the SPB have been identified with various approaches (Rose and Fink, 1987; Rout and Kilmartin, 1990; Winey *et al.*, 1991; Sobel and Snyder, 1995; Knop *et al.*, 1997; Brachat *et al.*, 1998; Chen *et al.*, 1998; Wigge *et al.*, 1998; Jaspersen *et al.*, 2002; Kilmartin, 2003) and were subsequently assigned to the SPB substructures by immuno-EM and fluorescence resonance energy transfer analysis (Rout and Kilmartin, 1990; Donaldson and Kilmartin, 1996; Wigge *et al.*, 1998; Adams and Kilmartin, 1999; Muller *et al.*, 2005).

The *S cerevisiae* γ-tubulin, Tub4, is essential for nucleation of both, intranuclear and cytoplasmic microtubules. It forms a stable complex with two other evolutionarily conserved proteins, Spc98 and Spc97 (Geissler *et al.*, 1996; Spang *et al.*, 1996; Knop *et al.*, 1997; Brachat *et al.*, 1998). This complex assembles in the cytoplasm and is targeted to the nucleus where it is anchored to the IP by Spc110 (Knop and Schiebel, 1997; Pereira *et al.*, 1998). It is also anchored to the OP and half-bridge by Spc72 (Rout and Kilmartin, 1990; Knop *et al.*, 1997; Knop and Schiebel, 1998). Components required for the integrity of the OP and thus a stable connection of microtubules to the SPB, include Cnm67 and Nud1 (Brachat *et al.*, 1998; Elliott *et al.*, 1999; Gruneberg *et al.*, 2000; Schaerer *et al.*, 2001). In contrast to Spc72, which can be found associated with the half-bridge or OP depending on the cell cycle stage, Cnm67 and Nud1 are localized exclusively to the OP of the SPB (Brachat *et al.*, 1998; Adams and Kilmartin, 1999; Pereira *et al.*, 1999).

Except for Spc72 and Cnm67, deletions of *S. cerevisiae* genes encoding mitotic SPB proteins are lethal (reviewed in Jaspersen and Winey, 2004). Cells lacking Spc72 and Cnm67 show cytoplasmic microtubule defects, which lead to impaired nuclear positioning and spindle mis-orientation and consequently to the formation of bi-nucleate mother- and anucleate daughter cells (Brachat *et al.*, 1998; Soues and Adams, 1998; Hoepfner *et al.*, 2000; Hoepfner *et al.*, 2002). While *S. cerevisiae* cells lacking *SPC72* can only generate very short and unstable cytoplasmic microtubules (Hoepfner *et al.*, 2002), *CNM67*-deleted cells are still able to form cytoplasmic microtubules from the half-bridge. However, upon SPB separation these microtubules are released and fail to be anchored to the cytoplasmic side of the SPB because of the absence of an OP (Brachat *et al.*, 1998; Hoepfner *et al.*, 2000).

The filamentous fungus *Ashbya gossypii* shared a common ancestor with *S. cerevisiae* before the duplication of the budding yeast genome. Annotation of both genomes revealed a high degree of synteny (gene order conservation) between the two organisms (Dietrich *et al.*, 2004). In particular, *A. gossypii* has syntenic homologs for all components involved in microtubule nucleation, including α-, β- and γ-tubulin and all 18 mitotic SPB components (Part I of this thesis). Nevertheless, the organization of cytoplasmic microtubules and

nuclear dynamics are very different in *A. gossypii* and *S. cerevisiae*. In contrast to the mono-nucleate yeast cells, hyphae of the filamentous fungus *A. gossypii* contain many nuclei in a common cytoplasm. Nuclear dynamics include not only asynchronous division and long-range transport towards the hyphal tip, but also non-synchronous oscillations, occasional bypassing of nuclei and overall nuclear distance control (Alberti-Segui *et al.*, 2001; Gladfelter *et al.*, 2006; Kaufmann and Philippsen, 2008). Previously, we showed that every nucleus in *A. gossypii* is connected to several cytoplasmic microtubules via its SPB OP. EM and live cell imaging demonstrated that *A. gossypii* SPBs are able to nucleate two distinct types of cytoplasmic microtubules: short perpendicular microtubules like in budding yeast and in addition, long, tangential microtubules that extend along the growth axis of the hypha (Part I of this thesis). This latter class of cytoplasmic microtubules often extend beyond adjacent nuclei but they do not align with each other to from a network of anti-parallel microtubule bundles. Instead, each SPB forms its own cytoskeletal subdomain. This unique arrangement likely accounts for the independent behavior of every nucleus.

Little is known about the contribution of individual *A. gossypii* SPB components that control the different aspects of its nuclear dynamics. How is it possible to build such a complex microtubule cytoskeleton with SPB proteins homologous to those of *S. cerevisiae*? To better understand how the particular *A. gossypii* microtubule arrangement is controlled by its SPB, we deleted components of the *A. gossypii* SPB outer plaque, half-bridge and the γ-tubulin complex. The observed unexpected phenotypes illustrate the evolution of functional roles of some SPB components.

Materials and Methods

A. gossypii media and growth conditions

A. gossypii media and culturing are described in (Ayad-Durieux *et al.*, 2000; Wendland *et al.*, 2000) and strains are listed in Table 1.

Plasmid and strain construction

Plasmids generated and used in this study are described below. All DNA manipulations were carried out according to (Sambrook, 2001) with *E. coli* DH5αF' as host (Hanahan, 1983). PCR amplification was performed using standard methods with Taq DNA polymerase, Expand High Fidelity PCR system or the Expand Long Template PCR system (Roche Diagnostics). Oligonucleotides are listed in Table 2 and were synthesized by Microsynth. For recombination of plasmids and PCR products, both were co-transformed into the budding yeast host strain DY3 (*MATα his3Δ200 trp1Δ63 leu2Δ1 ura3-52Δ*) according to (Gietz *et al.*, 1995). Plasmids were isolated from yeast using the High Pure Plasmid Purification Kit (Roche Diagnostics) with a modified protocol as previously described (Schmitz *et al.*, 2006).

The deletion cassettes were amplified from a plasmid containing the *GEN3* (Wendland *et al.*, 2000) cassette that mediates resistance to G418, using 'gene name'_NS1/F2 oligonucleotide pairs. Correct integration of the deletion cassettes was verified with oligonucleotide primer pairs 'gene name'_A1/Gen2_A2 (N-terminus) and 'gene name'_A4/Gen2_A3 (C-terminus). Three independent transformants were characterized for each mutant. Transformation of multi-nucleate mycelium leads to heterokaryotic cells, which contain a mixture of transformed and wild-type nuclei. For subsequent analysis, homokaryotic mycelia were obtained by isolating and growing single spores. To evaluate phenotypes of lethal mutants or mutants with sporulation deficiencies, spores from heterokaryotic mycelium were germinated and analyzed under selective conditions (200 µg/ml G418, ForMedium, England).

pAGT123 (kindly provided by Andreas Kaufmann) was used as a template to amplify *YFP-LEU2* using oligonucleotides AgSPC72_F1/F2. The resulting PCR product was co-transformed into yeast cells with pAG17134 to generate the replicative plasmid *pAgSPC72-YFP-LEU2*. *pAgSPC72-LEU2* was transformed into an *A. gossypii* wild-type strain to generate *AgSPC72-YFP*. To maintain the plasmid, *AgSPC72-YFP* was always grown in minimal medium lacking leucine.

To generate *AgSPC72-YFP AgTUB4-RFP*, the plasmid *pAgTUB4-RFP* (kindly provided by Sandrine Grava) was transformed into *AgSPC72-YFP.* This strain was always grown under selective conditions with 200 µg/ml G418 in minimal medium lacking leucine to maintain both plasmids.

To construct pCB69, the *AgCNM67* ORF plus 498 bp upstream and 191 bp downstream was amplified from BAG2301 (Dietrich *et al.*, 2004) and subcloned into pRS415 (Sikorski and Hieter, 1989). pAGT213 (kindly provided by Andreas Kaufmann) was then used as a template to amplify Td-Tomato-NATPS with oligonucleotides AgCNM67_F5/F2.

Table 1. *A. gossypii* strains used in this study

Strain	Genotype[a]	Reference
Δ*l*Δ*t* (referred to as wild-type)	*Agleu2*Δ *Agthr4*Δ	(1)
AgH4-GFP	*Agade2::AgADE2-AgHHF1-GFP Agleu2*Δ *Agthr4*Δ	(2)
*Agade2*Δ*1*	*Agade2(310-566)*Δ*::GEN3, Agleu2*Δ*, Agthr4*Δ	(3)
AgTUB4-YFP	*AgTUB4-YFP-LEU2 Agleu2*Δ *Agthr4*Δ	this study
GFP-AgTUB1	*Agade2::AgADE2-GFP-AgTUB1 Agleu2*Δ *Agthr4*Δ	this study
*Agcnm67*Δ	*Agcnm67*Δ*::GEN3 Agleu2*Δ *Agthr4*Δ	this study
*AgH4-GFP cnm67*Δ	*Agcnm67*Δ*::GEN3 Agade2::AgADE2-AgHHF1-GFP Agleu2*Δ *Agthr4*Δ	this study
*AgTUB4-YFP cnm67*Δ	*Agcnm67*Δ*::GEN3 AgTUB4-YFP-LEU2 Agleu2*Δ *Agthr4*Δ	this study
*GFP-AgTUB1 cnm67*Δ	*Agcnm67*Δ*::GEN3 Agade2::AgADE2-GFP-AgTUB1 Agleu2*Δ *Agthr4*Δ	this study
*Agspc72*Δ	*Agspc72*Δ*::GEN3 Agleu2*Δ *Agthr4*Δ	this study
*AgH4-GFP spc72*Δ	*Agspc72*Δ*::GEN3 Agade2::AgADE2-AgHHF1-GFP Agleu2*Δ *Agthr4*Δ	this study
*AgTUB4-YFP spc72*Δ	*Agspc72*Δ*::GEN3 AgTUB4-YFP-LEU2 Agleu2*Δ *Agthr4*Δ	this study
*AgH4-GFP tub4*Δ	*Agtub4*Δ*::GEN3 Agade2::AgADE2-AgHHF1-GFP Agleu2*Δ *Agthr4*Δ	this study
*AgH4-GFP nud1*Δ	*Agnud1*Δ*::GEN3 Agade2::AgADE2-AgHHF1-GFP Agleu2*Δ *Agthr4*Δ	this study
*AgH4-GFP kar1*Δ	*Agkar1*Δ*::GEN3 Agade2::AgADE2-AgHHF1-GFP Agleu2*Δ *Agthr4*Δ	this study
*AgH4-GFP cdc31*Δ	*Agcdc31*Δ*::GEN3 Agade2::AgADE2-AgHHF1-GFP Agleu2*Δ *Agthr4*Δ	this study
*AgH4-GFP spc97*Δ	*Agspc97*Δ*::GEN3 Agade2::AgADE2-AgHHF1-GFP Agleu2*Δ *Agthr4*Δ	this study
*AgH4-GFP spc98*Δ	*Agspc98*Δ*::GEN3 Agade2::AgADE2-AgHHF1-GFP Agleu2*Δ *Agthr4*Δ	this study
*AgH4-GFP stu2*Δ	*Agstu2*Δ*::GEN3 Agade2::AgADE2-AgHHF1-GFP Agleu2*Δ *Agthr4*Δ	this study
AgCNM67-Tomato	*Agcnm67*Δ*::GEN3 Agleu2*Δ *Agthr4*Δ *(pAgCNM67-tdTomato-LEU2)*	this study
AgSPC72-YFP	*Agleu2*Δ *Agthr4*Δ *(pAgSPC72-YFP-LEU2)*	this study
AgSPC72-YFP AgTUB4-RFP	*Agleu2*Δ *Agthr4*Δ *(pAgSPC72-YFP-LEU2) (pAgTUB4-ZRedStar2-GEN3)*	this study

[a] A plasmid name in parentheses indicates a replicating plasmid which is maintained under selection pressure. With the exception of those plasmidic strains all analyzed mycelia were homokaryotic (all nuclei have the same genotype). This was obtained either by sporulating homokaryotic strains or by applying selective pressure during germination.

(1) (Altmann-Johl and Philippsen, 1996)
(2) (Helfer and Gladfelter, 2006)
(3) (Knechtle, 2002)

Table 2. Olignucleotide primers used in this study

Name	Sequence[a] 5' – 3'
AgCNM67_NS1	GCAAGATACACAGAAGCAGTTCAAGAGTAGCACAGACGTTTTAGAGATCAGCATTGAGCGccagtgaattcgagctcgg
AgCNM67_F2	TCTCACTTTTACGTATTTTAAATTTCACCAAGCACCGAAAAAAACGTTCATCATGATTACcatgattacgccaagcttgc
AgCNM67_F5	AGAAATATGTCTAGAGAAACTATATGATGAAGTTCGCTCCAGGTTAAAATATggtgacggtgctggttta
Start_CNM67_pAG	AACCGGAATTCCGGGCTTGGCTGGACCCATGGCGAGGGCC
End_AgCNM67_pAG	AACCGGAATTCCGGCCGAAGCACCCGAATCCACACCCAGC
AgSPC72_NS1	TGTTAGAGGCGATAATCCAATCTGTGCTGAATGGAGCAGGCGACGGGACCAAAGTGGATAcggggatcctctagagtcgacc
AgSPC72_F1	AAGAAGAAAATGTACAGCTTCGCGAAAGATTAAGGAGAGTAGACATGCTTaaaacgacggccagtgaattcg
AgSPC72_F2	TTACTAAGTGTATATTAAGTTAATCCACCTATATAAATTAATAACATGCAAAGCAATTTAaccatgattacgccaagcttgc
AgTUB4_NS1	AATTGTCCTTGTATGTACCATTGAGCACTTATGACTGGGGAAATAATATCTATTCAGGTCccagtgaattcgagctcgg
AgTUB4_F1	TGGGTGGAGATGCTGAGATGATCGATATTGAAAGTAACGACGACATCATAAaaacgacggccagtgaattcg
AgTUB4_F2	AGGTCCCGTTTCTAGTATCTACTAATGATGAAGCCAATGGTTACTAGCCTATTTACGCGAaccatgattacgccaagcttgc
AgNud1_NS1	AAGCCACAGGCAGAGAGGGTTTTGAGACCACAGGGAGCGGCAGCCTGGGCTGGCATCCGCccagtgaattcgagctcgg
AgNud1_F2	ATCCGAGAGGGGTGCAGCAGACGCCGTGCACGGTCCGATGGAACCTGCCCCTATATCCTGcatgattacgccaagcttgc
AgKar1_NS1	TTTTTGTGAAGTTTTCATACCGCGCCGCACAAAAACAAGCTGAAGCAGGACCAGGCTGGCccagtgaattcgagctcgg
AgKar1_F2	TTTCATTAAAGTTTTGATATATGTAGATAGTCCTTGTCGAGAGTACAGCTGGTTCACTCTcatgattacgccaagcttgc
AgCdc31_NS1	AGATCTATCGTTAGACAGAGTTGAGGGACAGATTAGCAGCGTGCACTAGATACTGGCAGAccagtgaattcgagctcgg
AgCdc31_F2	CGGCCGCATCGCGTGTTCGCTGCTTTCCACCGATGCGCGCGGAGCGCGCCGCAGAATAGCcatgattacgccaagcttgc
AgSpc97_NS1	TAGGCAGTAAAGATCAGCATTATAGAGTTGTAAAAGTTGCTACAAGGACTCTGGTAGATCccagtgaattcgagctcgg
AgSpc97_F2	GTCTGATTGTCTCAGAAGGCTGTGAACAGAAATTTTGTGCCAGCACCCGGCAGGTGGCGAcatgattacgccaagcttgc
AgSpc98_NS1	ACGACGCGATCTTGTAACACTTAGTATCAGTAAGGTCGTTGATGCCAAGGTCGTTCTTTGccagtgaattcgagctcgg
AgSpc98_F2	AGCGGAGGATTCTGCTCAACTTTGCCATGTCTTCGTTACCGTCCAGCTTGAGGTCCTTGAcatgattacgccaagcttgc
GEN3_A2	cggctcgatcatctctgcctcc
GEN3_A3	ccatcctatggaactgcctcgg
L3	aactggtgatttaggtggttcc
Green2.2	tgtagttcccgtcatctttg
AgCNM67_A1	ggctattaagctgcttgctgcc
AgCNM67_A2	atccggcgacacaagctcatcc
AgCNM67_A3	tttgccaacaagttgcacttcc
AgCNM67_A4	tgttgcttgctgaacatttccg

Table 2 (continued). Olignucleotide primers used in this study

AgSPC72_A1	ccattggctgctgcattaacgg
AgSPC72_A2	gctcgcctcgctatctgtctcc
AgSPC72_A3	tctatcccaggtgtcgcagggc
AgSPC72_A4	acggatggcttgcacaaggagg
AgTUB4_A1	gccagtcccatctttagggcgc
AgTUB4_A2	atcgccaattgcactcggctcg
AgTUB4_A3	cgttatattcaaacgcggtgcc
AgTUB4_A4	gtccatttgcatctccaccccc
AgNud1_A1	tccatctgcgactgctatgc
AgNud1_A2	cacctggactgttccgtagttc
AgNud1_A3	agtacctccgcacactacgac
AgNud1_A4	ttggtgccagtggctttcc
AgKar1_A1	ctgccggtaacacctttgg
AgKar1_A2	aggtcgtagtgggcgaacag
AgKar1_A3	gctatcatgaactcccgattgg
AgKar1_A4	ccaagaacttcgggtacattgg
AgCdc31_A1	gccaaggtaccgcacaacac
AgCdc31_A2	tctcgccaacgaccaggtag
AgCdc31_A3	cgtacgacgacttctacc
AgCdc31_A4	cttcagctgcctctatgg
AgSpc97_A1	cacgtgaccacaaacttc
AgSpc97_A2	ggccctacgatgtcatac
AgSpc97_A3	cctccgtcctaacctaacaaac
AgSpc97_A4	taatcaccacgcgaggattc
AgSpc98_A1	ggagcagtgtggttacactgag
AgSpc98_A2	gttcagcaccgtcaggtacttc
AgSpc98_A3	agcatcctcgacaacaag
AgSpc98_A4	tcggtcattgtgcagttc
AgStu2_A1	agccttctcaatcgtccgtctc
AgStu2_A2	acgaactcacgcccttctc
AgStu2_A3	ttccaatgccgggctaacc
AgStu2_A4	ggtcccgctcttagtacatgc

[a] Lowercase letters are regions of homology to the cassette containing a selectable marker.

The resulting PCR product was co-transformed into yeast cells with pCB69 to generate pCB74, which was transformed into *Agcnm67*Δ to generate *AgCNM67-Tomato. AgCNM67-Tomato* was always grown in minimal medium lacking leucine to maintain the plasmid.

Fluorescence microscopy and image processing

DNA (Hoechst) and immuno-fluorescence stainings were performed as previously described (Ayad-Durieux *et al.*, 2000; Gladfelter *et al.*, 2006). Rat anti-α-tubulin (YOL1/34, Serotec, UK) was used at a 1:25 dilution and Alexa Fluor 568 goat-

anti-rat IgG (Molecular Probes, USA) at a 1:200 dilution.

An Axioplan2 microscope equipped with the objectives Plan-Apochromat 100x/1.40 NA Oil DIC, and Plan-Apochromat 63x/1.40 NA Oil DIC (Carl Zeiss AG, Feldbach, Switzerland) and appropriate filters (Zeiss and Chroma Technology, Brattleboro, VT) was used for microscopy. The light source for fluorescence microscopy was either a 75 W XBO lamp (OSRAM GmbH, Augsburg, Germany), controlled by a MAC2000 shutter and filter wheel system (Ludl Electronics, Hawthorne, NY), or a Polychrome V monochromator (TILL Photonics GmbH, Gräfelfing, Germany). Images were acquired at room temperature using a cooled charge-coupled device camera CoolSNAP HQ (Photometrics, Tucson, AZ) with MetaMorph 6.2r5 software (Molecular Devices Corp., Downingtown, PA). Out-of-focus shading references were used for DIC image acquisitions.

For time-lapse image acquisition, a glass slide was covered with 1 ml of *A. gossypii* minimal medium containing 1% agarose. Once the medium had solidified, either small pieces of mature mycelium from the border of three-day-old *A. gossypii* colonies or young mycelia cultured in liquid medium were spotted onto the slides. 70 µl of liquid minimal medium was added to mycelium before cells were covered with a coverslip and incubated for at least 1 hour before image acquisition. For still images, multiple planes with a distance between 0.3 and 1 µm in the Z-axis were taken.

Image processing was performed with MetaMorph 6.2r5 software. Z-stacks were deconvolved with Nearest Neighbor and compressed by maximum or average projection with Stack Arithmetic. Brightness and contrast were adjusted using Scale Image. Images were colored and overlaid by using Overlay Images and exported from MetaMorph as 8-bit grayscale or RGB TIFF files. Z-Stacks and time-lapse picture series were converted to QuickTime H.264 movies with QuickTime Player Pro (Apple Inc., Cupertino, CA).

Transmission electron microscopy

Spores were grown for 10 - 14 hours in liquid AFM to give rise to small mycelia containing no more than 100 nuclei. Samples were frozen on the Leica EM-Pact at ~ 2050 bar, then transferred under liquid nitrogen into 2% osmium tetroxide/0.1% uranyl acetate/acetone and transferred to the Leica AFS. The freeze substitution protocol was as follows: -90°C for 16 hours, up 4°C an hour for 7 hours, -60°C for 19 hours, up 4°C an hour for 10 hours, -20°C for 20 hours. Samples were then removed from the AFS and placed in the refrigerator for 4 hours, then allowed to incubate at room temperature for 1 hour. Samples went through 3 changes of acetone over 1 hour and were removed from the planchettes. Then, they were embedded in acetone/Epon mixtures to final 100% Epon over several days in a stepwise procedure as described (McDonald, 1999). 60 nm serial thin sections were cut on a Leica UC6, stained with uranyl acetate and Sato's lead and imaged on a FEI Technai Spirit (Hillsboro, OR). Serial section images were aligned using AutoAligner (Bitplane AG, Zurich, Switzerland). For the *AgNUD1* deletion and some samples of the *AgCNM67* deletion, mycelium of the border of 3 days old colonies was frozen and subsequently treated as described above. We could not detect any differences in the SPB structure between either methods of sample preparation.

Bioinformatic analysis

Nuclear localization signal (NLS) search was performed with PredictNLS (http://cubic.bioc.columbia.edu/predictNLS/) and Prosite (http://www.expasy.org/prosite/PS50079). Protein alignments were performed with sequences retrieved from the *Ashbya* Genome Database (AGD, http://agd.vital-it.ch/) (Gattiker *et al.*, 2007) and the *Saccharomyces* Genome Database (SGD, http://www.yeastgenome.org/) using the EMBOSS Pairwise Alignment Algorithms (Blosum62 Matrix, gap open 10, gap extend 0.5).

Results

Components of the γ-tubulin complex are essential in *A. gossypii*

SPBs are the sole site of microtubule nucleation in *A. gossypii* and homologs of all known *S. cerevisiae* SPB components are encoded within its genome (Part I of this thesis). Nevertheless, compared to *S. cerevisiae* SPBs, *A. gossypii* SPBs organize a more complex microtubule cytoskeleton. How can this be achieved? One possibility is that the functions of core SPB components have diverged. This seems plausible based on the low sequence identity between most of the SPB proteins (Table 3, in Part I of this thesis). To address this issue, we created deletion mutants for components of the

γ-tubulin complex, OP and half-bridge since all of these SPB sub-structures have a well-documented role in cytoplasmic microtubule organization in *S. cerevisiae* (Rose and Fink, 1987; Geissler *et al.*, 1996; Spang *et al.*, 1996; Knop *et al.*, 1997; Brachat *et al.*, 1998; Chen *et al.*, 1998; Pereira *et al.*, 1999; Gruneberg *et al.*, 2000; Hoepfner *et al.*, 2000; Hoepfner *et al.*, 2002; Usui *et al.*, 2003).

We found that components of the γ-tubulin complex (*AgTUB4*, *AgSPC97* and *AgSPC98*) are essential, even though small mycelia with up to 12 branches could develop before cells stopped growing (Figure 1B). This ability to grow in the absence of genes of the γ-tubulin complex is most likely due to a maternal effect or the lack of a morphogenesis checkpoint because hyphal elongation is not coupled to nuclear division cycles (Alberti-Segui *et al.*, 2001). In *A. gossypii*, deletions constructed by homologous recombination initially generate heterokaryotic strains since only some nuclei in the hyphae are transformed with the knock-out construct. Upon starvation, mono-nucleate spores are produced that contain either the wild-type or the deletion allele. Wild-type protein from the heterokaryon is likely present in the spores, and this maternal protein could account for early growth and division in otherwise fatal deletions.

Nonetheless, visualization of nuclei lacking *AgTUB4*, *AgSPC97* or *AgSPC98* revealed a clear nuclear segregation defect: nuclear density was decreased approximately 10-fold compared to wild-type (n>100) and most likely as a secondary reaction, nuclei were often elongated or fragmented (Figure 1, A and B). Time-lapse studies of *Agtub4*Δ germlings with histone H4-GFP (AgH4-GFP) labeled nuclei revealed that nuclear division occurs at the very early growth stages. Once nuclei migrated into the newly forming germtube they stopped dividing and finally often to merged (Figure 1B and Movie 1B). Since the γ-tubulin complex is most likely

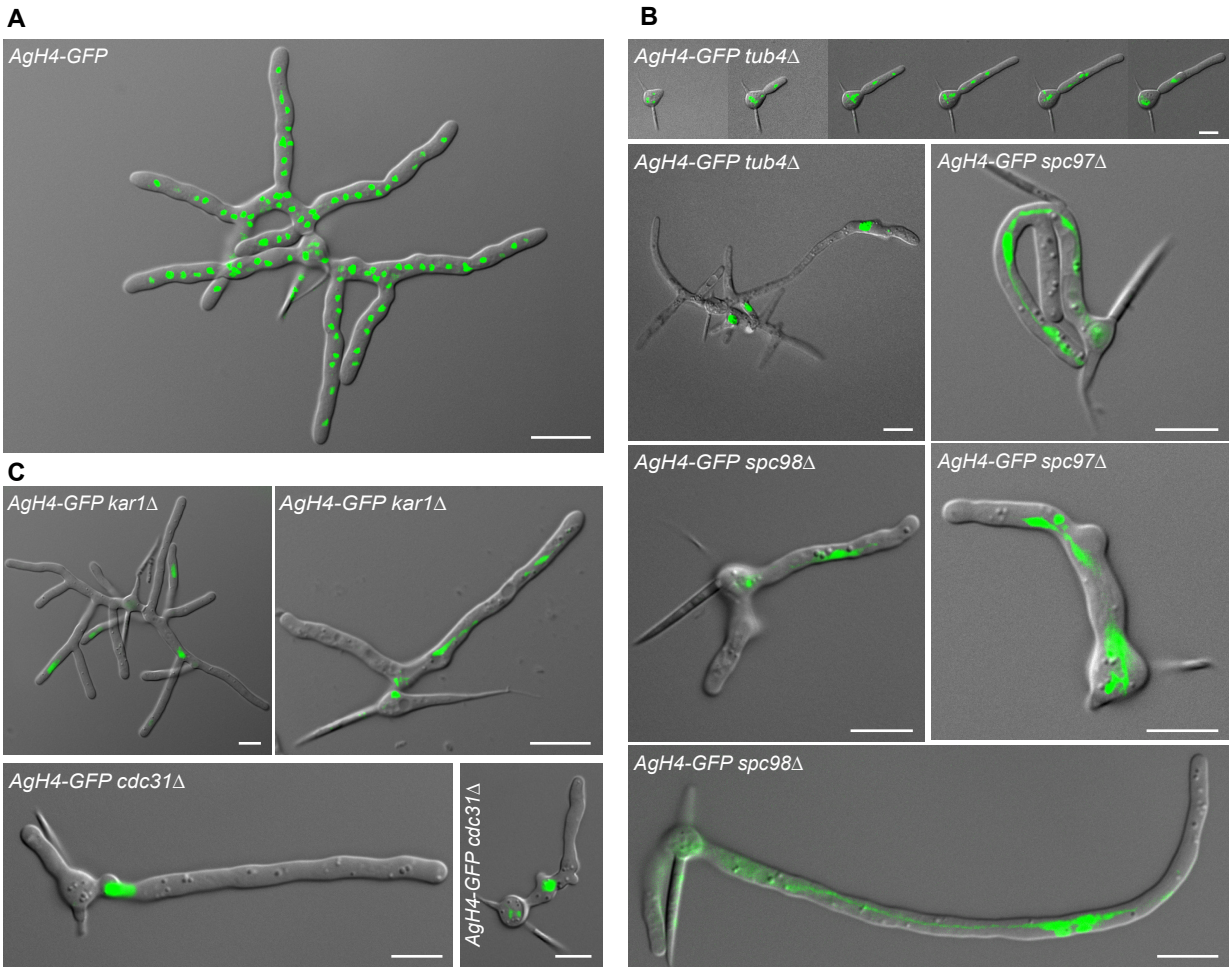

Figure1. Essential components of the *A. gossypii* SPB.
Overlay of a DIC image and AgH4-GFP signals of young mycelia 14 hours after spore incubation in full medium at 30°C. Remnants of the needle shaped spores mark the origin of the mycelia. (A) A typical wild-type mycelium at this stage contains multiple branches and approximately 100 nuclei. (B and C) Mutant hyphae lacking components of the γ-tubulin complex (B) or half-bridge (C) arrest as small mycelium with few branches and a reduced density of nuclei. For *AgH4-GFP tub4*Δ, representative frames of Movie S1 are presented. Bars, 10 μm.

present at both the OP and IP of the SPB, the lethality of these mutants could be due to defects in nuclear microtubules as well as cytoplasmic microtubule organization.

AgSPC72 is required for accurate nuclear distribution and dynamics in *A. gossypii*

Spc72 is the cytoplasmic γ-tubulin complex anchor in *S. cerevisiae* (Knop and Schiebel, 1998; Pereira *et al.*, 1999). The *Ashbya* genome project disclosed one homolog of *ScSPC72* in *A. gossypii*: ADR400W, which was referred to as *AgSPC72* (Dietrich *et al.*, 2004). Sequence comparison of ScSpc72 and AgSpc72 revealed an identity of only 22% between the two amino acid sequences (Part I of this thesis, Table 3). Like AgTub4-YFP (the *A. gossypii* γ-tubulin), AgSpc72-YFP localizes as one or two bright foci at the nuclear periphery (Figure 2A). When AgSpc72-YFP and AgTub4-RFP where expressed in the same strain, we found that they co-localized in 149 of 151 analyzed SPBs, indicating that AgSpc72 is present at the SPB during all nuclear cycle stages (Figure 2B).

To specifically interfere with cytoplasmic microtubule nucleation, we deleted *AgSPC72*. *A. gossypii* mutants lacking *AgSPC72* were viable and grew at a rate similar to that of wild-type (Figure 3A). However, labeling of nuclei revealed that nuclear distribution was severely perturbed (Figure 3B). In contrast to nuclei of wild-type cells that are fairly evenly distributed in hyphae, nuclei of *Agspc72*Δ cells form clusters that often lead to anucleate tip regions (Figure 3, B and C; Figure 5A). These clusters contained up to 20 nuclei and were often found at sites of tip branching (Figure 5A). Time-lapse studies of AgH4-GFP labeled *Agspc72*Δ cells showed that cluster formation already begins in germlings (Figure 4A) and is due to an impaired ability of nuclei to separate efficiently after division (Figure 4B). Moreover, we found that the nuclear oscillations and bypassing observed in wild-type cells are abolished in *Agspc72*Δ mutants (Figure 4, C and D; Movies S2 and S3).

Immuno-staining with antibodies to α-tubulin revealed that *Agspc72*Δ cells lack short cytoplasmic microtubules. Long cytoplasmic microtubules that run along the growth axis of the hypha were still present even though they were frequently detached from nuclei and sometimes detached microtubules could be found in the tip region (Figure 5A). To distinguish whether the γ-tubulin complex would also detach from nuclei, we examined AgTub4-YFP in the *Agspc72*Δ mutant. γ-tubulin was still exclusively localized as one or two foci at the nuclear periphery and could not be detected at detached microtubules (Figure 5B).

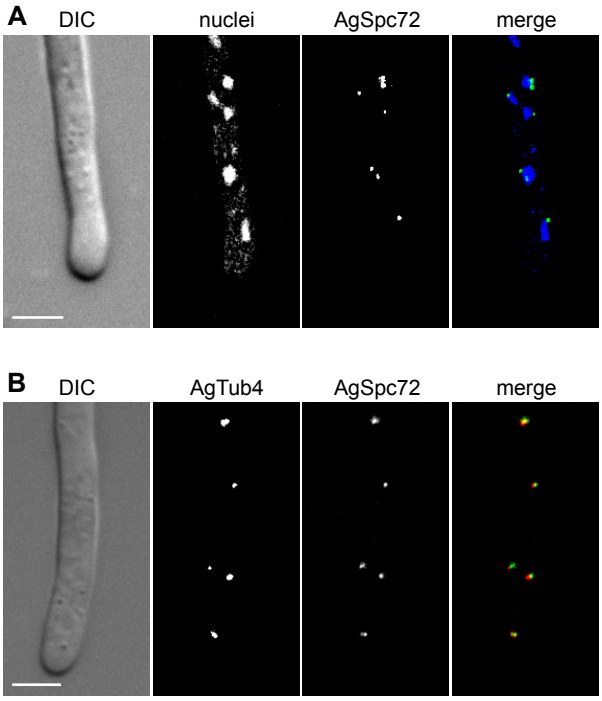

Figure 2. Localization of AgSpc72.
(A) AgSpc72-YFP localizes as one or two foci to the nuclear periphery. Nuclei are stained with Hoechst. Bar, 5 μm. (B) AgSpc72-YFP and AgTub4-RFP co-localize. Bar, 5μm.

EM analysis confirmed the decrease in the number of cytoplasmic microtubules in *Agspc72*Δ mutants. In contrast to wild-type cells where 98% (n = 50) of all observed SPBs were associated with one to five cytoplasmic microtubules, we could only find at most two cytoplasmic microtubules per SPB in 15% of all analyzed *Agspc72*Δ SPBs (n = 33) (Figure 11A). All observed cytoplasmic microtubules associated with the SPB in *Agspc72*Δ mutants were tangential (Figure 5C and 11A); perpendicular cytoplasmic microtubules were not detected. Since we propose that short microtubules are the perpendicular microtubules seen in EM and tangential microtubules correspond to long cytoplasmic microtubules (Part I of this thesis), this result is consistent with our immuno-fluorescence studies showing only long cytoplasmic microtubules in the mutant.

Both the OP and Intermediate layer 1 (IL1) were less visible by EM in SPBs from *Agspc72*Δ cells compared to wild-type (Figure 5D and Figure 4A in Part I of this thesis). A clearly distinguishable OP and IL1 was seen in only 23% and 40% of *Agspc72*Δ mutants, respectively, compared to 67% and 70% of wild-type (wild-type n = 46, *Agspc72*Δ n = 30; we only included SPBs in this analysis when serial section images were available) (Figure 11A). Other layers of the SPB were apparently

unaffected by deletion of *AgSPC72*, (Figure 5, C and D; Figure 11B). Thus, deletion of *AgSPC72* specifically leads affects cytoplasmic microtubules and their attachment to the SPB.

The fraction of mitotic nuclei is increased in *Agspc72*Δ mutants.

Clustering of nuclei in *Agspc72*Δ mutants could also be detected by EM (Figure 6). These nuclei often were deformed and the atypical curved structure of the spindle microtubules pointed to a defect in nuclear division. To investigate the process of nuclear division in *AgSPC72*-deleted cells, we first determined the percentage of nuclei that were in distinct nuclear cycle stages according to their number of SPBs and the length of the spindle (Figure 7A). In wild-type cells 76% of all counted nuclei (n = 234) had a single SPB, 16% had two adjacent SPBs without a connecting spindle and 8% had two separated SPBs that were connected by a spindle. This last class were considered as metaphase if the spindle length was < 2.8 µm (6%) and as anaphase if spindle length was ≥ 2.8 µm (2%). Compared to wild-type, *Agspc72*Δ strains had decreased numbers of nuclei with one and two SPBs (67% and 14% respectively from a total of n = 150 counted nuclei) while the fraction of mitotic nuclei was more than doubled (19%). In particular, the four-fold increase in anaphase spindles from 2% in wild-type to 8% in *Agspc72*Δ mutant cells was conspicuous (Figure 7, B and E).

Next, we measured the angle between the spindle of mitotic nuclei and the axis of growth (Figure 7C). During metaphase, spindles were oriented randomly in wild-type as well as in *Agspc72*Δ mutants with angles varying from < 3° to 90° (Figure 7, D and E). Anaphase spindles were mostly aligned along the lateral axis in wild-type cells (88% of anaphase spindles with < 15° divergence to the axis of growth). In *Agspc72*Δ however, only 64% of anaphase spindles were oriented along the axis of growth. Furthermore, spindles were longer on average (6.1 µm +/- 0.49,

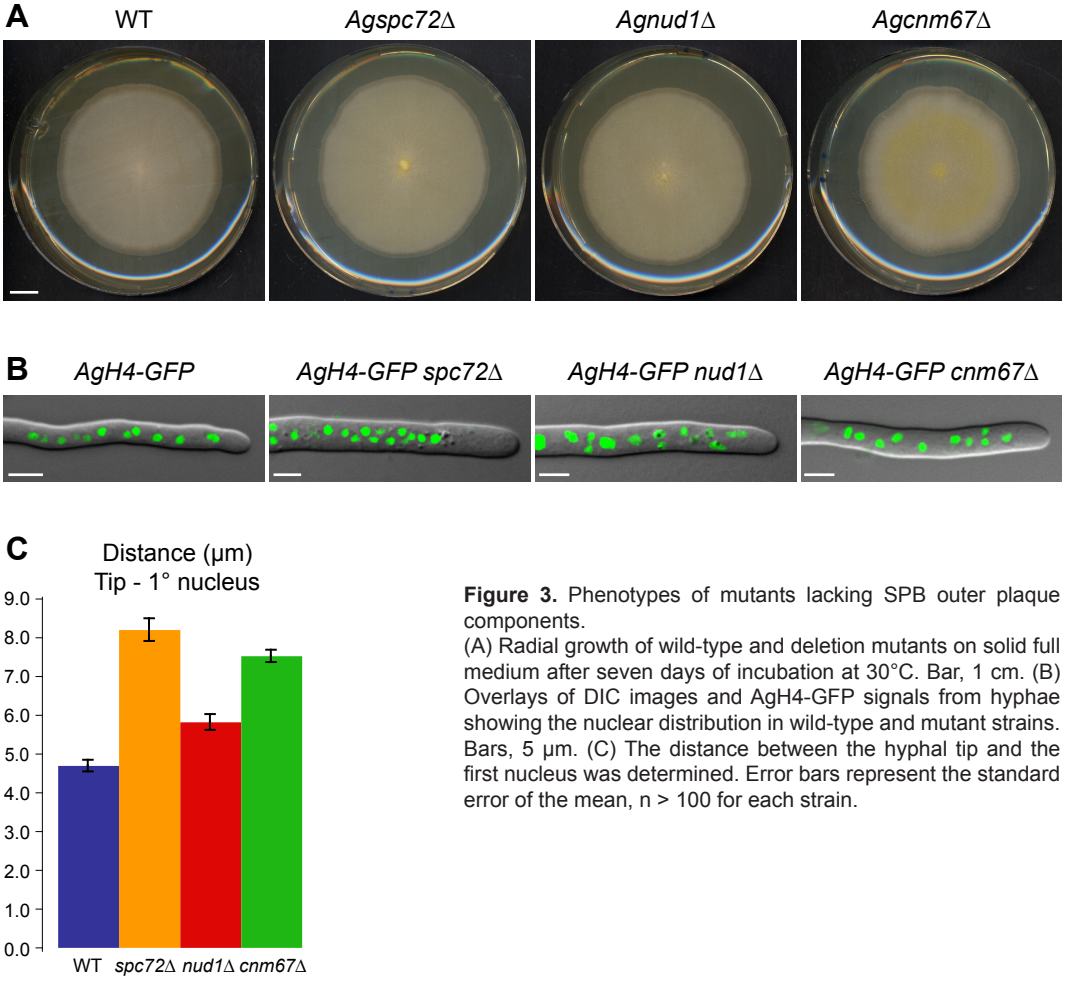

Figure 3. Phenotypes of mutants lacking SPB outer plaque components.
(A) Radial growth of wild-type and deletion mutants on solid full medium after seven days of incubation at 30°C. Bar, 1 cm. (B) Overlays of DIC images and AgH4-GFP signals from hyphae showing the nuclear distribution in wild-type and mutant strains. Bars, 5 µm. (C) The distance between the hyphal tip and the first nucleus was determined. Error bars represent the standard error of the mean, n > 100 for each strain.

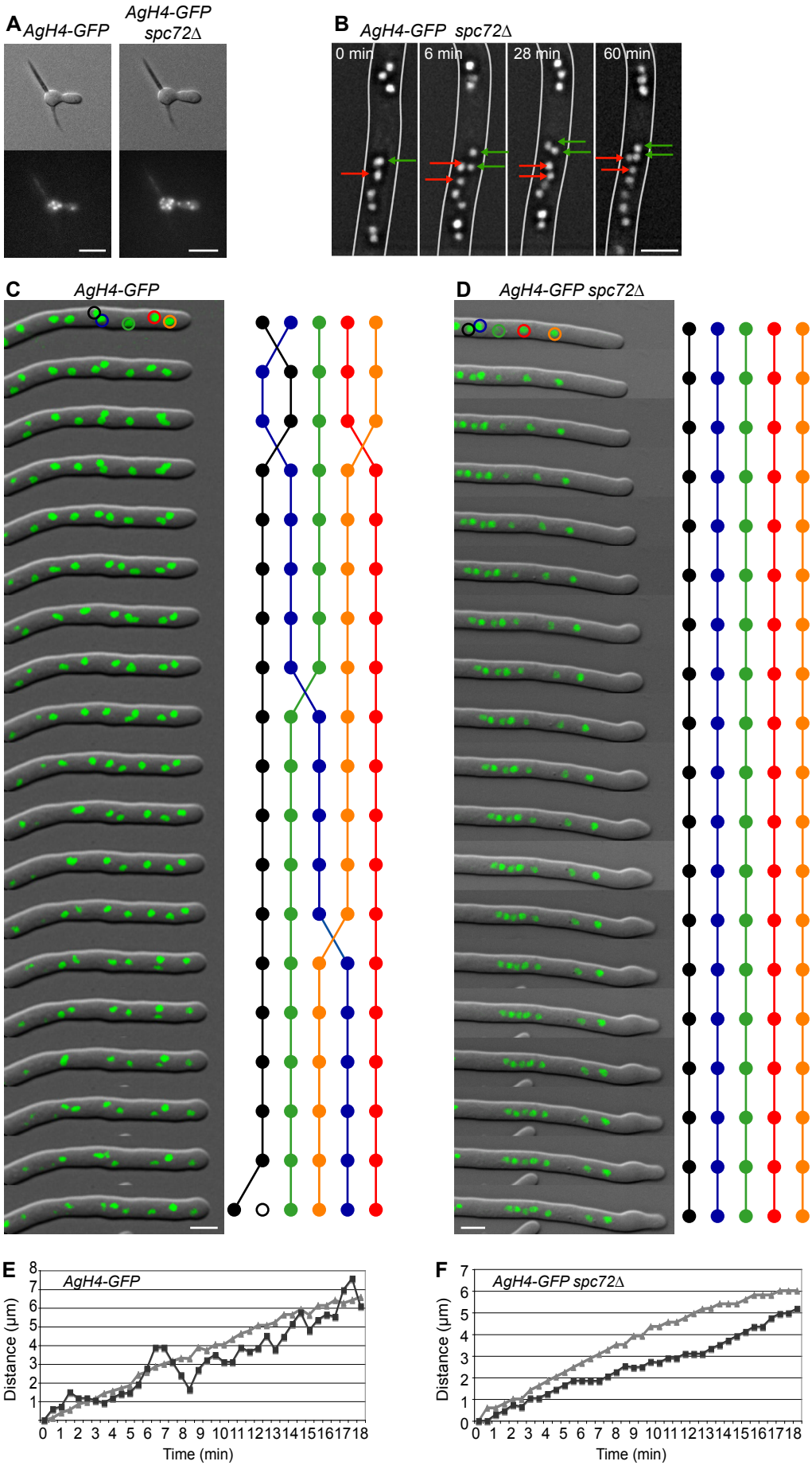
A
AgH4-GFP
AgH4-GFP spc72Δ
B
AgH4-GFP spc72Δ
0 min
6 min
28 min
60 min
C
AgH4-GFP
D
AgH4-GFP spc72Δ
E
AgH4-GFP
Distance (µm)
Time (min)
F
AgH4-GFP spc72Δ
Distance (µm)
Time (min)

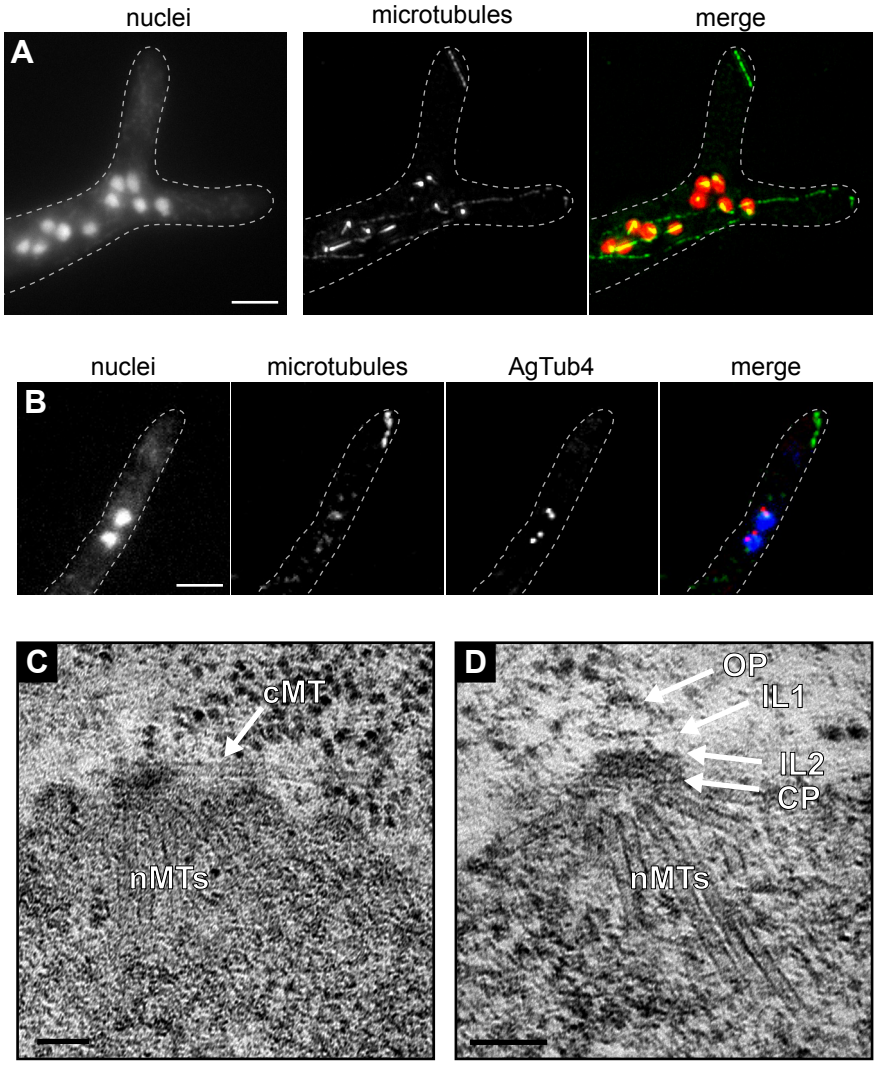

Figure 4 (previous page). Nuclear dynamics are impaired in *Agspc72*Δ mutants.
(A) Nuclei in wild-type and *Agspc72*Δ germlings were visualized using AgH4-GFP. In wild-type, ~four nuclei are seen in the germ bubble and one nucleus has migrated out of the germ bubble into the germ tube. In *Agspc72*Δ at least seven nuclei appear clustered in the germ bubble, while a few have left the germ tube. Bars, 5µm. (B) Time lapse imaging of *Agspc72*Δ *AgH4-GFP* cells shows that nuclei remain in close proximity after division, which leads to cluster formation. The nuclei marked with red and green arrows divide between 0 and 6 minutes, and the daughter nuclei remain associated for up to 60 minutes. Bar, 5 µm. (C and D) Overlay of DIC and AgH4-GFP signal from time-lapse video imaging of wild-type (C) and *Agspc72*Δ (D) hyphae (Movies S2 and S3). Images were captured every 30 seconds and 1 minute interval frames are shown. Migration of the first five nuclei was monitored and their tracks are schematically documented. (C) In wild-type, the nuclei were observed to undergo bypassing and rapid oscillations (see Movie S2). (D) These dynamic nuclear movements were not detected in *Agspc72*Δ mutants (see Movie S3). (E and F) Graphical representations of the oscillatory migration of a nucleus (black) compared to the tip elongation (grey) over the time course are superimposed.

Figure 5. *Agspc72*Δ mutants have defects in the cytoplasmic microtubule cytoskeleton and the SPB outer plaque.
(A) *Agspc72*Δ cells were were stained with Hoechst to visualize DNA and anti-α-tubulin antibodies to detect microtubules. A cluster of nuclei can be seen at a tip-splitting site. These cells lack short cytoplasmic microtubules while long cytoplasmic microtubules that extend along the growth axis are still present even though they are frequently not connected to nuclei. A detached microtubule can be seen in the upper tip region. Bar, 5 µm. (B) *Agspc72*Δ cells expressing AgTub4-YFP were stained with Hoechst and anti-α-tubulin antibodies to detect the DNA and microtubules, respectively. The SPBs were visualized by AgTub4-YFP epifluroescence. (C and D) Electron micrographs of *Agspc72*Δ mutants. Bars, 100 nm. (C) The SPB in these mutants is associated with nuclear microtubules (nMTs) but shows reduced numbers of cytoplasmic microtubules (cMT). In this image, a tangential cytoplasmic microtubule can be seen in the vicinity of the SPB (arrow). In a total of 33 analyzed *Agspc72*Δ SPBs we did not observe any perpendicular microtubules. (D) The central plaque (CP) and intermediate layers 1 and 2 (IL1 and IL2) were observed in SPBs from *Agspc72*Δ mutants. In some cases, a small amount of amorphous material could also be detected above IL1, which could be part of the outer plaque (OP). However, the size of this layer was greatly reduced compared to wild-type (see Figure 4A, Part I of this thesis).

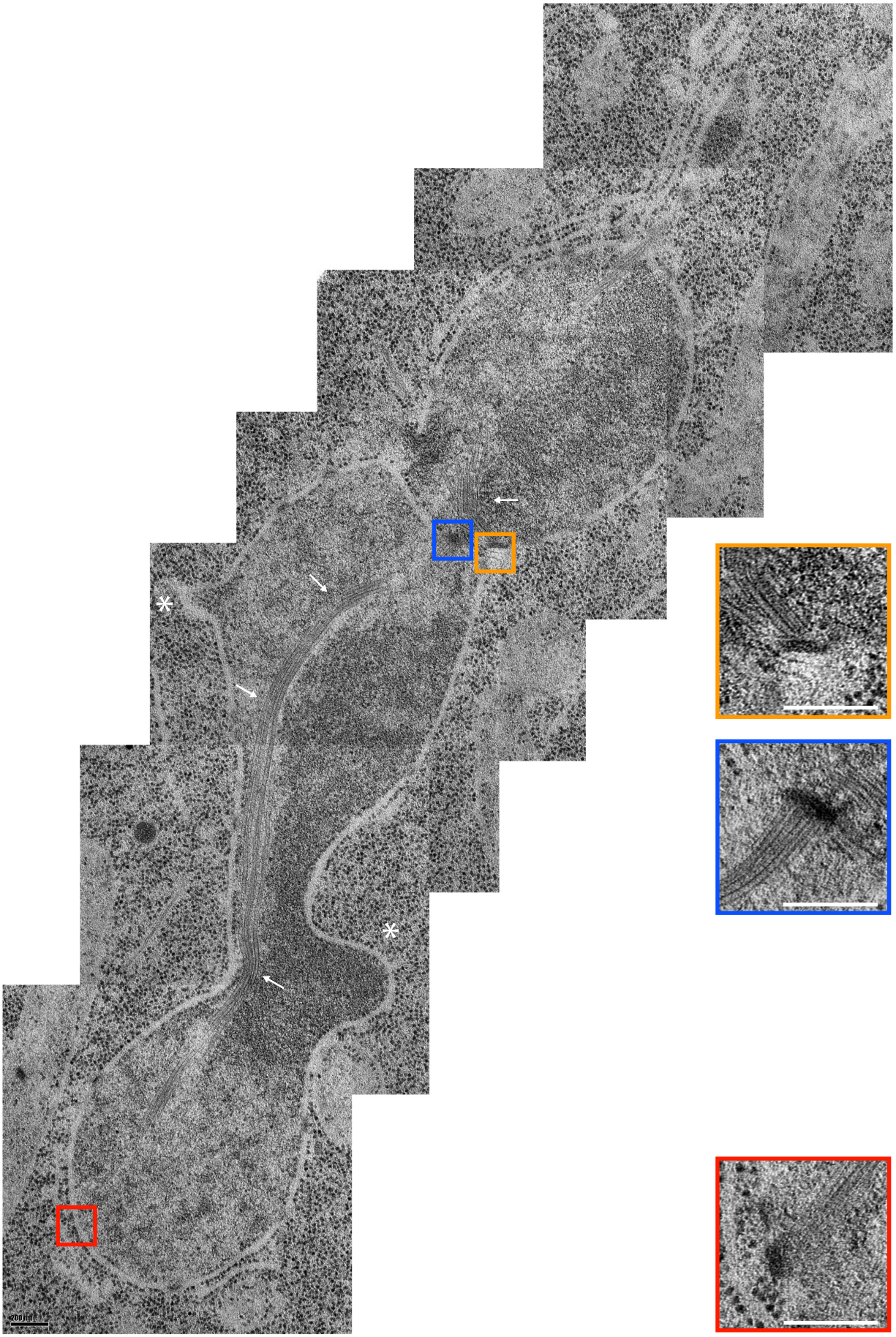
200nm

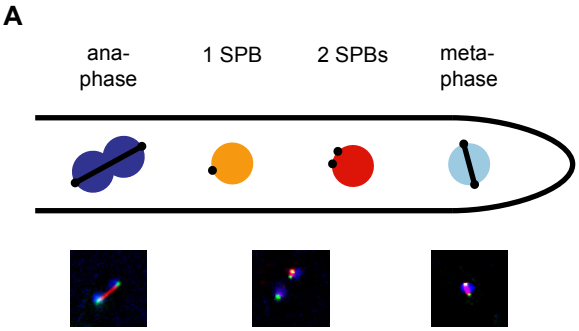

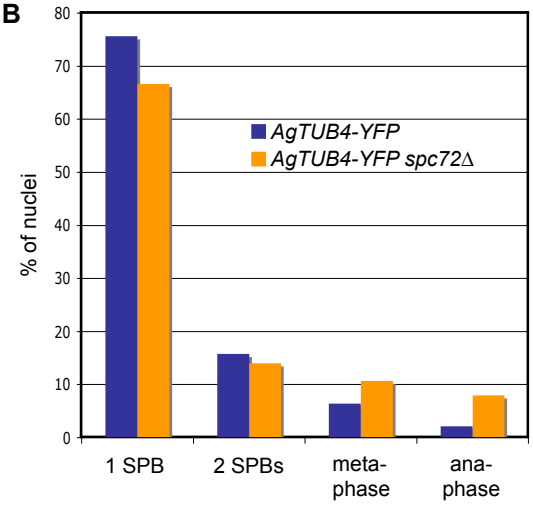

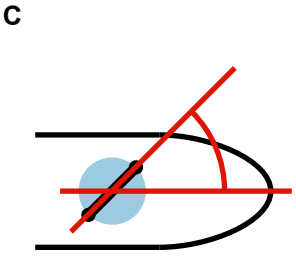

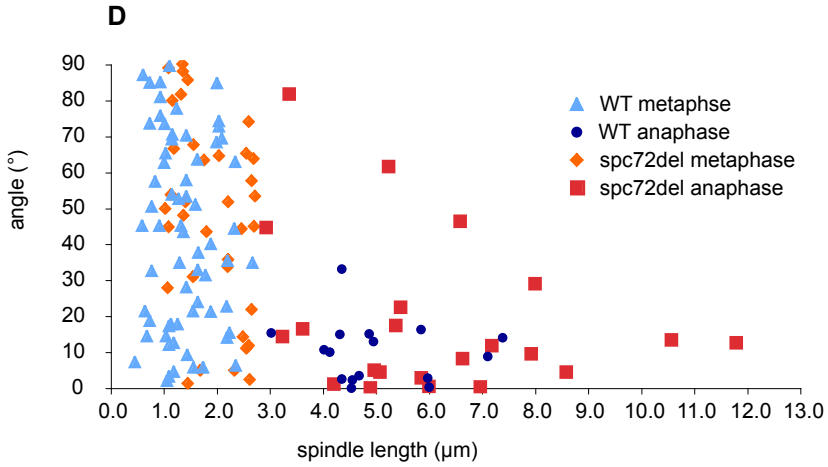

E

	nuclei in metaphase	average angle metaphase	min-max angle metaphase	distribution	nuclei in anaphase	average angle anaphase	min-max angle anaphase	< 15°	average spindle length anaphase
Wt	6%	42°	2° - 90°	random	2%	10°	0° - 33°	88%	5.0 µm
spc72Δ	11%	48°	1° - 90°	random	8%	19°	0° - 82°	64%	6.1 µm

Figure 6 (previous page). EM of nuclear clusters in *Agspc72Δ* cells.
Montage of seven EM images showing the clustering of nuclei in a hyphae of a *SPC72*-deletion mutant. The nuclei exhibit abnormal protuberances (asterisks) and spindle microtubules are remarkably curved (arrows). The colored boxes mark locations of SPBs. Higher magnifications of these SPBs are shown in the respective boxes on the side. For the blue and red framed examples, the SPBs images were taken from thin sections adjacent to the composite image. Bars, 200 nm.

Figure 7. Analysis of mitosis in *AgTUB4-YFP* and *AgTUB4-YFP spc72Δ* cells.
MTOCs were labeled with AgTub4-YFP, spindles with anti-α-tubulin, nuclei with Hoechst. Spindle lengths of less than 2.8 µm were defined as metaphase, spindles of 2.8 µm and more as anaphase. (A and B) The number of nuclei in distinct cell-cycle stages was counted according to their number of MTOCs per nucleus and the length of the spindle. (C and D) The angle between the spindle of mitotic nuclei and the axis of growth was measured and plotted as a function of the spindle length. (E) Table summarizing the results of (B) and (D).

n = 22) compared to wild-type (5.0 µm +/- 0.29 µm, n = 16). Interestingly, we noticed a tendency of longer spindles to be better aligned along the growth axis (Figure 7, D and E).

To further investigate this aberration in spindle orientation and length in *Agspc72*Δ cells, we followed nuclear divisions *in vivo*. Six mitotic events of *AgH4-GFP* and *AgH4-GFP spc72*Δ strains were analyzed as described in (Alberti-Segui *et al.*, 2001). The time for complete separation of nuclear masses was increased from an average of 9.5 ± 0.6 min in wild-type to 11.5 ± 0.6 min in *AgSPC72*-deleted cells (Figure 8). When we measured the time until the angle between the spindle and the axis of growth was less then 15°C, we found that this process was accomplished 4.8 ± 0.6 min after the starting point of nuclear elongation in the *Agspc72*Δ mutant compared to 2.2 ± 0.7 in wild-type. Thus the delay in nuclear division is due to a less efficient spindle orientation in elongating nuclei along the axis of growth.

The half-bridge is essential in *A. gossypii*

Spc72 binds to multiple sites on the cytoplasmic side of the *S. cerevisiae* SPB. During G1 phase of the cell cycle, it interacts with Kar1 on the half-bridge to nucleate cytoplasmic microtubules from this site but redistributes to the OP in early S phase where it associates with Nud1 and Cnm67 (Pereira *et al.*, 1999). We were interested in determining if deletion of any of these SPB components resulted in cytoplasmic microtubule and nuclear migration defects similar to *Agspc72*Δ mutants.

Small mycelium containing up to 10 nuclei were observed in cells deleted for *AgKAR1* (Figure 1C), however, further nuclear divisions did not occur. This indicates that *AgKAR1* is an essential gene. The fact that deletion of *AgCDC31*, another half-bridge protein not involved in Spc72 binding and cytoplasmic microtubule organization, resulted in the same phenotype (Figure 1C) suggests that lethality in cells lacking *AgKAR1* is due to general SPB duplication defects rather than a specific effect on cytoplasmic microtubules.

Deletion of *AgCNM67* and *AgNUD1* result in loss of the SPB outer plaque and microtubule nucleation form the bridge

Next, we examined cells lacking *AgNUD1* or *AgCNM67*. These mutants were viable and displayed radial growth on agar similar to wild-type cells (Figure 3A). Both mutants showed only mild defects in nuclear distribution compared to *Agspc72*Δ (Figure 3, B and C), and nuclear dynamics were not obviously affected: nuclear oscillations and bypassing could still be observed in *Agnud1*Δ and *Agcnm67*Δ strains (Movies S4 and S5).

Examination of SPB structure by EM showed defects in the OP and cytoplasmic microtubules in *Agnud1*Δ and *Agcnm67*Δ mutants. However, we observed distinct differences in the SPB ultra structure between the two mutants and *Agspc72*Δ. In *Agnud1*Δ mutants, the OP was clearly absent

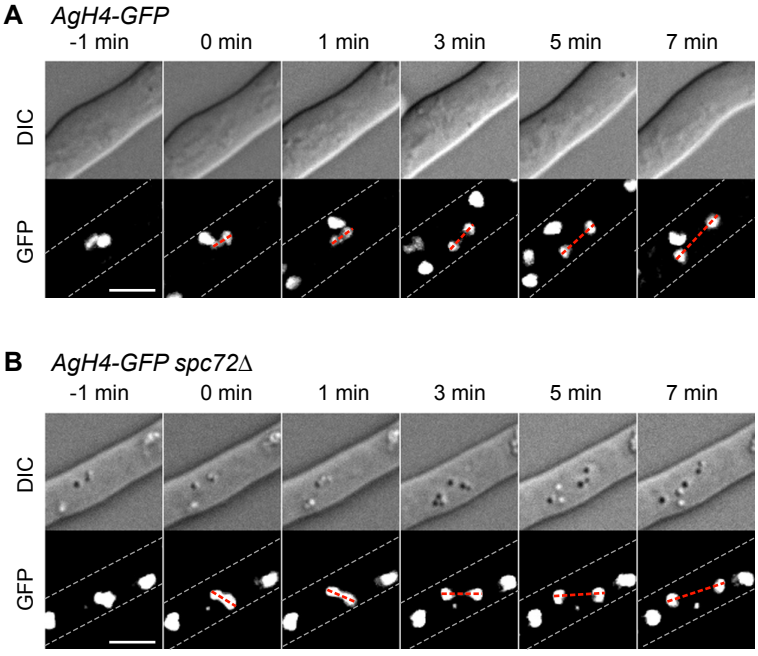

Figure 8. *In vivo* analysis of nuclear division in *AgH4-GFP* and *AgH4-GFP spc72*Δ cells. Representative time-lapse series of dividing nuclei in *H4-GFP* (A) and *H4-GFP spc72*Δ (B) strains. The angle between the axis of nuclear elongation and the axis of growth was measured every 60 seconds. Six time points are shown for both strains. Nuclei start to elongate at T = 0 min. In wild-type, orientation of the dividing nuclei along the axis of growth is completed one minute after the starting point of nuclear elongation, in *Agspc72*Δ this process takes seven minutes. Bars, 5 µm.

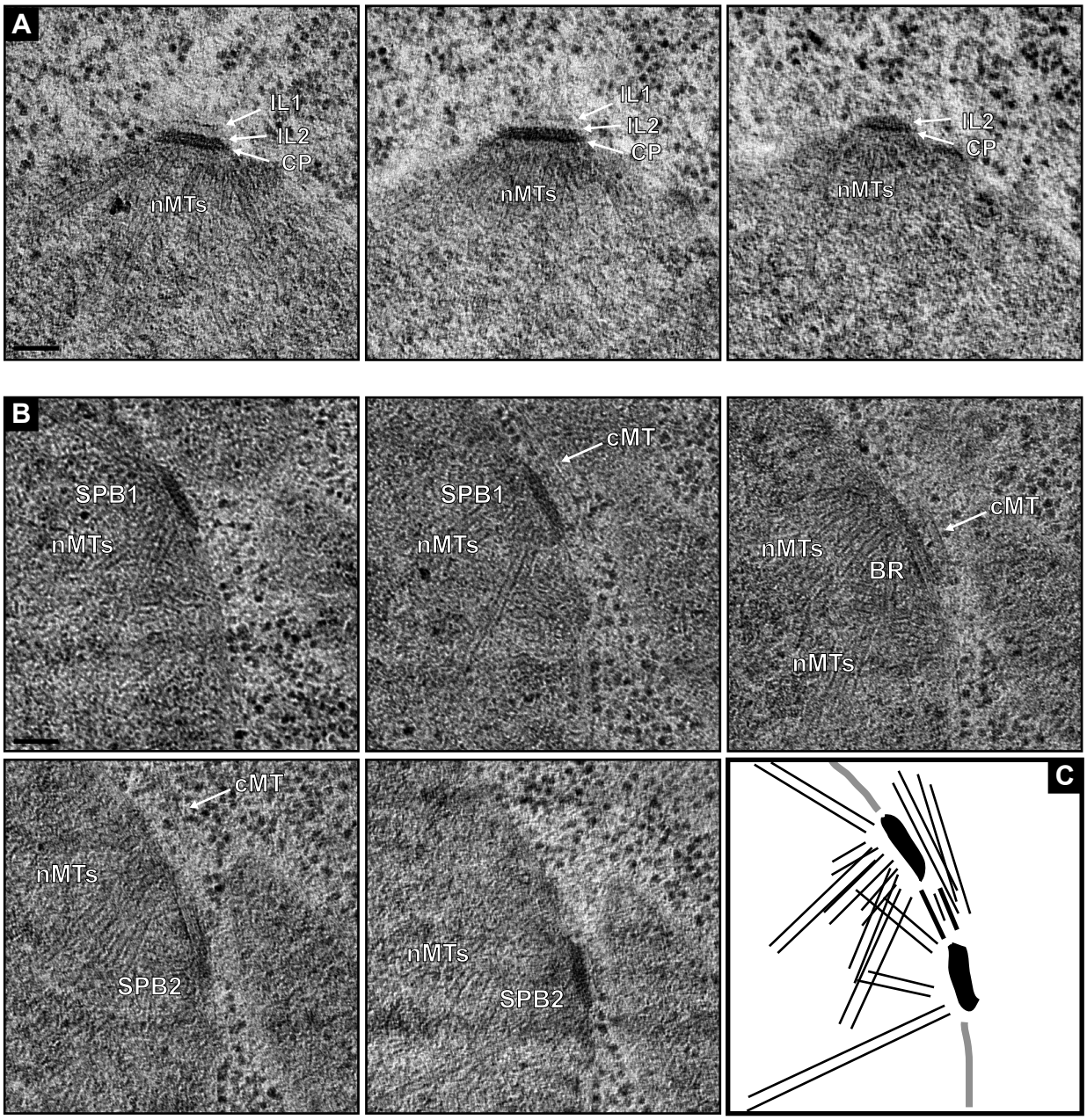

Figure 9. SPBs of *Agnud1*Δ mutants lack the outer plaque.
(A) Serial section images of a single SPB of a *Agnud1*Δ mutant. The central plaque (CP) and intermediate layers 1 and 2 (IL1 and IL2) were observed while the outer plaque could not be detected in any section. Bar, 100 nm. (B) Serial section images of duplicated side-by-side SPBs (SPB1 and SPB2) connected by a bridge (BR). Nuclear microtubules (nMTs) as well as two cytoplasmic microtubules (cMT) can be seen. The cytoplasmic microtubules seem to emerge from the bridge region. (C) A schematic drawing summarizing the five serial sections images of (B).

Figure 10 (next page). Cytoplasmic microtubule defects in *Agcnm67*Δ mutants.
(A) Serial sections of duplicated side-by-side SPBs (SPB1 and SPB2) connected by a bridge (BR), which nucleates three cytoplasmic microtubules (cMTs). Nuclear microtubules (nMTs) are formed at the SPB inner plaque (IP). Images were aligned using AutoAligner to produce the schematic drawing. Bar, 100 nm. (B) Representative, deconvolved images of a Z-stack through an *Agcnm67*Δ hyphae expressing GFP-AgTub1. The complete stack is available as Movie S6. Short and long cytoplasmic microtubules can be seen emerging form both sides of a mitotic spindle (M) and from bright foci that represent the SPBs. Compared to wild-type, the number of cytoplasmic microtubules is reduced. An arrow points to a SPB lacking any associated cytoplasmic microtubules. Bar, 5 µm. (C) The number of short and long cytoplasmic microtubules per SPB was quantitated in wild-type and in the *Agcnm67*Δ mutant and average values observed for both classes are presented along with a combined total. Error bars indicate standard error of the mean (n=55 and 95 SPBs for *GFP-AgTUB1* and *GFP-AgTUB1 cnm67*Δ respectively). (D) EM of a mitotic spindle in *Agcnm67*Δ cells. Bar, 100 nm. (E) Wild-type and *Agcnm67*Δ mutants expressing AgTub4-YFP were stained with anti-α-tubulin antibodies to determine the number of nuclei containing a single SPB focus, two SPB foci but no mitotic spindle or two SPB foci and a spindle. Error bars indicate standard error of the mean (n>200).

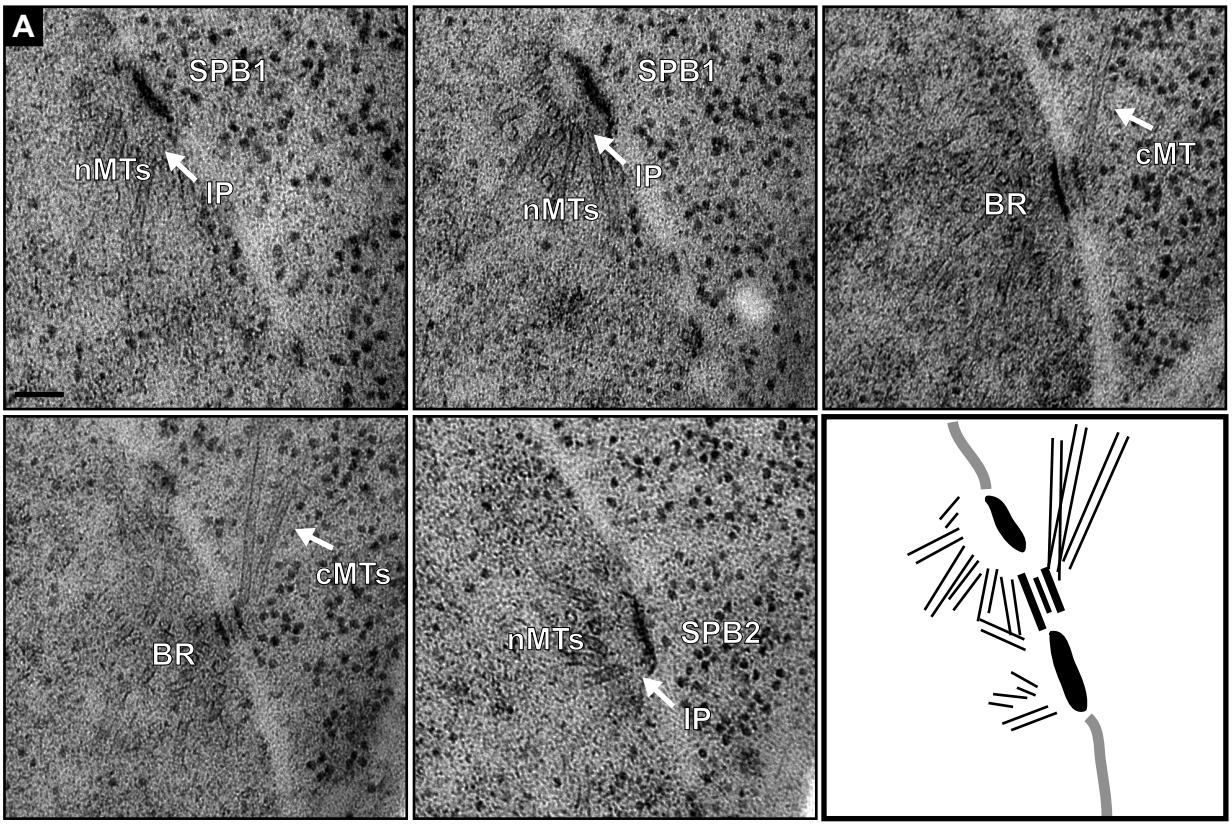
A
SPB1
nMTs
IP
SPB1
IP
nMTs
cMT
BR
cMTs
BR
nMTs
SPB2
IP

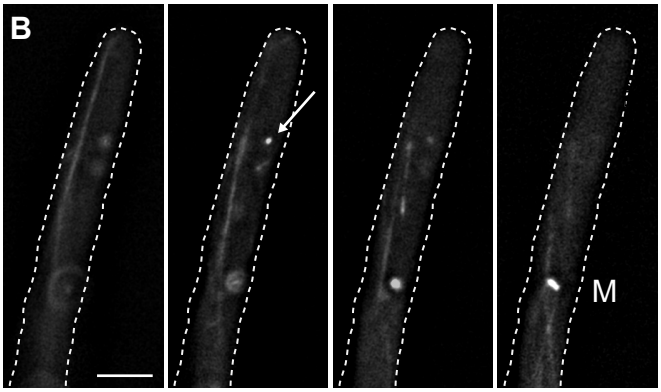
B
M

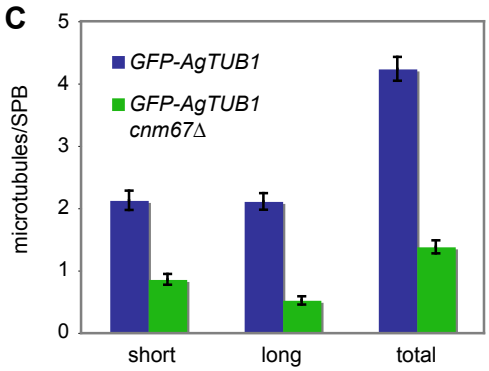
C
microtubules/SPB
GFP-AgTUB1
GFP-AgTUB1
cnm67Δ
0
1
2
3
4
5
short
long
total

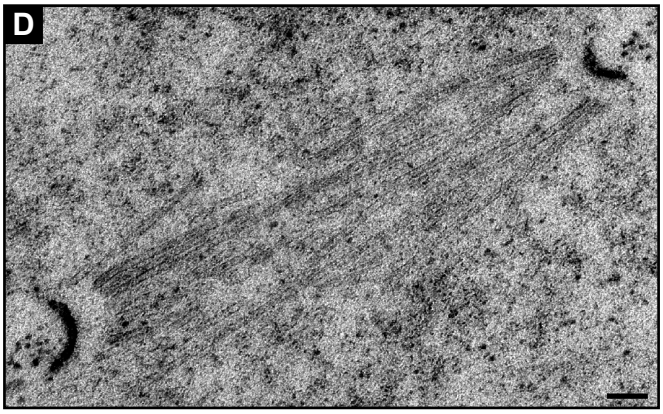
D

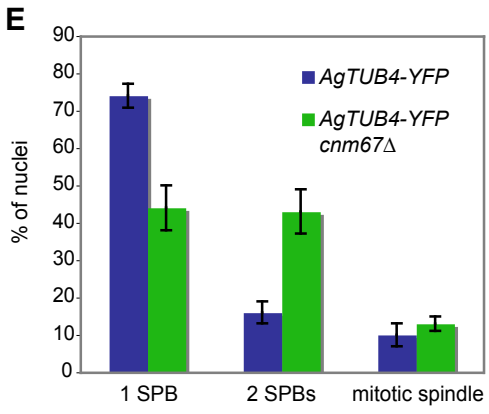
E
% of nuclei
AgTUB4-YFP
AgTUB4-YFP
cnm67Δ
0
10
20
30
40
50
60
70
80
90
1 SPB
2 SPBs
mitotic spindle

and the number of cytoplasmic microtubules was decreased (6 of 18 SPBs had 1 – 4 attached tangential and/or perpendicular cytoplasmic microtubules while 49 of 50 wild-type SPBs had 1 – 5 cytoplasmic microtubules attached). Distinct IL1 and IL2 layers were visible in 66% of the *Agnud1*Δ SPBs (Figures 9 and 11), which is equal to wild-type. In one case where we could track duplicated SPBs in the side-by-side position over several sections, we observed microtubules emanating from the connecting bridge (Figure 9 B).

We also noticed a significant increase in the width of the CP in *Agnud1*Δ mutants (Figure 11B and Table S1, Supplementary material). This could be due to the fact that those samples were prepared form agar plates instead of liquid cultures. However, since we could not detect a difference in the SPB structure between samples prepared with either method in wild-type and *Agcnm67*Δ cells, we believe that this is a true phenotype of *Agnud1*Δ mutants rather than an artifact from sample handling.

The OP was also absent in *Agcnm67*Δ cells, but in contrast to *AgNUD1*-deleted cells, these mutants lacked the IL1 plaque as well (Figure 10, A and D and Figure 11). Moreover, we observed a decrease in cytoplasmic microtubules: 11 of 33 *Agcnm67*Δ SPBs were associated with 1 – 3 tangential and/or perpendicular cytoplasmic microtubules (Figure 11A). Unlike wild-type cells where both classes of cytoplasmic microtubules are nucleated at the OP, the cytoplasmic microtubules we observed in *Agcnm67*Δ cells most often emanated from the bridge or half-bridge region (Figure 10A). Live cell imaging of *GFP-AgTUB1* in *Agcnm67*Δ confirmed that the mutants show a reduced number of both long and short cytoplasmic microtubules compared to wild-type cells (Figure 10, B and C; Movie S6). In some cases we could even observe SPBs without any associated cytoplasmic microtubules but in contrast to *Agspc72*Δ, we did not observe detached microtubules in the cytoplasm of *Agcnm67*Δ hyphae (Figure 10B).

EM analysis also revealed an additional phenotype in *Agcnm67*Δ mutants. More often than in wild-type, nuclei frequently contained two SPBs, in the side-by-side or separated configuration or associated with a mitotic spindle (Figure 10D). Evaluation of *Agcnm67*Δ *AgTUB4-YFP* cells by fluorescence microscopy confirmed this finding. Compared to wild-type, ~3-fold more *Agcnm67*Δ nuclei had two SPBs (Figure 10E), indicating that

A

	wild-type			*Agspc72*Δ			*Agnud1*Δ			*Agcnm67*Δ		
cMT	#	%	n	#	%	n	#	%	n	#	%	n
total	1-5	98	50	1-2	15	33	1-4	33	18	1-3	33	33
tangential	1-5	90	50	1-2	15	33	1-2	33	18	1-2	21	33
perpendicular	1-3	38	50	0	0	33	1-2	28	18	1-3	15	33
layer		%	n		%	n		%	n		%	n
IL1		70	46		40	30		66	18		0	30
OP		67	46		23	30		0	18		0	30

B

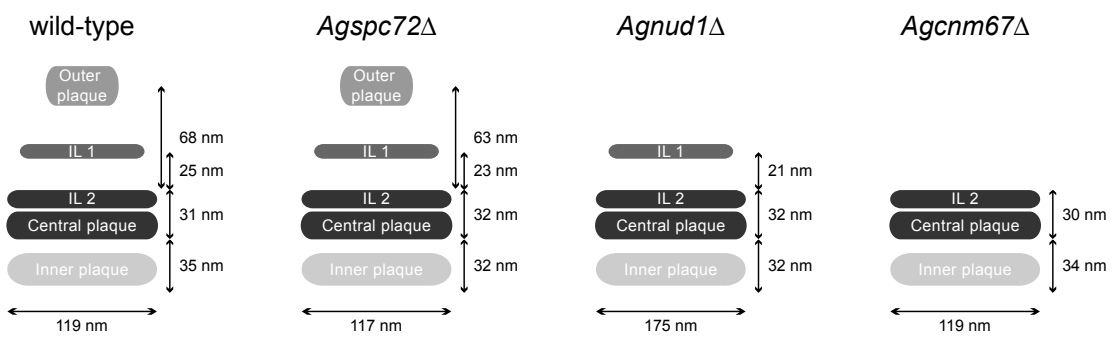

Figure 11. Comparison of *A. gosspyii* wild-type and mutant SPB structure and cytoplasmic microtubule nucleation based on EM analysis.
(A) Quantitation of cytoplasmic microtubules that emerge per SPB and of the observed layers are shown for wild-type and mutant SPBs. (B) Schematics of wild-type and mutant SPBs depicting the observed layers and averaged distances between the layers. Detailed numbers are shown in Table S1 (Supplementary Material).

AgCnm67 is not only a structural component of the *A. gossypii* SPB but also may have an additional role in regulation of the mitotic division cycle.

Discussion

The overall structure of the *A. gossypii* SPB is similar as in *S. cerevisiae*, yet the phenotypes we observed in several deletion mutants of SPB components of the cytoplasmic side differ from those of budding yeast. *S. cerevisiae* s*pc72*Δ mutants form very short and unstable cytoplasmic microtubules, resulting in spindle orientation and nuclear positioning defects that, depending on the strain background, often lead to cell death (Brachat *et al.*, 1998; Chen *et al.*, 1998; Pereira *et al.*, 1999; Gruneberg *et al.*, 2000; Hoepfner *et al.*, 2002; Usui *et al.*, 2003). Even though *Agspc72*Δ mutants have defects in nuclear dynamics, cell viability is not affected. However, this is not the most perplexing phenotype we observed, rather it was the persistence of long cytoplasmic microtubules in cells lacking the cytoplasmic γ-tubulin receptor. Possibly, additional proteins tether the γ-tubulin complex to the SPB in the absence of *AgSPC72*. A leading candidate is *AgSTU2*, which encodes the *A. gossypii* XMAP215/Dis1 microtubule-associated protein. In budding yeast, Stu2 is essential and binds to the γ-tubulin complex. Interestingly *Agstu2*Δ mutants are viable and display similar defects in nuclear positioning, oscillations and bypassing as *Agspc72*Δ (Figure 12, Movie S7). A second candidate is the SPB IP γ-tubulin complex binding protein, AgSpc110, a portion of which might remain in the cytoplasm of *A. gossypii*. Interestingly, Spc110 can function in cytoplasmic microtubule nucleation if it is tethered to the *S. cerevisiae* OP (Knop and Schiebel, 1998), but it is normally targeted to the nucleus by a N-terminal nuclear localization sequence (Adams and Kilmartin, 1999). This domain is not conserved in AgSpc110 and other nuclear localization motifs were not detected (C.B. and S.L.J., unpublished observations), so how AgSpc110 enters the nucleus is unknown. Finally, *A. gossypii* contains roughly 100 NOHBY genes (no homologues in bakers yeast) (Brachat *et al.*, 2003) that might play a role in SPB functions specific to multinucleate yeast, including nucleation of different classes of cytoplasmic microtubules. A NOHBY gene may function in the absence of *AgSPC72* to tether the γ-tubulin complex to the SPB.

The deletion phenotype of *AgNUD1* was also unexpected since *nud1* mutants in *S. cerevisiae* arrest in anaphase due to the role of Nud1 in recruitment of mitotic regulatory proteins to the SPB OP (reviewed in Pereira and Schiebel, 2001; Stegmeier and Amon, 2004). Our finding that *AgNUD1* is not essential suggests that the mitotic exit network is either non-essential in *A. gossypii* or does not depend on SPB recruitment for its activation. Instead, we find that *Agnud1*Δ mutants have phenotypes similar to *nud1-2*, an allele that is defective in Nud1's non-essential functions, namely loss of the SPB OP, defects in cytoplasmic microtubules and impaired nuclear dynamics (Gruneberg *et al.*, 2000).

Upon genome duplication, *S. cerevisiae* obtained two copies of every gene. About 1 in 10 of these so called twin ORFs can still be found in current *S. cerevisiae* strains while the rest of the duplicated genes were lost during evolution. *AgCNM67* is one of these genes that has two homologs in *S. cerevisiae*: *ScCNM67* and *ScADY3*. The products of those twin ORFs exhibit highly diverged amino acid sequences (16% identity) and perform different functions (Figure 13A). So far it was not clear which functions of the *S. cerevisiae* proteins is fulfilled by the single AgCnm67. We show that even though the identity between the ScAdy3 and AgCnm67 amino acid sequences is greater than that between ScCnm67 and AgCnm67 (Figure 13A), *Agcnm67*Δ mutants lack the OP in mitotically dividing nuclei of *A. gossypii*. Moreover, AgCnm67 localizes to the nuclear periphery during all nuclear cycle stages (Figure 13B). Together, our results indicate that AgCnm67 serves the mitotic function of ScCnm67.

The SPB structures in *Agspc72*Δ, *Agnud1*Δ and *Agcnm67*Δ cells (summarized in Figure 11B)

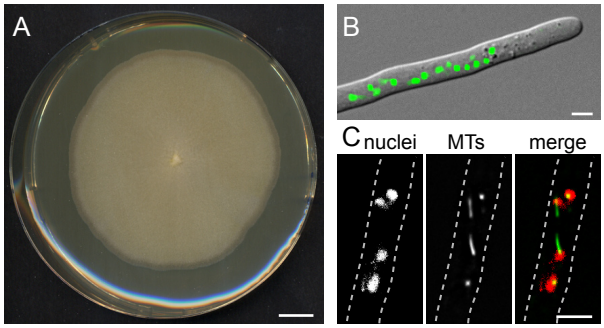

Figure 12. Stu2 is not essential in *A. gossypii*.
(A) An *Agstu2*Δ colony formed on solid full medium after 7 days of incubation at 30°C. Compared to wild-type, no difference in radial colony growth can be observed. Bar, 1 cm. (B) Overlay of a DIC image and AgH4-GFP signal showing an *Agstu2*Δ hyphae with nuclei clustering distal to the hyphal tip. Bar, 5 µm. (C) Immuno-fluorescence staining of an *Agstu2*Δ mutant. Only very short cytoplasmic microtubules can be detected emerging from two SPBs. The SPBs from two other nuclei do not nucleate any cytoplasmic microtubules. Bar, 5 µm.

suggest that this organelle is assembled in a stepwise fashion. By analogy to *S. cerevisiae* SPB assembly, binding of AgCnm67 to components of IL2 drives assembly of AgNud1, followed by AgSpc72 and the γ-tubulin complex to form the OP. In the absence of AgCnm67, or AgNud1, cytoplasmic microtubules are nucleated from the bridge, but this results in mild defects in nuclear dynamics. Microtubule nucleation from the half-bridge is also observed in wild-type budding yeast cells during G1 and in *cnm67*Δ mutants (Brachat *et al.*, 1998) (Pereira *et al.*, 1999). We did not find evidence for cytoplasmic microtubule nucleation from the bridge in any EM images of *A. gossypii* wild-type SPBs although differences in nuclear division or SPB duplication regulation might make this difficult to observe. Alternatively, *A. gossypii* wild-type SPBs may not need to nucleate microtubules from the bridge since they do not undergo nuclear fusion (karyogamy).

Despite the fact that the number of cytoplasmic microtubules was reduced in both *Agcnm67*Δ and *Agnud1*Δ mutants, nuclear oscillations and bypassing were largely unaffected and cells displayed only subtle defects in nuclear spacing. When contrasted to cells lacking *AgSPC72*, the effect of these deletions is mild. This suggests that anchorage of cytoplasmic microtubules to the SPB and not necessarily the number of microtubules is the critical factor that controls nuclear dynamics. The fact that the *A. gossypii* nuclear cycle most probably pauses with duplicated SPBs in the side-by-side position could provide a prolonged time frame for alternative microtubule nucleation from the bridge in cells lacking the OP. Consequently, this could account for mild influence on nuclear dynamics observed in *Agnud1*Δ and *Agcnm67*Δ mutants.

Nuclear migration into a bud once every cell cycle does not apply in *A. gossypii* hyphae, thus cytoplasmic microtubules and SPB OP components are not critical for cell viability. The multi-nucleate growth mode of *A. gossypii* has resulted in different demands on the microtubule cytoskeleton that have driven evolution of SPB components to fit its unique life-style. Through our functional analysis of *A. gossypii* SPB genes, we can better understand the adaptive properties of the cytoskeleton involved in growth and development of many eukaryotic cells.

A

	ScCnm67	**ScAdy3**
localization	IL1, OP	MP
active cell cycle stage	Mitosis	Meiosis
Function	Spacer, anchors OP to CP	Spore wall formation
S.c./A.g. Protein length (AA)	581/862	790/862
S.c./A.g. Identitity (AA)	18.2 %	22.2 %

B

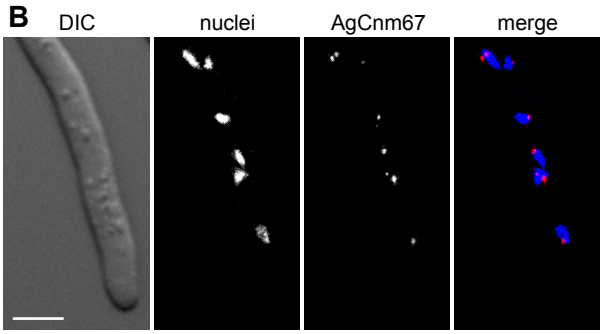

Figure 13. *AgCNM67* is the functional homolog of *ScCNM67*. (A) Summary of data about *ScCNM67* and *ScADY3*, the two homolog twin ORFs of *AgCNM67*. (B) AgCnm67-tdTomato localizes as one or two foci to the nuclear membrane. Bar 5 µm.

Acknowledgements

We thank Géraldine Käslin for the help in strain construction and Dominic Hoepfner for guidance in the early stage of this project. We are grateful to Jenny Friederichs, Teri Johnson and Fengli Guo for assistance with EM and Katie Perko for help with AutoAligner. We thank Mark Winey and Tom Giddings for advice and suggestions. This work was supported by a grant from the Swiss National Science Foundation to P.P. (No. 3100A0 – 112688). S.L.J. is supported by a March of Dimes Basil O'Connor Award and the Stowers Institute for Medical Research.

Part III

A search for a role of AgKar9 in multinucleate hyphae

Introduction

Positioning of the mitotic spindle with respect to the plane of cell division is crucial in many eukaryotes. The network that controls this process regulates whether a cell divides asymmetrically or symmetrically.

In Saccharomyces cerevisiae, the alignment of the mitotic spindle along the division axis of the cell ensures the accurate inheritance of a daughter nucleus by the bud. Two partially overlapping pathways are involved in the correct positioning of the spindle: the Kar9 - and the dynein pathway (Miller and Rose, 1998). Prior to anaphase, the old spindle pole body (SPB) is pulled toward the bud (Pereira *et al.*, 2001), thus aligning the spindle along the mother bud axis (Figure 1A). In addition to Kar9, this mechanism requires the microtubule binding protein Bim1, the type V myosin Myo2 and the kinesin Kip3 to link cytoplasmic microtubules emerging form the bud-proximal SPB with actin cables originating from the bud (Korinek *et al.*, 2000; Lee *et al.*, 2000; Yin *et al.*, 2000; Hwang *et al.*, 2003). The dynein pathway subsequently ensures nuclear migration through the bud neck (Figure 1A). This second mechanism depends the dynein/dynactin complex, Num1 and Bik1. Neither *KAR9* nor *DYN1* are essential, but deletion of either gene leads to misalignment of the spindle, resulting in spindle elongation within the mother cell and consequently binucleate mother cells (Eshel *et al.*, 1993; Li *et al.*, 1993; Miller and Rose, 1998). However, simultaneous inactivation of both pathways is lethal (Miller and Rose, 1998).

Kar9 and Dyn1 both localize asymmetrically to the bud-proximal SPB and cytoplasmic microtubules emanating form it (Liakopoulos *et al.*, 2003; Grava *et al.*, 2006). This asymmetry ensures that only one SPB is pulled towards the bud neck in metaphase and through the bud neck during anaphase.

The asymmetric localization of Kar9 is regulated by Cdc28. Phosporylation of Kar9 on serines 197 and 496 prevents Kar9 loading/maintenance on the mother bound pole (Liakopoulos *et al.*, 2003; Maekawa and Schiebel, 2004; Miller *et al.*, 2006; Moore *et al.*, 2006).

Spindle alignment is a crucial process in asymmetrically dividing cells. But what about cells where mitosis is uncoupled from cell division? *Ashbya gossypii* is a filamentous fungus that carries many nuclei in a continuous cytoplasm (Figure 1B). The asynchronous nuclear divisions trigger neither cell division nor septum formation. Therefore, asymmetric control of spindle positioning does not seem to be compulsory. Moreover, metaphase spindles do not pre-orient along the polarity axis, they rather seem to be randomly oriented prior to elongation (Figure 1B) ((Philippsen *et al.*, 2005) and Part II of this thesis). Nevertheless, the *Ashbya* genome project revealed orthologs for all known *S. cerevisiae* proteins involved in spindle positioning (Dietrich *et al.*, 2004).

To investigate whether asymmetric forces also play a role in spindle positioning in *A. gossypii*, we first tagged AgKar9 with fluorophores and examined its cellular localization.

We also characterized the *Agkar9*Δ mutant and studied the effect of the deletion on nuclear dynamics and distribution. Deletion of *AgDYN1*, the *A. gossypii* ortholog of the key player of the

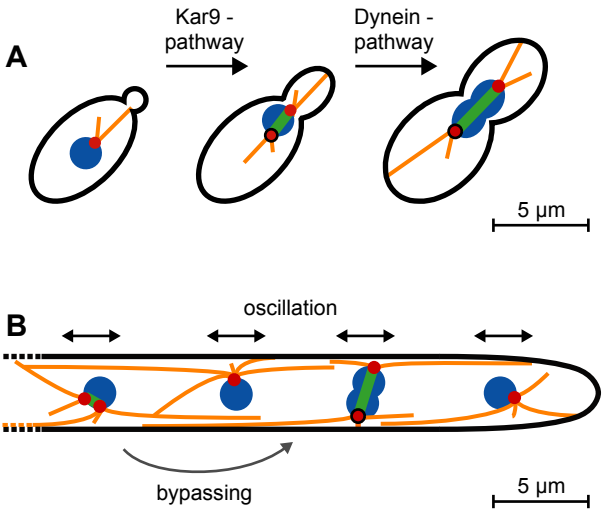

Figure 1. Nuclear dynamics in (A) *S. cerevisiae* and (B) *A. gossypii*.
Nuclei are blue, cytoplasmic microtubules orange, the mitotic spindle green and SPBs red. Additionally the new SPB is marked with a circle. (A) In *S. cerevisiae*, the nucleus is pulled toward the budding site in a Kar9 dependent manner prior to mitosis. During anaphase the dynein pathway pulls the SPB through the bud neck. (B) Hypha of *A. gossypii* contain multiple nuclei in different nuclear cycle stages. Nuclear dynamics include oscillations, bypassing and division of nuclei. However metaphase spindles do not pre-orient along the polarity axis prior to elongation.

Table 1. *A. gossypii* strains used in this study

Strain	Genotype[a]	Reference
Δ*l*Δ*t* (referred to as wild-type)	*Agleu2*Δ *Agthr4*Δ	(1)
AgH4-GFP	*Agade2::AgADE2-AgHHF1-GFP Agleu2*Δ *Agthr4*Δ	(2)
*Agkar9*Δ	*Agkar9*Δ*::GEN3 Agleu2*Δ *Agthr4*Δ	this study
*AgH4-GFP kar9*Δ	*Agade2::AgADE2-AgHHF1-GFP Agleu2*Δ *Agthr4*Δ *Agkar9*Δ*::GEN3*	this study
AgKAR9-GFP	*AgKAR9-GFP-GEN3 Agleu2*Δ *Agthr4*Δ	this study
AgH4-GFP KAR9-RFP	*Agade2::AgADE2-AgHHF1-GFP Agleu2*Δ *Agthr4*Δ *AgKAR9-RedStar2-GEN3*	this study
AgKAR9-GFP_L2	*AgKAR9-GFP-LEU2 Agleu2*Δ *Agthr4*Δ	this study
AgKAR9-GFP TUB4-RFP	*AgKAR9-GFP-LEU2 Agleu2*Δ *Agthr4*Δ *(pAgTUB4-RedStar2-GEN3)*	this study

[a] A plasmid name in parentheses indicates a replicating plasmid which is maintained under selection pressure. With the exception of those plasmidic strains all analyzed mycelia were homokaryotic (all nuclei have the same genotype). This was obtained either by sporulating homokaryotic strains or by applying selective pressure during germination.

(1) (Altmann-Johl and Philippsen, 1996)
(2) (Helfer and Gladfelter, 2006)

Table 2. Olignucleotide primers used in this study

Name	Sequence[a] 5' – 3'
AgKAR9_NS1	CTTATAAAGGGCAGCTGATAGCACAGTTGTAATATTTCAAAGTGAGGTGGTGTCCGCA GCaaaacgacggccagtgaattcg
AgKAR9_F1	TCGAGATTGAAGGAGCCCACGCCGTTGGCGGATCTTCTTAACTTATCAaaaacgacggcc agtgaattcg
AgKAR9_F2a	GCATGTATTGGATACTACATTACCAAGCAAACCAAATATATCATTAAGTACGTCATATCA catgattacgccaagcttgc
AgKAR9_A1	agacatgccccagattcacccg
AgKAR9_A2	ctgtggcatgtgcgacaccacc
AgKAR9_A3	actgcgccgaacgaggacgacg
AgKAR9_A4	ggtggtgggacatgacagccgc
GEN3_A2	cggctcgatcatctctgcctcc
GEN3_A3	ccatcctatggaactgcctcgg
Green2.2	tgtagttcccgtcatctttg
Red II	tcggtagatggttcccaaccc

[a] Lowercase letters are regions of homology to the cassette containing a selectable marker.

second pathway involved in spindle positioning in budding yeast, has lead to severe defects in nuclear migration with formation of nuclear clusters at the hyphal tip (Alberti-Segui *et al.*, 2001). This raises the question whether deletion of *AgKAR9* affects nuclear migration in a similar way.

Material and Methods

A. gossypii media and growth conditions

A. gossypii media and culturing are described in (Ayad-Durieux *et al.*, 2000; Wendland *et al.*, 2000) and strains are listed in Table 1. To depolymerize microtubules, nocodazole (Sigma-Aldrich) was added to a final concentration of 15 µg/ml to liquid cultures. After 1 hour of incubation at 30°C under shaking conditions, cells were washed 2 times in AFM and transferred to a time-lapse slide for *in vivo* imaging. To disrupt the actin cytoskeleton, latrunculin A was added to a final concentration of 200 µM to liquid cultures. Cells were incubated for 10 minutes and subsequently analyzed by *in vivo* fluorescence microscopy. To control the disruption of the actin and microtubule cytoskeleton, samples were taken at all steps and immediately fixed for rhodamine phalloidin or immuno-fluorescence staining with anti-α-tubulin, respectively.

Plasmid and strain construction

Plasmids generated and used in this study are described below. All DNA manipulations were carried out according to (Sambrook, 2001) with *E. coli* DH5αF' as host (Hanahan, 1983). PCR amplification was performed using standard methods with Taq DNA polymerase, Expand High Fidelity PCR system or the Expand Long Template PCR system (Roche Diagnostics). Oligonucleotides are listed in Table 2 and were synthesized by Microsynth. For recombination of plasmids and PCR products, both were co-transformed into the budding yeast host strain DY3 (*MATα his3Δ200 trp1Δ63 leu2Δ1 ura3-52Δ*) according to (Gietz *et al.*, 1995). Plasmids were isolated from yeast using the High Pure Plasmid Purification Kit (Roche Diagnostics) with a modified protocol as previously described (Schmitz *et al.*, 2006).

To generate *AgKAR9-GFP*, pAGT141 (kindly provided by Andreas Kaufmann) was used as a template to amplify GFP-GEN3 using oligonucleotides AgKAR9_F1/F2a. The resulting PCR product was co-transformed into yeast cells with pAG17650 to generate pCB11. pCB11 was digested with BsrBI and PPuMI to tag the endogenous *AgKAR9* with GFP in the wild-type strain.

To generate *AgH4-GFP KAR9-RFP*, pAGT144 (kindly provided by Andreas Kaufmann) was used as a template to amplify RedStar2-GEN3 with oligonucleotides AgKAR9_F1/F2a. The resulting PCR product was co-transformed into yeast cells with pAG17650 to generate pCB12. pCB12 was digested with BsrBI and XmnI to tag the endogenous *AgKAR9* with RFP in the *AgH4-GFP* strain.

pAGT121 (kindly provided by Andreas Kaufmann) was used as a template to amplify GFP-LEU2 using oligonucleotides AgKAR9_F1/F2a. The resulting PCR product was co-transformed into yeast cells with pAG17650 to generate pCB13. pCB13 was digested with PvuI, DraIII and AseI to tag the endogenous *AgKAR9* with GFP in the wild-type strain resulting in *AgKAR9-GFP_L2*. To construct *AgKarAR9-GFP TUB4-RFP*, *AgKAR9-GFP_L2* was transformed with the plasmid pTub4-RFP (kindly provided by Sandrine Grava). This strain was always grown under selective conditions with 200 µg/ml G418 (ForMedium, England) to maintain the plasmid.

The *AgKAR9*-deletion mutants were made using the PCR-based one-step gene targeting approach with heterologous selection markers (Wendland *et al.*, 2000). The deletion cassettes were amplified from a plasmid containing the *GEN3* cassette (Wendland *et al.*, 2000) that mediates resistance to G418, using the AgKAR9_NS1/F2a oligonucleotide pair. Correct integration of the deletion cassettes was verified with oligonucleotide primer pairs AgKAR9_A1/Gen2_A2 (N-terminus) and AgKAR9_A4/Gen2_A3 (C-terminus).

Fluorescence microscopy and image processing

Actin (rhodamine phalloidin), DNA (Hoechst) and immuno-fluorescence stainings were performed as previously described (Ayad-Durieux *et al.*, 2000; Gladfelter *et al.*, 2006). Rat anti-α-tubulin (YOL1/34, Serotec, UK) was used at a 1:25 dilution and Alexa Fluor 568 goat-anti-rat IgG (Molecular Probes, USA) at a 1:200 dilution.

An Axioplan2 microscope equipped with the objectives Plan-Apochromat 100x/1.40 NA Oil DIC and Plan-Apochromat 63x/1.40 NA Oil DIC (Carl Zeiss AG, Feldbach, Switzerland) and appropriate filters (Zeiss and Chroma Technology, Brattleboro, VT) was used for microscopy. The light source for fluorescence microscopy was either a 75 W XBO lamp (OSRAM GmbH, Augsburg, Germany), controlled by a MAC2000 shutter and filter wheel system (Ludl Electronics, Hawthorne, NY) or a Polychrome V monochromator (TILL Photonics GmbH, Gräfelfing, Germany). Images were acquired at room temperature using a cooled charge-coupled device camera CoolSNAP HQ (Photometrics, Tucson, AZ) with MetaMorph 6.2r5 software (Molecular Devices Corp., Downingtown,

PA). Out-of-focus shading references were used for DIC image acquisitions. For time-lapse image acquisition, a glass slide was covered with 1 ml of *A. gossypii* minimal medium containing 1% agarose. Once the medium had solidified, either small pieces of mature mycelium from the border of three-day-old *A. gossypii* colonies or young mycelia cultured in liquid medium were spotted onto the slides. 70 µl of liquid minimal medium was added to mycelium before cells were covered with a coverslip and incubated for at least 1 hour before image acquisition. For still images, multiple planes with a distance between 0.3 and 1 µm in the Z-axis were taken.

Image processing was performed with MetaMorph 6.2r5 software. Z-stacks were deconvolved with Nearest Neighbor and compressed by maximum or average projection with Stack Arithmetic. Brightness and contrast were adjusted using Scale Image. Images were colored and overlaid by using Overlay Images and exported from MetaMorph as 8-bit grayscale or RGB TIFF files. Z-Stacks were converted to QuickTime H.264 movies with QuickTime Player Pro (Apple Inc., Cupertino, CA).

Bioinformatic analysis

The protein alignment was performed with sequences retrieved from the *Ashbya* Genome Database (AGD, http://agd.vital-it.ch/) (Gattiker *et al.*, 2007) and the *Saccharomyces* Genome Database (SGD, http://www.yeastgenome.org/) using the EMBOSS Pairwise Alignment Algorithms (Blosum62 Matrix, gap open 10, gap extend 0.5).

Results

Kar9 has a syntenic homolog in *A. gossypii*

Genome analysis revealed one syntenic homolog for *ScKAR9* in *A. gossypii*: *ACR023W*, termed *AgKAR9* (Dietrich et al., 2004). The identity between the two protein sequences is only 22.7% and AgKar9 is considerably longer than ScKar9 (769 AA in *A. gossypii* versus 644 AA in *S. cerevisiae*). This is mainly due to a 158 AA long, unaligned stretch at the C-terminus of AgKar9 (Figure S1, Supplementary Material). However, the two serines (located at position 197 and 496) that are required for the asymmetric localization of Kar9 in *S. cerevisiae* (Liakopoulos *et al.*, 2003; Maekawa and Schiebel, 2004; Moore *et al.*, 2006; Moore and Miller, 2007) are conserved between the two organisms (position 186 and 462 in *A. gossypii*) (Figure S1, Supplementary Material).

In vivo localization of AgKar9

To localize Kar9 *in vivo*, AgKAR9 was fused to GFP and RFP. Kar9-GFP was visible along the entire hyphae as faint filamentous structures and bright foci (Figure 2A and Movie S1). Kar9-RFP localized in a similar manner, even though the filaments were often better visible (Figure 2, B and C; Movies S2 – S4). One fraction of AgKar9-XFP foci were predominantly observed near the cortex where they moved forward (Figure 2A, 38 – 56 sec) as well as backward (Figure 2A, 144 – 164 sec and Figure 2B) with similar velocities for both directions (7 – 21 µm/min). An accumulation of AgKar9 could frequently be observed in the tip region and in many of the analyzed hyphae 1-2 filaments extended to the tip region (Figure 2, B and C; Movies S1 – S4). Co-labeling of nuclei with AgH4-GFP revealed that the filaments seemed to emerge form the nuclear periphery (Figure 2, B and C).

AgKar9 localization depends on microtubules

To investigate whether AgKar9 localization depends on either actin or microtubules, AgKar9-GFP and H4-GFP Kar9-RFP cells were treated with latrunculin A or nocodazole to disrupt the actin- or microtubule cytoskeleton, respectively. After 10 min of incubation with latrunculin A, hyphae showed swelling of the hyphal tip that is typically observed after disruption of the actin cytoskeleton in *A. gossypii* (Knechtle *et al.*, 2006; Kohli *et al.*, 2008) (Figure 3A). However, neither AgKar9-GFP nor AgKar9-RFP localization was affected (Figure 3A). On the other hand, AgKar9 of nocodazole-treated cells could only be seen as bright foci in the hypha (Kar9-GFP) or dots and ring-like structures around nuclei (Kar9-RFP) (Figure 3B). The tip localization and filaments could no longer be detected after the disruption of the microtubule cytoskeleton.

AgKar9 localizes symmetrically to SPBs

One of the main questions we addressed was whether AgKar9 localizes asymmetrically to SPBs as in *S. cerevisiae* (Liakopoulos *et al.*, 2003). In cells treated with nocodazole we could sometimes observe two foci at the nuclear periphery (Figure 4A). If one would assume that those foci represent

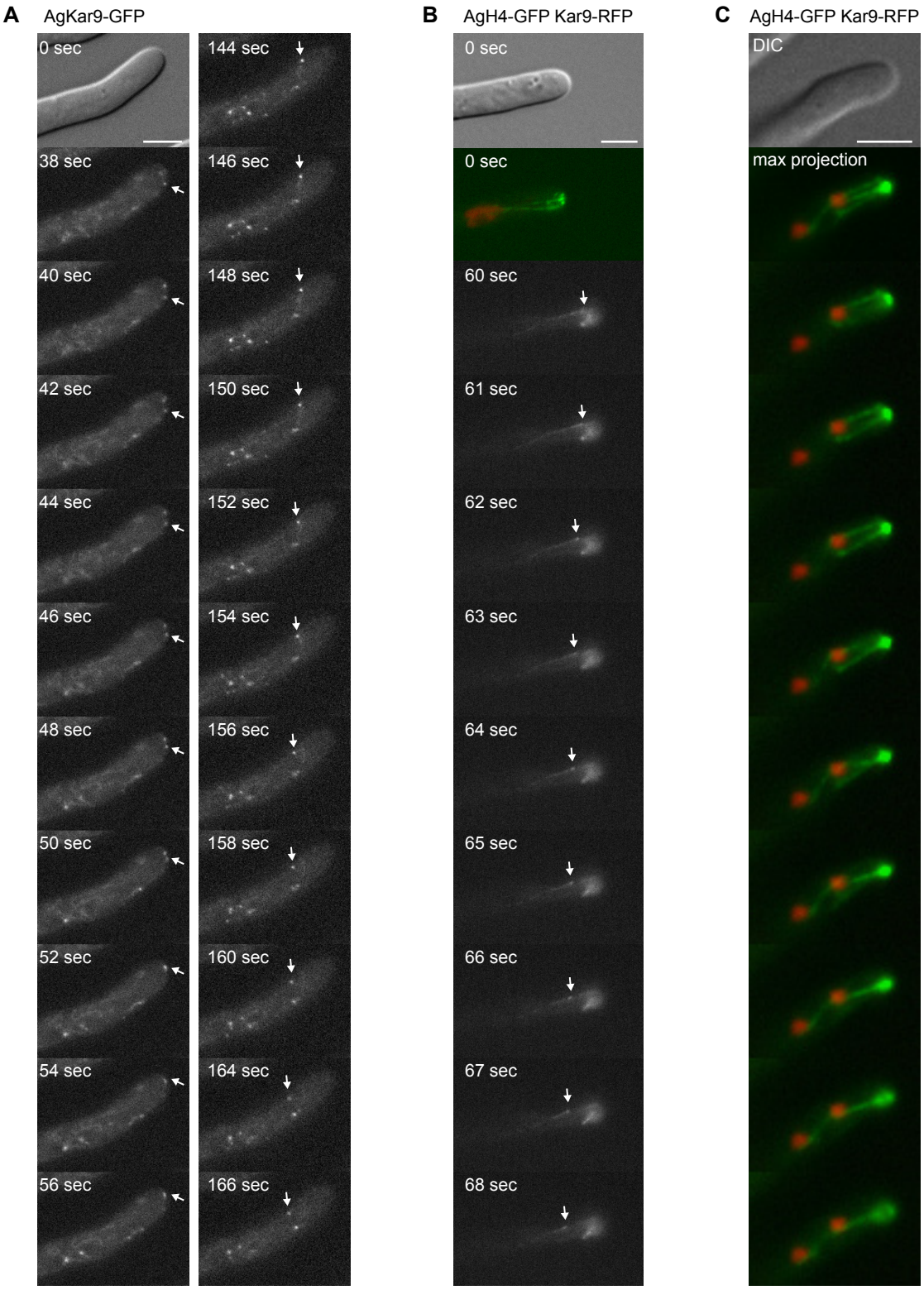

Figure 2. AgKar9 localization.
(A) A DIC image and representative frames of Movie S1 of a hypha expressing AgKar9-GFP are shown. Bright foci and faint filaments can be observed. Two examples of foci moving towards the tip (38 – 56 sec) and in the opposite direction (114 – 164 sec) are marked with arrows. (B) The dynamic localization of AgKar9 was visualized in a hypha expressing AgH4-GFP and AgKar9-RFP. A DIC, one RFP/GFP overlay image and representative frames of Movie S3 are shown. A cortically located filament with a more intensely fluorescent end seems to move away form the tip (arrows). Additionally, an accumulation of AgKar9 can be observed in the tip region. RFP images were acquired every second. Bar 5µm. (C) Z-stack through a hypha expressing AgH4-GFP (red) and AgKar9-RFP (green). A DIC, a maximum projection image and nine single planes of a Z-stack (Movie S4) through a hypha are shown. In addition to the strong fluorescence at the tip, Kar9-decorated filaments can be observed. They seem to emanate from the tip region and the periphery of the nuclei. Z-distance 0.3 µm. Bar, 5 µm.

duplicated SPBs, this would imply that AgKar9 might strictly localizes in a symmetric manner. To test this hypothesis we constructed a strain expressing AgTub4-RFP in addition to AgKar9-GFP. AgKar9 foci co-localized with all analyzed SPBs (n = 80) (Figure 4B, upper panel). This was also true when two AgTub4 signals were in very close proximity of each other, most likely representing duplicated SPBs (Figure 4B, upper panel, marked by an asterisk). In this Figure, AgKar9 filaments emanating from both of those presumably duplicated SPBs are also observable.

Since SPB localization of AgKar9 becomes more prominent after incubation with nocodazole, we also analyzed cells after treatment with that drug. As in untreated cells, AgKar9-GFP localized to all observed SPBs (n > 100) (Figure 4B, lower panel). In maximum projection images, the size of the Kar9-GFP dots of two adjacent SPBs sometimes seems unequal, suggesting a possible partial asymmetry. By visual inspection of single planes of

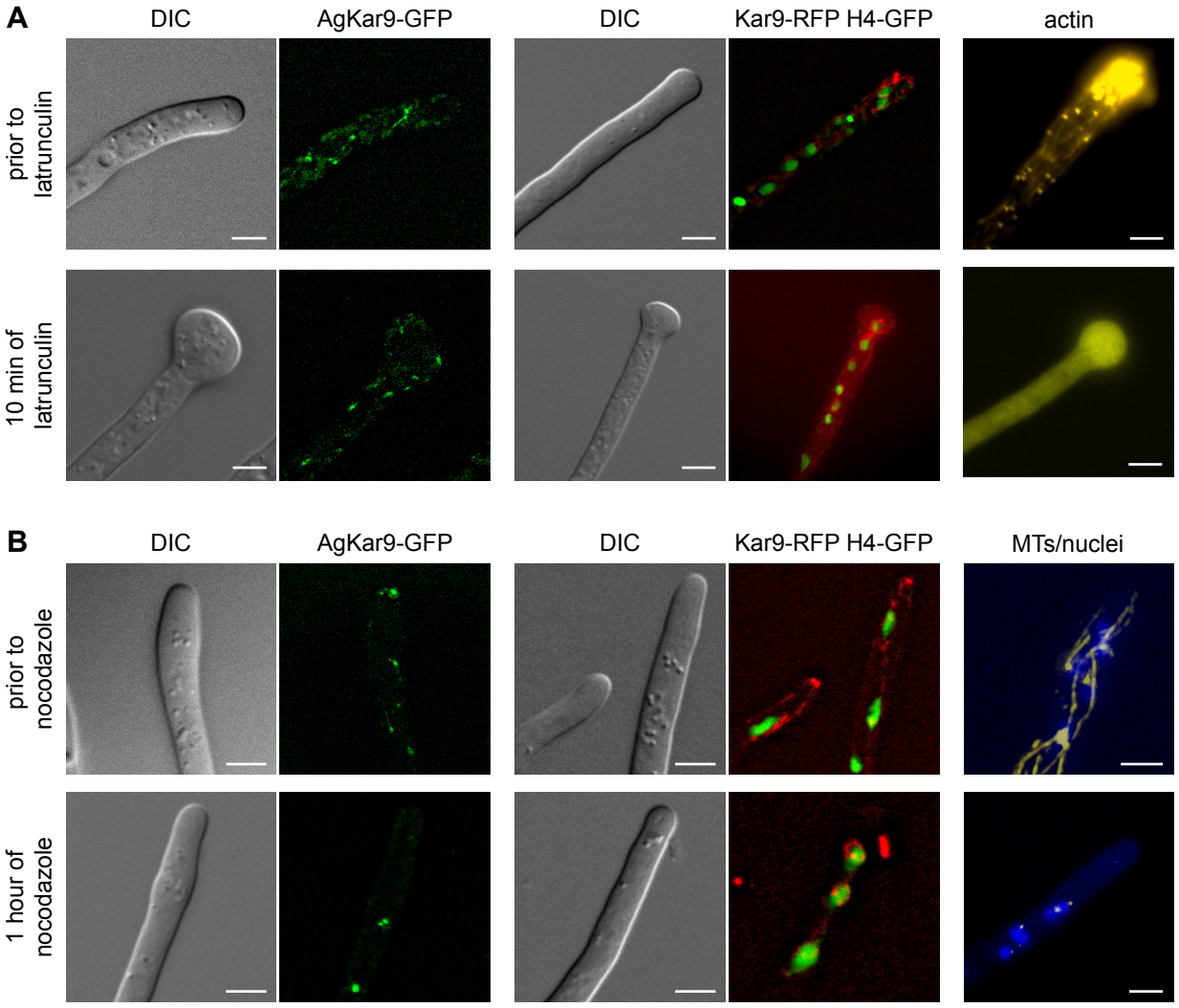

Figure 3. AgKar9 localization depends on an intact microtubule cytoskeleton.
(A) AgKar9-GFP and AgH4-GFP Kar9-GFP cells were treated with latrunculin A to disrupt the actin cytoskeleton. Hyphae were examined *in vivo* directly before and after 10 minutes of incubation with latrunculin A. AgKar9 localizes as bright foci and filaments before and after the drug treatment. In addition, samples were fixed and stained with rhodamine phalloidin. Untreated hyphae show a normal actin cytoskeleton with actin filaments and polarized actin patches. 10 minutes after addition of latrunculin, the tip of the hyphae is swollen and the actin cytoskeleton has disassembled. (B) AgKar9-GFP and AgH4-GFP Kar9-GFP cells were treated with 15 µg/ml nocodazole to disrupt the microtubule cytoskeleton. Hyphae were examined *in vivo* directly before and after 1 hour of incubation with nocodazole. Before the drug treatment, AgKar9 localizes to the tip region and as foci and filaments within the hyphae. After treatment with nocodazole, AgKar9 can only be observed as bright foci (AgKar9-GFP) or foci and ring-like structures around nuclei (AgH4-GFP Kar9-GFP). As a control for microtubule disassembly, samples were fixed and stained with Hoechst and anti-α-tubulin antibodies to label nuclei and microtubules respectively. Untreated hyphae show a normal microtubule cytoskeleton with long and short cytoplasmic microtubules. 1 hour after addition of nocodazole, only SPB foci at the nuclear periphery are detectable with anti-α-tubulin antibodies.

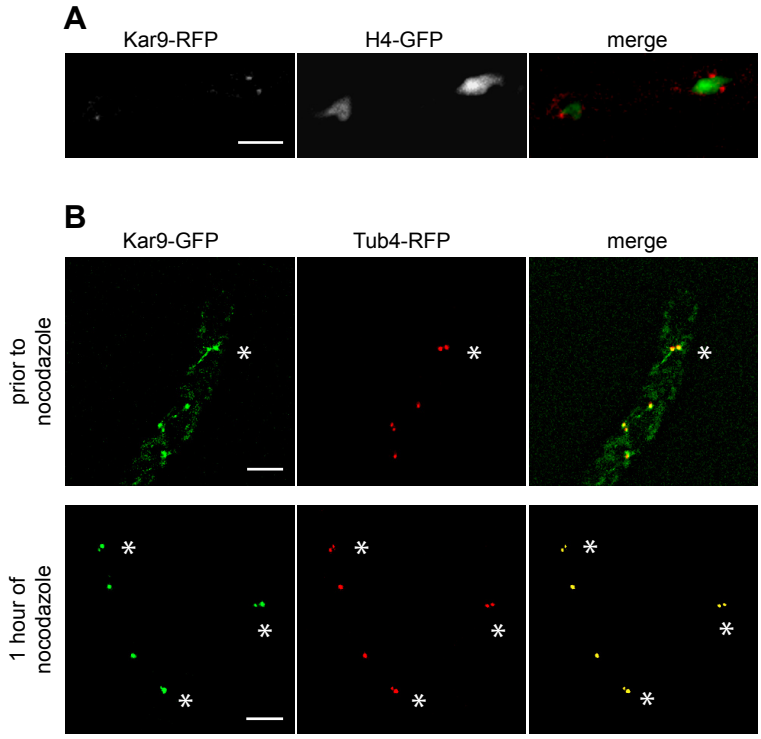

Figure 4. AgKar9 localizes symmetrically to SPBs.
(A) AgKar9-GFP Tub4-RFP cells were treated for 1 hour with nocodazole. AgKar9 localizes as one or two dots to the nuclear periphery. (B) AgKar9-GFP foci co-localize with AgTub4-RFP in untreated (upper panel) as well as in nocodazole treated (lower panel) cells. The asterisks marks presumably duplicated SPBs. AgKar9 always localizes to both of these SPBs and in untreated cells SPB associated filaments can be observed emanating from either SPB.

Z-stacks through hyphae we could not confirm an unequal distribution between Kar9-GFP signals of adjacent SPBs. Thus, the observed difference may be due to the fact that the position of the SPBs is not parallel to the focal plane.

Nuclear dynamics are only slightly affected in *Agkar9*Δ strains

Deletion of *AgKAR9* did neither affect radial colony growth speed (Figure 5A) nor the normal pattern of mycelial development (Figure 5B) (Ayad-Durieux *et al.*, 2000; Knechtle *et al.*, 2003). Staining of the actin cytoskeleton did not reveal any obvious defects in *Agkar9*Δ hyphae. Actin cables as well as actin rings and polarized actin patches could be detected (Figure 5C). We also could not observe a decrease in sporulation efficiency of the mutant strains.

To investigate the effect of the *AgKAR9* deletion on nuclear distribution we deleted *Agkar9*Δ in an AgH4-GFP labeled strain and analyzed the distance between neighboring nuclei (Figure 5, D and E). The average distance was increased from 5.5 ± 0.3 µm in wild-type to 6.4 ± 0.3 µm (n > 100), leading to a decreased nuclear density. Surprisingly though, the distance between the tip and the most apical nucleus was the same in the deletion mutant as in wild-type (8.1 ± 0.4 µm). To address the question whether AgKar9 might function in nuclear dynamics of *A. gossypii*, we analyzed movies of H4-GFP-labeled wild-type and *Agkar9*Δ strains (see Movie S5). Hyphae of both strains grew with similar speeds of approximately 0.8 µm/min. In total 48 *Agkar9*Δ nuclei and 54 wild-type nuclei were observed over a time of 10 minutes. During this time, 15 of the 48 *Agkar9*Δ nuclei underwent a bypassing event, compared to 14 out of 56 wild-type nuclei. Thus the bypassing-frequency of *AgKAR9*-deletion mutants was increased to 31% compared to 25% in wild-type. On the other hand, oscillations of *Agkar9*Δ nuclei were not affected to a measurable degree (Movie S5).

Discussion

Coordination of spindle positioning with cell division is crucial in asymmetrically dividing cells. Here, we analyzed the *A. gossypii* ortholog of Kar9, a protein required for the establishment of spindle asymmetry in *S. cerevisiae*, in the context of a continuous cytoplasm where nuclear division is not linked to cell division.

The bright foci we detected with AgKar9-GFP labeled strains most likely correspond to SPBs as they co-localized with AgTub4-RFP. A second fraction of very motile but less bright dots could be observed to move along the cortex. In

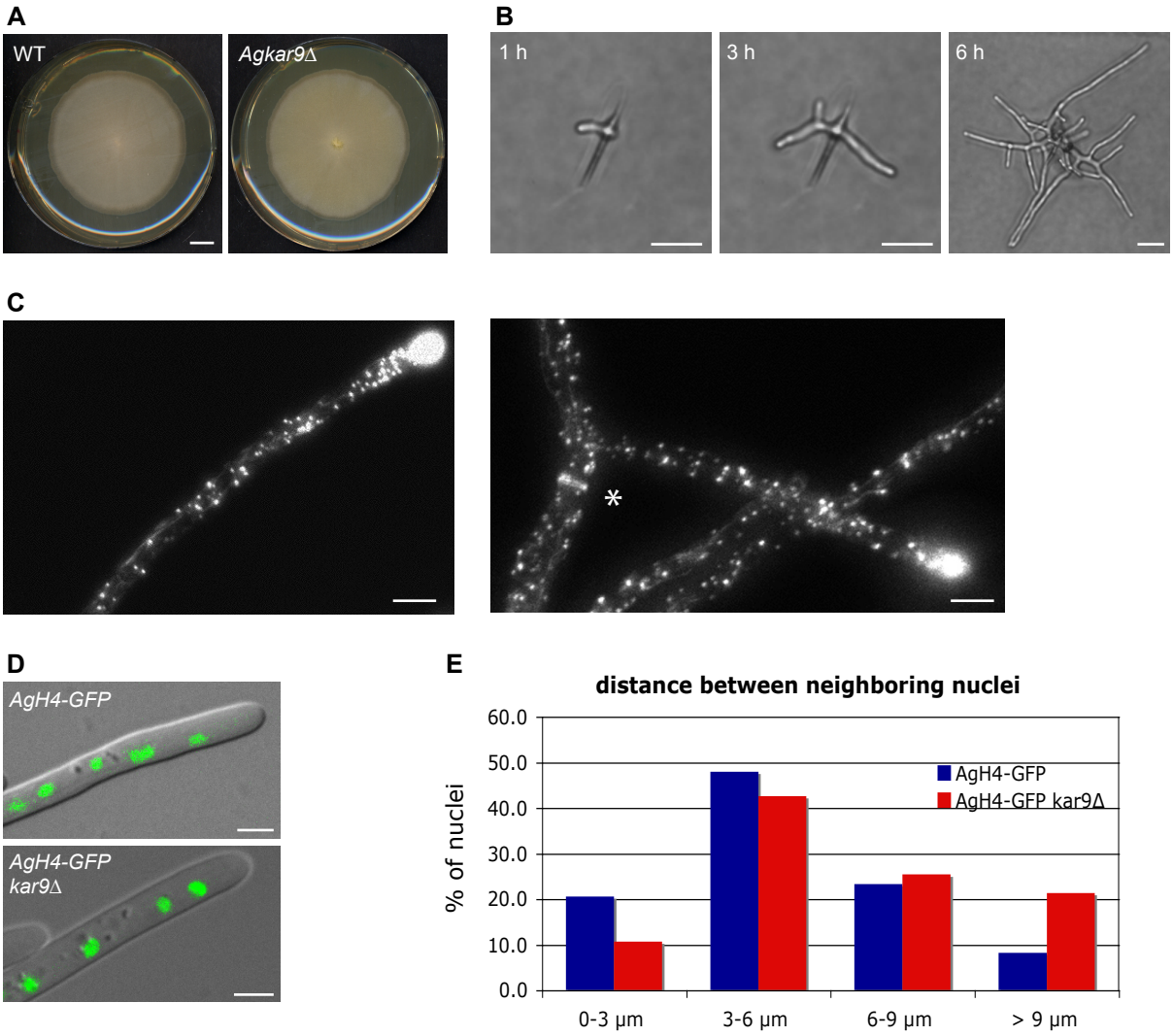

Figure 5. AgKar9 is not essential.
(A) Radial growth of wild-type and *Agkar9*Δ on solid full medium after seven days of incubation at 30°C. Bar, 1 cm. (B) Representative images from a time-lapse movie showing a developing *Agkar9*Δ mycelium. Growth speed as well as growth pattern are similar as in wild-type. Bars, 20 µm. (C) Rhodamine phalloidin staining of *Agkar9*Δ hyphae. An actin ring (asterisk), actin patches polarized at hyphal tips and actin cables can be observed. Bars, 5 µm. (D) Overlays of DIC images and AgH4-GFP signals from wild-type and *Agkar9*Δ hyphae showing the nuclear distribution. Bars, 5 µm. (E) The distance between neighboring nuclei was measured in *AgH4-GFP* and *AgH4-GFP kar9*Δ strains (n > 100).

AgH4-GFP Kar9-RFP strains, these dots were often associated with the end of faintly labeled filaments that emerged from the nuclear periphery. Thus, those dots probably represent the plus ends of cytoplasmic microtubules. We therefore propose that AgKar9 localizes to SPBs and along cytoplasmic microtubules, predominantly at their plus end. This could explain the accumulation of fluorescent Kar9 signal in the tip region, as we already have shown by *in vivo* imaging of GFP-AgTub1 that the tip region is frequently contacted by several microtubules (Part I of this thesis). Interestingly, the velocity of the movements of these presumptive microtubule plus ends was approximately 10 times greater than that observed for cytoplasmic microtubule shrinking and growing rates in *S. cerevisiae* (Carminati and Stearns, 1997). One possible explanation for this effect could be that *A. gossypii* has only one gene coding for α-tubulin (*AgTUB1*) while *S. cerevisiae* has two (*TUB1* and *TUB3*). Microtubules in *S. cerevisiae* containing only one of the two α-tubulin isoforms exhibit altered microtubule shrinking and catastrophe rates (Bode *et al.*, 2003), suggesting that the ratio of α-tubulin variants is important for the regulation microtubule dynamics.

In contrast to *S. cerevisiae*, where Kar9 distributes asymmetrically to the bud-directed SPB and cytoplasmic microtubules emanating from it during metaphase, we could not detect any

measurable asymmetry in AgKar9 localization. The two phosphorylation sites that are required for the asymmetric loading of Kar9 onto cytoplasmic microtubules in *S. cerevisiae* are present in *A. gossypii*. However, since the region containing S496/S462 (*S. cerevisiae*/*A. gossypii*) is not very well conserved, it may have lost its function as a target of Cdc28 in *A. gossypii*. AgBfa1, AgBub2 and AgDyn1, the *A. gossypii* homologs of three other components that localize asymmetrically in *S. cerevisiae* could also be observed on both SPBs of mitotic nuclei (Sandrine Grave, personal communication). The lack of asymmetric localization of components involved spindle positioning could explain why metaphase spindles are randomly oriented in *A. gossypii* hyphae.

Analysis of *AgKAR9*-deletion mutants did not reveal any striking phenotypes. The observed increase in the nuclear bypassing frequency might be due to altered microtubule dynamics in *Agkar9*Δ cells. This seems plausible assuming that AgKar9 localizes to the plus end of cytoplasmic microtubules and given the fact that microtubule plus end binding proteins are known to be involved in microtubule dynamics (Carvalho *et al.*, 2003). We also observed a slight increase in the inter-nuclear distances. However, compared to the dramatic nuclear migration defects of the *Agdyn1*Δ mutant (Alberti-Segui *et al.*, 2001), these effects were mild.

Together, our data suggest that asymmetric spindle orientation is not critical in *A. gossypii* and thus AgKar9 function has adapted to a life-style lacking cell division during evolution. However, in future, more detailed measurements of parameters typically involved in nuclear dynamics of *A. gossypii* may reveal more subtle defects in nuclear behavior of the *Agkar9*Δ mutant and help to gain further insight into the function of Kar9 in a non-dividing cell.

Acknowledgements

Acknowledgements

I am very grateful to Peter Philippsen, for giving me the opportunity to do my PhD in his laboratory. He let me many liberties but offered help, suggestions and advice (and chocolate) whenever it was needed. I especially appreciate his enormous support during the last weeks.

Special thanks also to Sue Jaspersen to welcome me in her group at the Stowers Institute for Medical Research in Kansas City, USA. She was a wonderful mentor and the EM I could perform in her laboratory was a crucial part for my PhD. Rhonda Trimble did a great job in EM preparation and always tried to fulfill my never-ending wishes and demands. Thanks to all the Jaspersen-girls and Gerton-boys the stays in Kansas City were a great experience for me, not only form the scientific point of view.

It is also a pleasure to work in the Philippsen group and I would like to thank all present and former members for help, inspiration, tips, tricks, and the good times we spent together. Special thanks to Kumiko Masai for ending my lonely life in 5014, to Michael Köhli for being the best imaginable dancing partner and to Andreas Kaufmann for finding answers to countless questions and a solution for almost every problem.

Special thanks to Nicole, Corinne, Marco, Isabella, Kerstin, Ivi, Michi and Andi for being wonderful friends in good and less good times.

I would like to thank Reto Birrer for many years of support. It was mostly due to his encouragement that I started that PhD at all.

Finally I want to thank my family for supporting me during all those PhD years. My grandma Ida Lang shared her flat with me for a long time and the wise advise and encouragement of my aunt Regula Perret was always very important to me.

References

References

Adams, I.R., and Kilmartin, J.V. (1999). Localization of core spindle pole body (SPB) components during SPB duplication in Saccharomyces cerevisiae. J Cell Biol *145*, 809-823.

Aist, J.R., and Williams, P.H. (1972). Ultrastructure and time course of mitosis in the fungus Fusarium oxysporum. J Cell Biol *55*, 368-389.

Alberti-Segui, C., Dietrich, F., Altmann-Johl, R., Hoepfner, D., and Philippsen, P. (2001). Cytoplasmic dynein is required to oppose the force that moves nuclei towards the hyphal tip in the filamentous ascomycete Ashbya gossypii. J Cell Sci *114*, 975-986.

Altmann-Johl, R., and Philippsen, P. (1996). AgTHR4, a new selection marker for transformation of the filamentous fungus Ashbya gossypii, maps in a four-gene cluster that is conserved between A. gossypii and Saccharomyces cerevisiae. Mol Gen Genet *250*, 69-80.

Ashby, S.F., and Nowell, W. (1926). The fungi of Stigmatomycosis. Annals of Botany *os-40*, 69-84.
Ayad-Durieux, Y., Knechtle, P., Goff, S., Dietrich, F., and Philippsen, P. (2000). A PAK-like protein kinase is required for maturation of young hyphae and septation in the filamentous ascomycete Ashbya gossypii. J Cell Sci *113 Pt 24*, 4563-4575.

Batra, L.R. (1973). Nematosporaceae (Hemiascomycetidae): Taxonomy, pathogenicity, distribution, and vector relations. USDA Technical Bulletin *1469*, 1-71.

Bode, C.J., Gupta, M.L., Suprenant, K.A., and Himes, R.H. (2003). The two alpha-tubulin isotypes in budding yeast have opposing effects on microtubule dynamics in vitro. EMBO reports *4*, 94-99.

Brachat, A., Kilmartin, J.V., Wach, A., and Philippsen, P. (1998). Saccharomyces cerevisiae cells with defective spindle pole body outer plaques accomplish nuclear migration via half-bridge-organized microtubules. Mol Biol Cell *9*, 977-991.

Brachat, S., Dietrich, F.S., Voegeli, S., Zhang, Z., Stuart, L., Lerch, A., Gates, K., Gaffney, T., and Philippsen, P. (2003). Reinvestigation of the Saccharomyces cerevisiae genome annotation by comparison to the genome of a related fungus: Ashbya gossypii. Genome biology *4*, R45.

Bullitt, E., Rout, M.P., Kilmartin, J.V., and Akey, C.W. (1997). The yeast spindle pole body is assembled around a central crystal of Spc42p. Cell *89*, 1077-1086.

Byers, B., and Goetsch, L. (1974). Duplication of spindle plaques and integration of the yeast cell cycle. Cold Spring Harbor symposia on quantitative biology *38*, 123-131.

Byers, B., and Goetsch, L. (1975a). Behavior of spindles and spindle plaques in the cell cycle and conjugation of Saccharomyces cerevisiae. Journal of bacteriology *124*, 511-523.

Byers, B., and Goetsch, L. (1975b). Electron microscopic observations on the meiotic karyotype of diploid and tetraploid Saccharomyces cerevisiae. Proceedings of the National Academy of Sciences of the United States of America *72*, 5056-5060.

Byers, B., Shriver, K., and Goetsch, L. (1978). The role of spindle pole bodies and modified microtubule ends in the initiation of microtubule assembly in Saccharomyces cerevisiae. J Cell Sci *30*, 331-352.

Carminati, J.L., and Stearns, T. (1997). Microtubules orient the mitotic spindle in yeast through dynein-dependent interactions with the cell cortex. J Cell Biol *138*, 629-641.

Carvalho, P., Tirnauer, J.S., and Pellman, D. (2003). Surfing on microtubule ends. Trends in cell biology *13*, 229-237.

Chen, X.P., Yin, H., and Huffaker, T.C. (1998). The yeast spindle pole body component Spc72p interacts with Stu2p and is required for proper microtubule assembly. J Cell Biol *141*, 1169-1179.

Czymmek, K.J., Bourett, T.M., Shao, Y., DeZwaan, T.M., Sweigard, J.A., and Howard, R.J. (2005). Live-cell imaging of tubulin in the filamentous fungus Magnaporthe grisea treated with anti-microtubule and anti-microfilament agents. Protoplasma *225*, 23-32.

Dietrich, F.S., Voegeli, S., Brachat, S., Lerch, A., Gates, K., Steiner, S., Mohr, C., Pohlmann, R., Luedi, P., Choi, S., Wing, R.A., Flavier, A., Gaffney, T.D., and Philippsen, P. (2004). The Ashbya gossypii genome as a tool for mapping the ancient Saccharomyces cerevisiae genome. Science *304*, 304-307.

Ding, R., West, R.R., Morphew, D.M., Oakley, B.R., and McIntosh, J.R. (1997). The spindle pole body of Schizosaccharomyces pombe enters and leaves the nuclear envelope as the cell cycle proceeds. Mol Biol Cell *8*, 1461-1479.

Donaldson, A.D., and Kilmartin, J.V. (1996). Spc42p: a phosphorylated component of the S. cerevisiae spindle pole body (SPD) with an essential function during SPB duplication. J Cell Biol *132*, 887-901.

Elliott, S., Knop, M., Schlenstedt, G., and Schiebel, E. (1999). Spc29p is a component of the Spc110p subcomplex and is essential for spindle pole body duplication. Proceedings of the National Academy of Sciences of the United States of America *96*, 6205-6210.

Eshel, D., Urrestarazu, L.A., Vissers, S., Jauniaux, J.C., van Vliet-Reedijk, J.C., Planta, R.J., and Gibbons, I.R. (1993). Cytoplasmic dynein is required for normal nuclear segregation in yeast. Proceedings of the National Academy of Sciences of the United States of America *90*, 11172-11176.

Gattiker, A., Rischatsch, R., Demougin, P., Voegeli, S., Dietrich, F.S., Philippsen, P., and Primig, M. (2007). Ashbya Genome Database 3.0: a cross-species genome and transcriptome browser for yeast biologists. BMC genomics *8*, 9.

Gietz, R.D., Schiestl, R.H., Willems, A.R., and Woods, R.A. (1995). Studies on the transformation of intact yeast cells by the LiAc/SS-DNA/PEG procedure. Yeast (Chichester, England) *11*, 355-360.

Gladfelter, A.S., Hungerbuehler, A.K., and Philippsen, P. (2006). Asynchronous nuclear division cycles in multinucleated cells. J Cell Biol *172*, 347-362.

Grava, S., Schaerer, F., Faty, M., Philippsen, P., and Barral, Y. (2006). Asymmetric recruitment of dynein to spindle poles and microtubules promotes proper spindle orientation in yeast. Developmental cell *10*, 425-439.

Gruneberg, U., Campbell, K., Simpson, C., Grindlay, J., and Schiebel, E. (2000). Nud1p links astral microtubule organization and the control of exit from mitosis. Embo J *19*, 6475-6488.

Hanahan, D. (1983). Studies on transformation of Escherichia coli with plasmids. Journal of molecular biology *166*, 557-580.

Harper, R.A. (1895). Beitrag zur Kenntniss der Kerntheilung und Sporenbildung im Ascus. . Ber Dtsch Bot Ges, 67.

Harper, R.A. (1905). Sexual reproduction and the organization of the nucleus in certain mildews. Carnegie Institute of Washington Publication *No. 37*.

Heitz, M.J., Petersen, J., Valovin, S., and Hagan, I.M. (2001). MTOC formation during mitotic exit in fission yeast. J Cell Sci *114*, 4521-4532.

Hoepfner, D., Brachat, A., and Philippsen, P. (2000). Time-lapse video microscopy analysis reveals astral microtubule detachment in the yeast spindle pole mutant cnm67. Mol Biol Cell *11*, 1197-1211.

Hoepfner, D., Schaerer, F., Brachat, A., Wach, A., and Philippsen, P. (2002). Reorientation of mispositioned spindles in short astral microtubule mutant spc72Delta is dependent on spindle pole body outer plaque and Kar3 motor protein. Mol Biol Cell *13*, 1366-1380.

Horio, T., and Oakley, B.R. (2005). The role of microtubules in rapid hyphal tip growth of Aspergillus nidulans. Mol Biol Cell *16*, 918-926.

Horio, T., Uzawa, S., Jung, M.K., Oakley, B.R., Tanaka, K., and Yanagida, M. (1991). The fission yeast gamma-tubulin is essential for mitosis and is localized at microtubule organizing centers. J Cell Sci *99 (Pt 4)*, 693-700.

Hwang, E., Kusch, J., Barral, Y., and Huffaker, T.C. (2003). Spindle orientation in Saccharomyces cerevisiae depends on the transport of microtubule ends along polarized actin cables. J Cell Biol *161*, 483-488.

Jaspersen, S.L., Giddings, T.H., Jr., and Winey, M. (2002). Mps3p is a novel component of the yeast spindle pole body that interacts with the yeast centrin homologue Cdc31p. J Cell Biol *159*, 945-956.

Jaspersen, S.L., and Winey, M. (2004). The budding yeast spindle pole body: structure, duplication, and function. Annu Rev Cell Dev Biol *20*, 1-28.

Joglekar, A.P., Bouck, D., Finley, K., Liu, X., Wan, Y., Berman, J., He, X., Salmon, E.D., and Bloom, K.S. (2008). Molecular architecture of the kinetochore-microtubule attachment site is conserved between point and regional centromeres. J Cell Biol *181*, 587-594.

Kaufmann, A., and Philippsen, P. (2008). Of bars and rings: Hof1-dependent cytokinesis in multiseptated hyphae of Ashbya gossypii. Molecular and cellular biology.

Kilmartin, J.V. (2003). Sfi1p has conserved centrin-binding sites and an essential function in budding yeast spindle pole body duplication. J Cell Biol *162*, 1211-1221.

Knechtle, P. (2002). AgSPA2 and AgBOI control landmarks of filamentous growth in the filamentous ascomycete Ashbya gossypii. Ph.D. thesis. Biozentrum, Universität Basel, Basel, Switzerland., 69 pp.

Knechtle, P., Dietrich, F., and Philippsen, P. (2003). Maximal polar growth potential depends on the polarisome component AgSpa2 in the filamentous fungus Ashbya gossypii. Mol Biol Cell *14*, 4140-4154.

Knechtle, P., Wendland, J., and Philippsen, P. (2006). The SH3/PH domain protein AgBoi1/2 collaborates with the Rho-type GTPase AgRho3 to prevent nonpolar growth at hyphal tips of Ashbya gossypii. Eukaryotic cell *5*, 1635-1647.

Knop, M., Pereira, G., Geissler, S., Grein, K., and Schiebel, E. (1997). The spindle pole body component Spc97p interacts with the gamma-tubulin of Saccharomyces cerevisiae and functions in microtubule organization and spindle pole body duplication. Embo J *16*, 1550-1564.

Knop, M., and Schiebel, E. (1998). Receptors determine the cellular localization of a gamma-tubulin complex and thereby the site of microtubule formation. Embo J *17*, 3952-3967.

Kohli, M., Galati, V., Boudier, K., Roberson, R.W., and Philippsen, P. (2008). Growth-speed-correlated localization of exocyst and polarisome components in growth zones of Ashbya gossypii hyphal tips. J Cell Sci *121*, 3878-3889.

Konzack, S., Rischitor, P.E., Enke, C., and Fischer, R. (2005). The role of the kinesin motor KipA in microtubule organization and polarized growth of Aspergillus nidulans. Mol Biol Cell *16*, 497-506.

Korinek, W.S., Copeland, M.J., Chaudhuri, A., and Chant, J. (2000). Molecular linkage underlying microtubule orientation toward cortical sites in yeast. Science *287*, 2257-2259.

Lee, L., Tirnauer, J.S., Li, J., Schuyler, S.C., Liu, J.Y., and Pellman, D. (2000). Positioning of the mitotic spindle by a cortical-microtubule capture mechanism. Science *287*, 2260-2262.

Li, R., and Gundersen, G.G. (2008). Beyond polymer polarity: how the cytoskeleton builds a polarized cell. Nat Rev Mol Cell Biol *9*, 860-873.

Li, S., Sandercock, A.M., Conduit, P., Robinson, C.V., Williams, R.L., and Kilmartin, J.V. (2006). Structural role of Sfi1p-centrin filaments in budding yeast spindle pole body duplication. J Cell Biol *173*, 867-877.

Li, Y.Y., Yeh, E., Hays, T., and Bloom, K. (1993). Disruption of mitotic spindle orientation in a yeast dynein mutant. Proceedings of the National Academy of Sciences of the United States of America *90*, 10096-10100.

Liakopoulos, D., Kusch, J., Grava, S., Vogel, J., and Barral, Y. (2003). Asymmetric loading of Kar9 onto spindle poles and microtubules ensures proper spindle alignment. Cell *112*, 561-574.

Luders, J., and Stearns, T. (2007). Microtubule-organizing centres: a re-evaluation. Nat Rev Mol Cell Biol *8*, 161-167.

Maekawa, H., and Schiebel, E. (2004). Cdk1-Clb4 controls the interaction of astral microtubule plus ends with subdomains of the daughter cell cortex. Genes & development *18*, 1709-1724.

Marschall, L.G., Jeng, R.L., Mulholland, J., and Stearns, T. (1996). Analysis of Tub4p, a yeast gamma-tubulin-like protein: implications for microtubule-organizing center function. J Cell Biol *134*, 443-454.

McDonald, K. (1999). High-pressure freezing for preservation of high resolution fine structure and antigenicity for immunolabeling. Methods in molecular biology (Clifton, N.J *117*, 77-97.

Meraldi, P., McAinsh, A.D., Rheinbay, E., and Sorger, P.K. (2006). Phylogenetic and structural analysis of centromeric DNA and kinetochore proteins. Genome biology *7*, R23.

Miller, R.K., D'Silva, S., Moore, J.K., and Goodson, H.V. (2006). The CLIP-170 orthologue Bik1p and positioning the mitotic spindle in yeast. Current topics in developmental biology *76*, 49-87.

Miller, R.K., and Rose, M.D. (1998). Kar9p is a novel cortical protein required for cytoplasmic microtubule orientation in yeast. J Cell Biol *140*, 377-390.

Minke, P.F., Lee, I.H., and Plamann, M. (1999). Microscopic analysis of Neurospora ropy mutants defective in nuclear distribution. Fungal Genet Biol *28*, 55-67.

Moens, P.B., and Rapport, E. (1971). Spindles, spindle plaques, and meiosis in the yeast Saccharomyces cerevisiae (Hansen). J Cell Biol *50*, 344-361.

Moore, J.K., D'Silva, S., and Miller, R.K. (2006). The CLIP-170 homologue Bik1p promotes the phosphorylation and asymmetric localization of Kar9p. Mol Biol Cell *17*, 178-191.

Moore, J.K., and Miller, R.K. (2007). The cyclin-dependent kinase Cdc28p regulates multiple aspects of Kar9p function in yeast. Mol Biol Cell *18*, 1187-1202.

Morris, N.R. (2000). Nuclear migration. From fungi to the mammalian brain. J Cell Biol *148*, 1097-1101.

Mourino-Perez, R.R., Roberson, R.W., and Bartnicki-Garcia, S. (2006). Microtubule dynamics and organization during hyphal growth and branching in Neurospora crassa. Fungal Genet Biol *43*, 389-400.

Muller, E.G., Snydsman, B.E., Novik, I., Hailey, D.W., Gestaut, D.R., Niemann, C.A., O'Toole, E.T., Giddings, T.H., Jr., Sundin, B.A., and Davis, T.N. (2005). The organization of the core proteins of the yeast spindle pole body. Mol Biol Cell *16*, 3341-3352.

O'Toole, E.T., Winey, M., and McIntosh, J.R. (1999). High-voltage electron tomography of spindle pole bodies and early mitotic spindles in the yeast Saccharomyces cerevisiae. Mol Biol Cell *10*, 2017-2031.

Oakley, B.R., Oakley, C.E., Yoon, Y., and Jung, M.K. (1990). Gamma-tubulin is a component of the spindle pole body that is essential for microtubule function in Aspergillus nidulans. Cell *61*, 1289-1301.

Pereira, G., Grueneberg, U., Knop, M., and Schiebel, E. (1999). Interaction of the yeast gamma-tubulin complex-binding protein Spc72p with Kar1p is essential for microtubule function during karyogamy. Embo J *18*, 4180-4195.

Pereira, G., Tanaka, T.U., Nasmyth, K., and Schiebel, E. (2001). Modes of spindle pole body inheritance and segregation of the Bfa1p-Bub2p checkpoint protein complex. Embo J *20*, 6359-6370.

Philippsen, P., Kaufmann, A., and Schmitz, H.P. (2005). Homologues of yeast polarity genes control the development of multinucleated hyphae in Ashbya gossypii. Curr Opin Microbiol *8*, 370-377.

Robinow, C.F., and Marak, J. (1966). A fiber apparatus in the nucleus of the yeast cell. J Cell Biol *29*, 129-151.

Rose, M.D., and Fink, G.R. (1987). KAR1, a gene required for function of both intranuclear and extranuclear microtubules in yeast. Cell *48*, 1047-1060.

Rout, M.P., and Kilmartin, J.V. (1990). Components of the yeast spindle and spindle pole body. J Cell Biol *111*, 1913-1927.

Sambrook, J.a.D.R. (2001). Molecular Cloning: A Laboratory Manual. Cold Spring Harbor Laboratory Press.

Sawin, K.E., and Tran, P.T. (2006). Cytoplasmic microtubule organization in fission yeast. Yeast (Chichester, England) *23*, 1001-1014.

Schaerer, F., Morgan, G., Winey, M., and Philippsen, P. (2001). Cnm67p is a spacer protein of the Saccharomyces cerevisiae spindle pole body outer plaque. Mol Biol Cell *12*, 2519-2533.

Schmitz, H.P., Kaufmann, A., Kohli, M., Laissue, P.P., and Philippsen, P. (2006). From function to shape: a novel role of a formin in morphogenesis of the fungus Ashbya gossypii. Mol Biol Cell *17*, 130-145.

Sikorski, R.S., and Hieter, P. (1989). A system of shuttle vectors and yeast host strains designed for efficient manipulation of DNA in Saccharomyces cerevisiae. Genetics *122*, 19-27.

Sobel, S.G., and Snyder, M. (1995). A highly divergent gamma-tubulin gene is essential for cell growth and proper microtubule organization in Saccharomyces cerevisiae. J Cell Biol *131*, 1775-1788.

Spang, A., Geissler, S., Grein, K., and Schiebel, E. (1996). gamma-Tubulin-like Tub4p of Saccharomyces cerevisiae is associated with the spindle pole body substructures that organize microtubules and is required for mitotic spindle formation. J Cell Biol *134*, 429-441.

Stahmann, K.P., Revuelta, J.L., and Seulberger, H. (2000). Three biotechnical processes using Ashbya gossypii, Candida famata, or Bacillus subtilis compete with chemical riboflavin production. Applied microbiology and biotechnology *53*, 509-516.

Stearns, T., Evans, L., and Kirschner, M. (1991). Gamma-tubulin is a highly conserved component of the centrosome. Cell *65*, 825-836.

Steinberg, G., and Fuchs, U. (2004). The role of microtubules in cellular organization and endocytosis in the plant pathogen Ustilago maydis. J Microsc *214*, 114-123.

Steiner, S., and Philippsen, P. (1994). Sequence and promoter analysis of the highly expressed TEF gene of the filamentous fungus Ashbya gossypii. Mol Gen Genet *242*, 263-271.

Steiner, S., Wendland, J., Wright, M.C., and Philippsen, P. (1995). Homologous recombination as the main mechanism for DNA integration and cause of rearrangements in the filamentous ascomycete Ashbya gossypii. Genetics *140*, 973-987.

Straube, A., Brill, M., Oakley, B.R., Horio, T., and Steinberg, G. (2003). Microtubule organization requires cell cycle-dependent nucleation at dispersed cytoplasmic sites: polar and perinuclear microtubule organizing centers in the plant pathogen Ustilago maydis. Mol Biol Cell *14*, 642-657.

Van den Hoorn, T. (2004). In vivo visualization of microtubules, ER and vacuoles in the filamentous fungus Ashbya gossypii. Diploma Thesis. Biozentrum, Universität Basel, Basel, Switzerland.

Wach, A., Brachat, A., Alberti-Segui, C., Rebischung, C., and Philippsen, P. (1997). Heterologous HIS3 marker and GFP reporter modules for PCR-targeting in Saccharomyces cerevisiae. Yeast (Chichester, England) *13*, 1065-1075.

Wach, A., Brachat, A., Pohlmann, R., and Philippsen, P. (1994). New heterologous modules for classical or PCR-based gene disruptions in Saccharomyces cerevisiae. Yeast (Chichester, England) *10*, 1793-1808.

Wendland, J., Ayad-Durieux, Y., Knechtle, P., Rebischung, C., and Philippsen, P. (2000). PCR-based gene targeting in the filamentous fungus Ashbya gossypii. Gene *242*, 381-391.

Wiese, C., and Zheng, Y. (2006). Microtubule nucleation: gamma-tubulin and beyond. J Cell Sci *119*, 4143-4153.

Wigge, P.A., Jensen, O.N., Holmes, S., Soues, S., Mann, M., and Kilmartin, J.V. (1998). Analysis of the Saccharomyces spindle pole by matrix-assisted laser desorption/ionization (MALDI) mass spectrometry. J Cell Biol *141*, 967-977.

Winey, M., Goetsch, L., Baum, P., and Byers, B. (1991). MPS1 and MPS2: novel yeast genes defining distinct steps of spindle pole body duplication. J Cell Biol *114*, 745-754.

Winey, M., Mamay, C.L., O'Toole, E.T., Mastronarde, D.N., Giddings, T.H., Jr., McDonald, K.L., and McIntosh, J.R. (1995). Three-dimensional ultrastructural analysis of the Saccharomyces cerevisiae mitotic spindle. J Cell Biol *129*, 1601-1615.

Wright, M.C., and Philippsen, P. (1991). Replicative transformation of the filamentous fungus Ashbya gossypii with plasmids containing Saccharomyces cerevisiae ARS elements. Gene *109*, 99-105.

Yin, H., Pruyne, D., Huffaker, T.C., and Bretscher, A. (2000). Myosin V orientates the mitotic spindle in yeast. Nature *406*, 1013-1015.

Appendix

Appendix

Movie legends

Part I

Movies 8B and 8C. GFP-AgTub1 was visualized by live cell image analysis. Z-distance 0.3 µm, exposure time 1500 msec.

Part II

Movie S1. DIC (top) and AgH4-GFP maximum intensity projections (bottom) of a growing *Agtub4*Δ germling. Z-distance 0.75 µm.

Movie S2. Overlay of DIC and maximum intensity projections of AgH4-GFP signal of a wild-type hypha. Images were captured every 30 seconds. Z-distance 0.75 µm.

Movie S3. Overlay of DIC and maximum intensity projections of AgH4-GFP signal of a *Agspc72*Δ hypha. Images were captured every 30 seconds. Z-distance 0.75 µm.

Movie S4. Overlay of DIC and maximum intensity projections of AgH4-GFP signal of *Agnud1*Δ hyphae. Images were captured every 30 seconds. Z-distance 0.75 µm.

Movie S5. Overlay of DIC and maximum intensity projections of AgH4-GFP signal of *Agcnm67*Δ hyphae. Images were captured every 30 seconds. Z-distance 0.75 µm.

Movie S6. GFP-AgTub1 in *Agcnm67*Δ was visualized by live cell image analysis. Z-distance 0.3 µm, exposure time 1500 msec.

Movie S7. Overlay of DIC and maximum intensity projections of AgH4-GFP signal of a *Agstu2*Δ hypha. Images were captured every 30 seconds. Z-distance 0.75 µm.

Part III

Movie S1. Kar9-GFP. One plane of GFP signal was captured every two seconds. Bar, 5 µm.

Movie S2. AgH4-GFP Kar9-RFP. One plane of RFP signal was captured every second. Bar 5, µm.

Movie S3. AgH4-GFP Kar9-RFP. One plane of RFP signal was captured every two seconds. Bar, 5 µm.

Movie S4. Z-stack through a hypha expressing AgH4-GFP (red) and Kar9-RFP (green). Overlay images of the two fluorescent channels are shown. Z-distance 0.3 µm. Bar, 5 µm.

Movie S5. DIC (top) and AgH4-GFP maximum projection (bottom) of two *Agkar9*Δ hyphae. Z-distance 0.75 µm. Bar, 5 µm.

Supplementary material

Part I

Table S1. Dimensions of the *A. gossypii* SPB.

SPB category[b]	CP diameter[a] range (nm)	mean (nm)	SD	n
single	94-153	122.0	22.1	13
duplicated	92-147	116.8	17.4	12
side-by-side	85-158	117.2	22.0	21
total	85-158	118.5	20.6	46

SPB category[b]	IP-OP distance[a] range (nm)	mean (nm)	SD	n
single	130-178	163.7	12.6	12
duplicated	128-165	147.0	13.0	9
side-by-side	124-190	148.5	18.3	15
total	124-190	153.2	17.5	36

[a] Distances were measured in the serial section image were CP or IP/OP were most visible. In cases where a distinct IP or OP could not be distinguished, the microtubule nucleation sites were used to estimate their position.

[b] SPBs were grouped according to the number and duplication status to approximate the stage in the nuclear division cycle (see text for details).

Part II

Table S1. Dimensions[a] of *A. gossypii* wild-type and mutant SPBs.

	wild-type			***Agspc72*Δ**			***Agnud1*Δ**			***Agcnm67*Δ**		
	mean (nm)	SD	n	mean (nm)	SD	n	mean (nm)	SD	n	mean (nm)	SD	n
CP width	118.5	20.6	46	117.1	20.1	29	174.8	17.0	14	138.9	27.2	27
IP – CP	35.2	6.1	40	31.7	5.7	22	31.5	6.5	12	33.9	8.5	24
CP – IL2	31.3	3.2	41	32.2	4.4	29	31.8	3.3	14	30.1	5.6	29
IL2 – IL1	24.8	5.3	30	23.0	7.7	12	21.1	3.7	9			
IL2 – OP	67.6	9.9	28	62.8	11.1	8						

[a] Distances were measured in the serial section image were the plaques/layers were most visible. In cases where a distinct IP or OP could not be distinguished, the microtubule nucleation sites were used to estimate their position.

Part II

```
A. gossypii        1                       MIQVPNAFISPPLATTLGPGADSLEDVM     28
                                           :.::.|...|.....:|.....|:.:.:
S. cerevisiae      1 MDNDGPRSMTIGDDFQENFCERLERIHNTLHSINDCNSLNESTTSISETL     50

A. gossypii       29 LRIGNKNLSTEEIKQDLLRLVNLLQDLKVSLKGTFSRDVVVSHMPQYFDW     78
                     |         .:...||..:.:::.|| |:.|.....|:::     :.||
S. cerevisiae     51 L---------VQFYDDLENVASVIPDL-VNKKRLGKDDILL-----FMDW     85

A. gossypii       79 IQDGRGLFYPLYKCFSQIEPAMLKFLDPLEAQ-----QTSGALNRDQVAI    123
                     :...:.:.|........||......||.||.:     |.|...||.. .:
S. cerevisiae     86 LLLKKYMLYQFISDVHNIEEGFAHLLDLLEDEFSKDDQDSDKYNRFS-PM    134

A. gossypii      124 FNLIDQVSELVLSLKPLFQSVKNLFDTALEFNEIFKDHMNSLLEEIEGNM    173
                     |::|::.:::...|:|...::|.|.||:||||||.||||::|.:.|..|:
S. cerevisiae    135 FDVIEESTQIKTQLEPWLTNLKELLDTSLEFNEISKDHMDTLHKIINSNI    184

A. gossypii      174 KKCLALHQDCFASPVRHPPSFTLDQLVELISSSSNNQRLQMPTFNPLEKR    223
                     ..||.:.::.||||:||.|||||:|||:|:.:.:.....::|.|:|.|..
S. cerevisiae    185 SYCLEIQEERFASPIRHTPSFTLEQLVKLLGTHTETTEPKVPKFSPAEDI    234

A. gossypii      224 IYQDYCELENAIVPIQTSLRDVLKTRIQMFRDRDIINLNYLMRLLNHKYA    273
                     :.:.:..|:..|.||:.||.|:|..||..|..|:|.|:..|..:|..||.
S. cerevisiae    235 LSRKFLNLKKNIPPIEKSLTDILPQRIVQFGHRNITNITTLQTILQKKYE    284

A. gossypii      274 NIVEKYDHFHSELMALKAGIIDKRWNVLFTNLNMELASILTSVTRMYESL    323
                     .|::.|...:||...||..:||||||:||.|||.||..||..:    |.|
S. cerevisiae    285 LIMKDYRFMNSEFRELKVELIDKRWNILFINLNHELLYILDEI----ERL    330

A. gossypii      324 QDNPTISGDTRDTLI---QQIQQKSDTIFKTFEVIYKALDASILNPNVAE    370
                     |.....:..|:|..|   :|:::||.|:.|||.:||:||:|:|:..||.
S. cerevisiae    331 QSKLLTTKYTKDITIRLERQLERKSKTVSKTFNIIYRALEFSLLDAGVAS    380

A. gossypii      371 VTNTLADKWLVLREKVDPILPKETESDPIDVLTKRMSDMTISEPVDSKPF    420
                     .||.||.:||.::...|.||.|.:.|:.|....|:     |.:|   |..
S. cerevisiae    381 KTNELAQRWLNIKPTADKILIKSSASNKIATSKKK-----IPKP---KSL    422

A. gossypii      421 HFDRS-----------------------------------KRCSVGALLLR    436
                     .|.|.                                   |...:|..||:
S. cerevisiae    423 GFGRPNSVIGTITQDFQERVAINEGDSNKTPENSTTVALKGKKLGKALLQ    472

A. gossypii      437 KMNIKPILTSDPDEAEKPKFNRSYRSPSSADANGSPISSDYPPVPFS---    483
                     ||||||..:.:...|..|.|:  ..|||:    .|..|.|..||:|:.
S. cerevisiae    473 KMNIKPATSPNSSNAINPFFD--PESPN----KGKLILSSVPPLPYDETD    516

A. gossypii      484 ------LEPVHSKNPPVF-------KLQIGSPDQPPVVKLQNENVCTEDK    520
                           ....:.|:|..|       |:||  .:.|.:.|  |::|...:|
S. cerevisiae    517 ETTLRVSRGENEKSPDSFITSRHENKVQI--TETPLMAK--NKSVLDIEK    562
```

```
A. gossypii      521 ------KTLAPSNTATAEPIGATQMQLNPEYPCSPPPPGDPQPTSPAQN-    563
                         ::|........:.:....::..|.......||  .:.|:|...
S. cerevisiae    563 DKWNHYRSLPSRIPIYKDKVVKVTVENTPIAKVFQTPP--TKITTPNSQV    610

A. gossypii      564 ---ATRRPSDASLGYPGSHKDPQSPSAPFLSAGSSAPVSPREAPATKSPS    610
                        :|||         .:...|.:|.:..|        ||||....|:|:
S. cerevisiae    611 WVPSTRR---------RTRLRPPTPLSQLL--------SPREGRLDKTPT    643

A. gossypii      611 LSPKDCRPEFDHMEPPDFFRSGEDSYTWRRDRSRNSSVSSASAGELSGKL    660
                     ..
S. cerevisiae    644 Y*                                                  645

A. gossypii      661 LLSASPQSSQPGDFTACTTAPNEDDVSPTSLVSDDYIKQADHIKYIERIE    710

S. cerevisiae    646                                                   645

A. gossypii      711 EERFRYYANMHSRIPVMFSDLIPQPIHLSHFPRSPGTRHNYWSSRLKEPT    760

S. cerevisiae    646                                                   645

A. gossypii      761 PLADLLNLS    769

S. cerevisiae    646             645
```

Figure S1. Sequence comparison between *A. gossypii* and *S. cerevisiae* Kar9.
Serines 197 and 496 (in red) that are phosphorylated by Cdc28 in *S. cerevisiae* are conserved in *A. gossypii*.

The hidden chapter

Many hours spent in the dark resulted in some highlights

The presented examples where selected because they are particularly surprising, intriguing or just beautiful

cMTs and electron dense associates

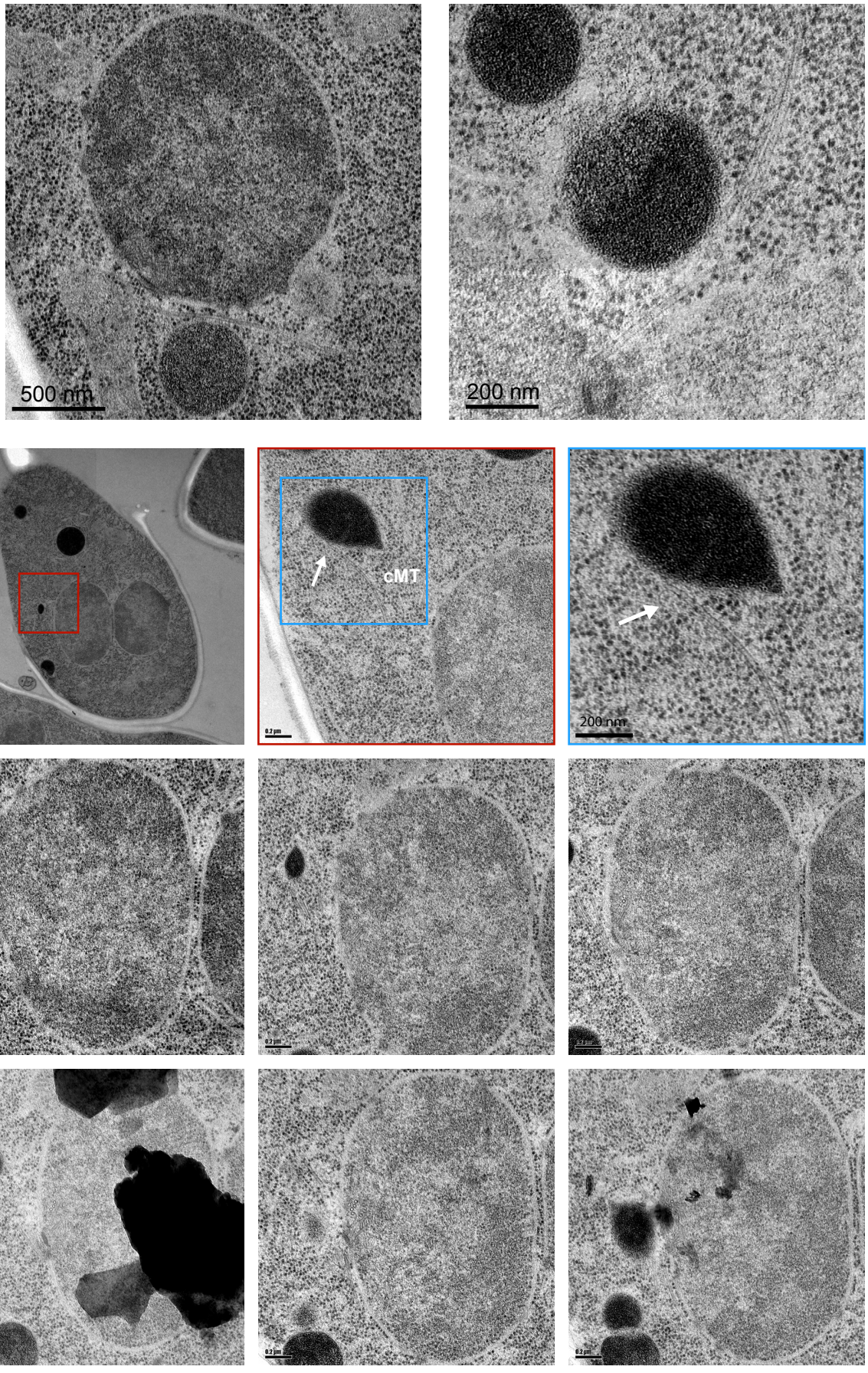

Eager to duplicate

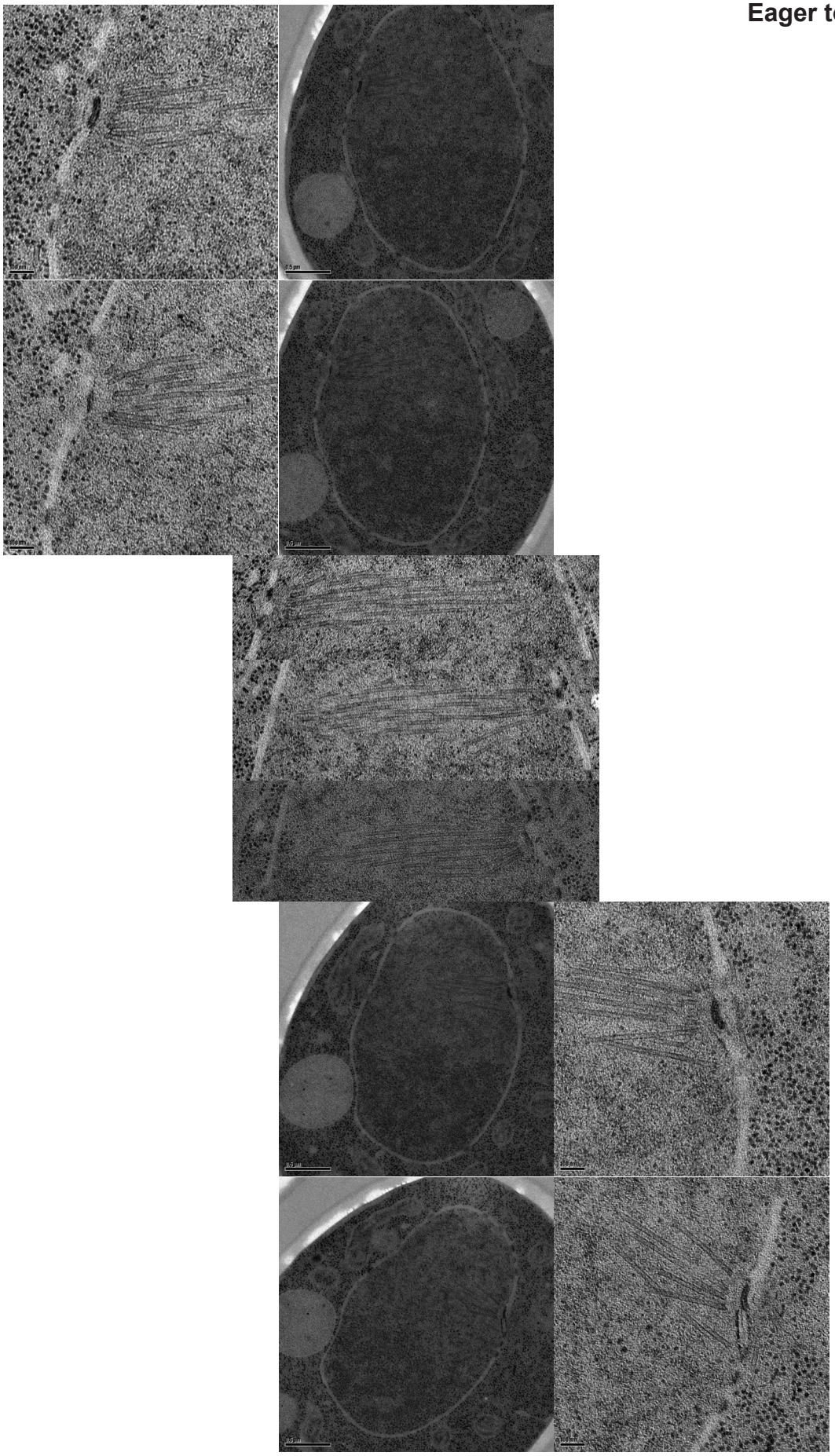

*Agcnm67*Δ spindle goes wild

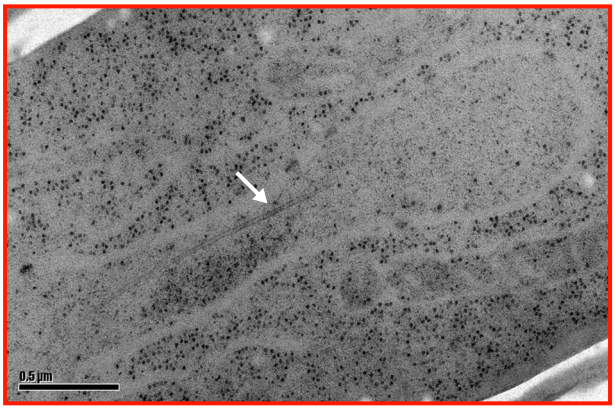

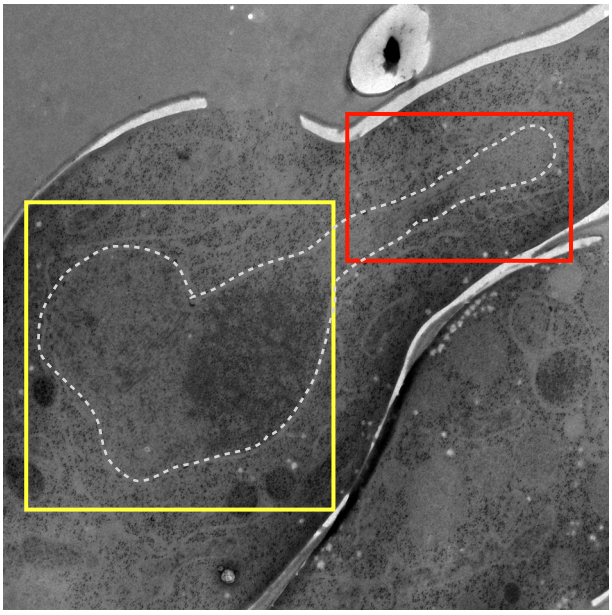

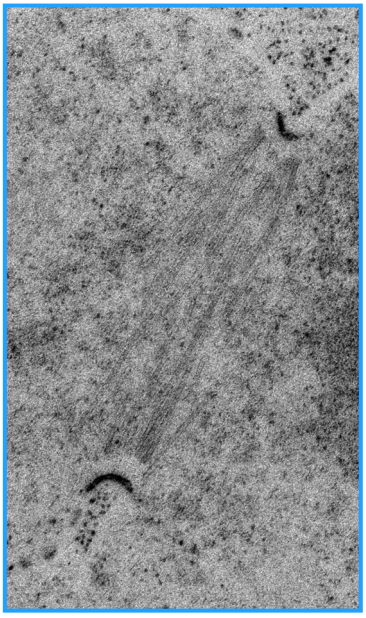

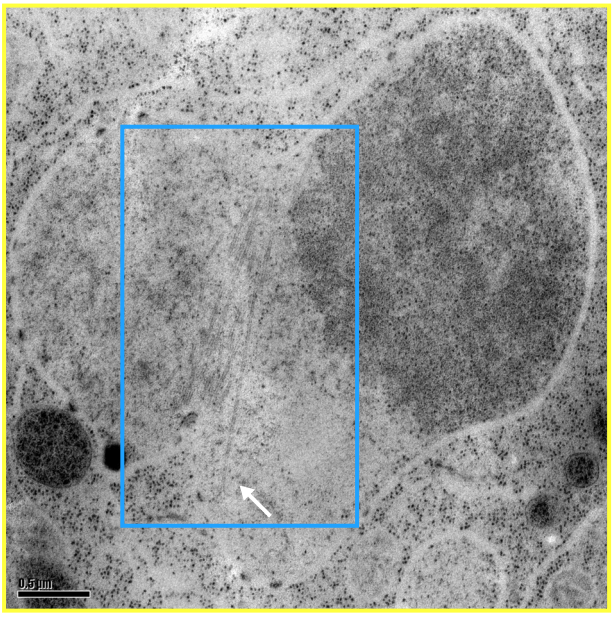

No karyogamy in *Ashbya*?

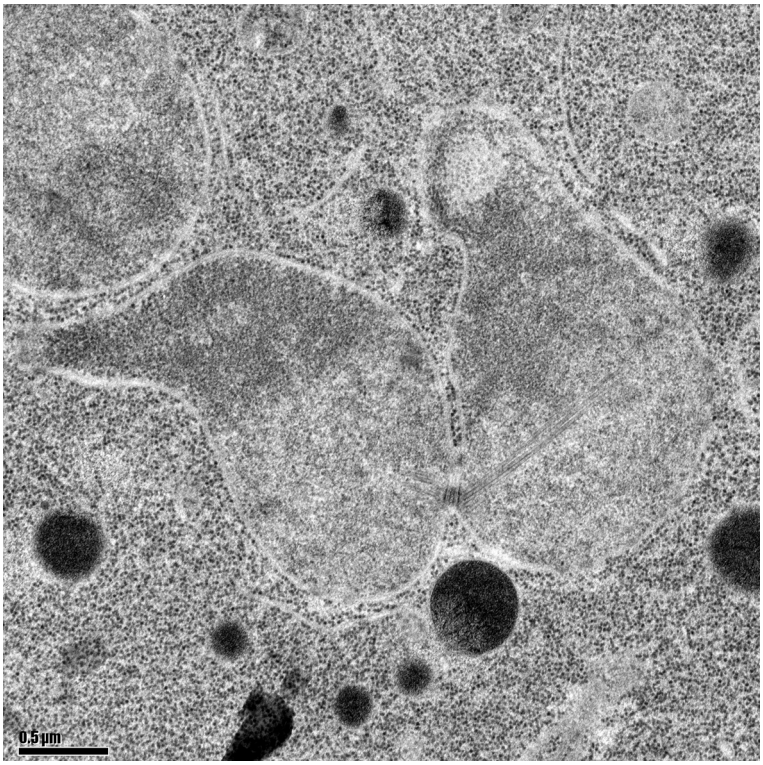

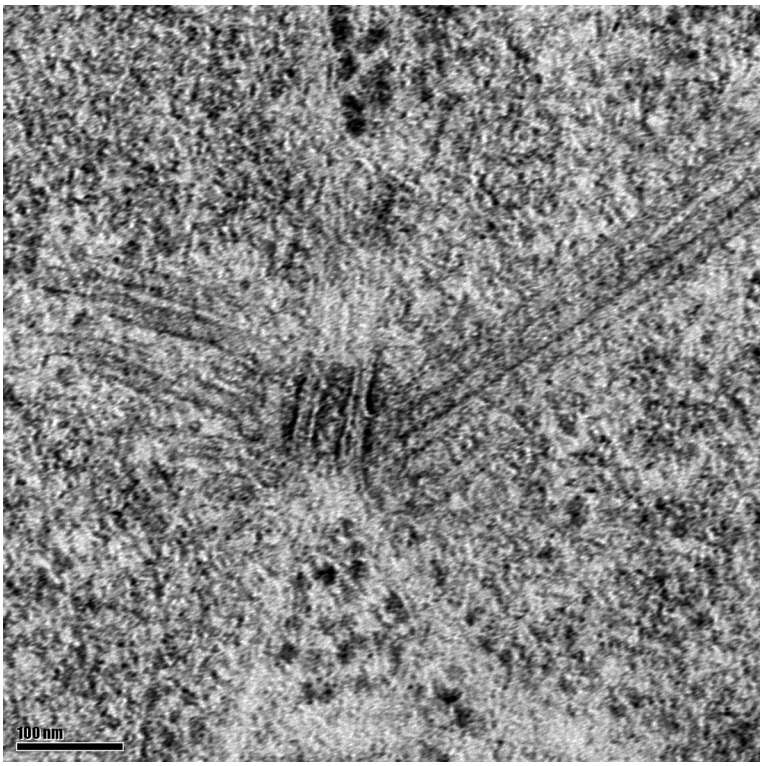

Again, no asymmetry...

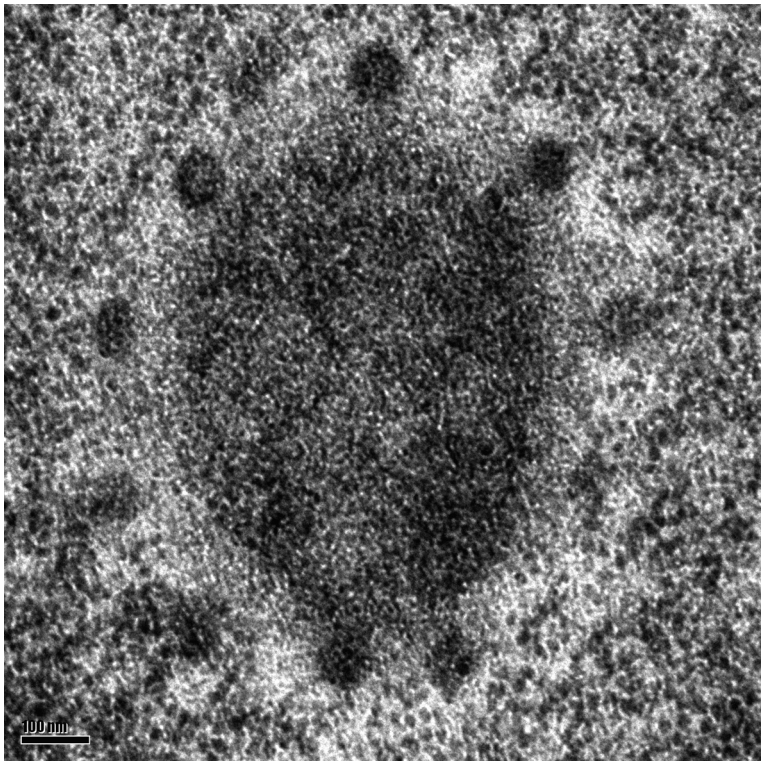

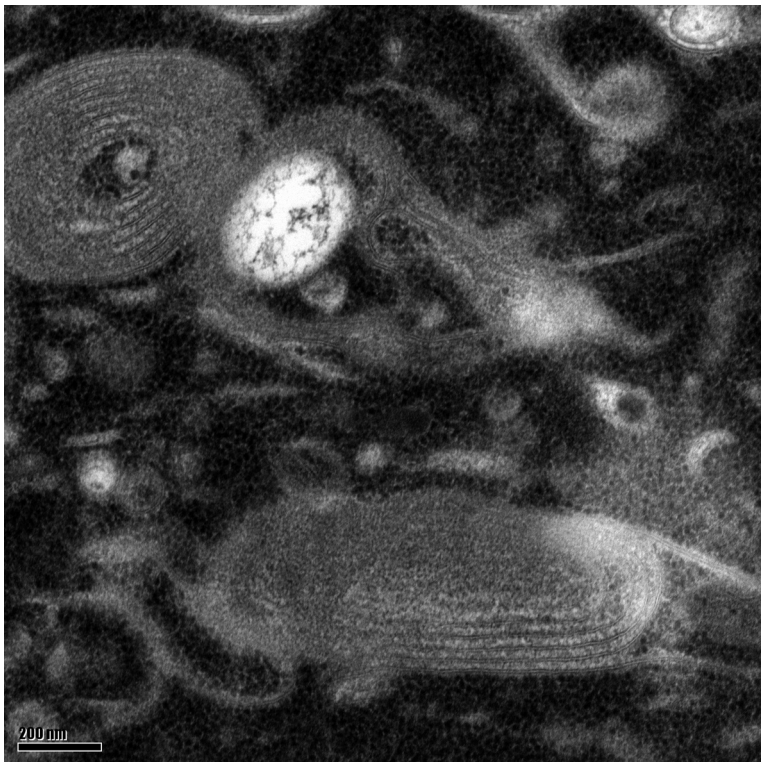

Ashbya with closed septa - and heart

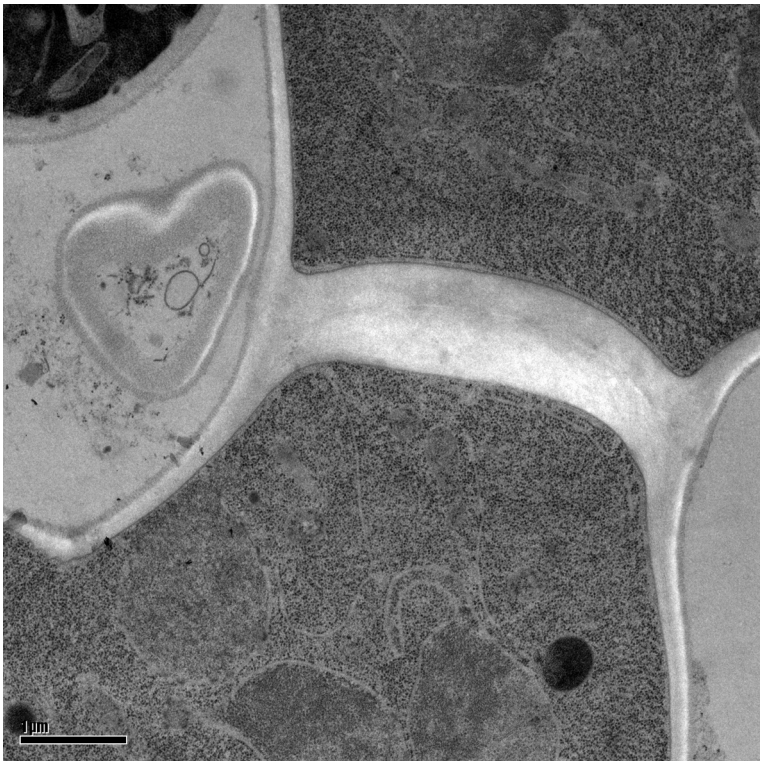

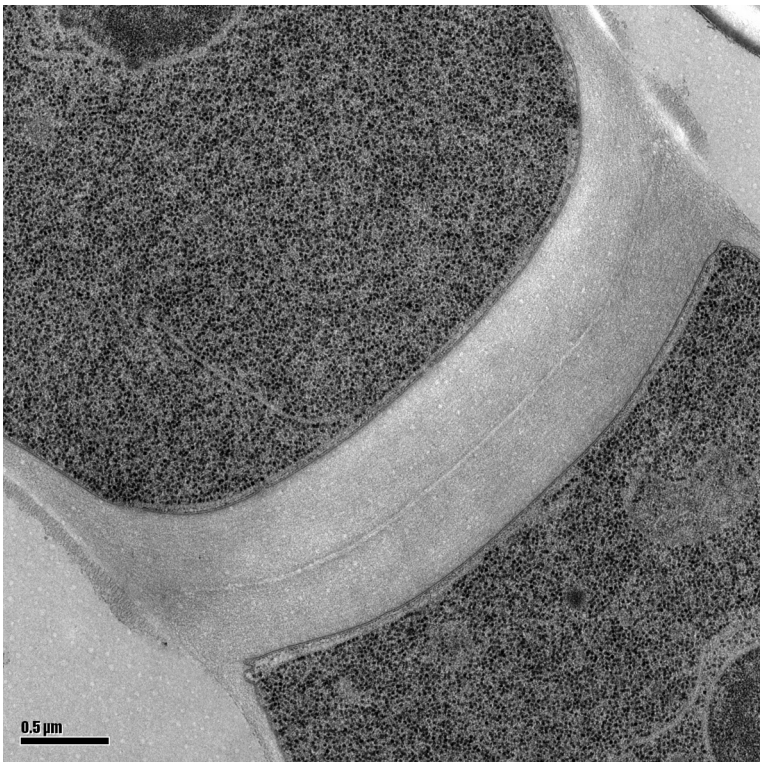

Curriculum vitae

Curriculum vitae

PERSONAL INFORMATION

Name Claudia Birrer
Address Erikastrasse 3
4057 Basel
Switzerland
Email claudia.lang@stud.unibas.ch

EDUCATION

2005 – 2009 **PhD Thesis** "The organization of the microtubule cytoskeleton and its role on nuclear dynamics in the multinucleate hyphae of *Ashbya gossypii* revealed by live cell imaging and electron microscopy"
Supervisors: Prof. Peter Philippsen, Biozentrum, University of Basel, Switzerland and Dr. Sue Jaspersen, Stowers Institute for Medical Research, Kansas City, USA

2004 – 2005 **Master of Science in Molecular Biology** "Proteins influencing nuclear dynamics in the filamentous fungus *Ashbya gossypii*"
Supervisor: Prof. Peter Philippsen, Biozentrum, University of Basel, Switzerland

2001 – 2004 **Bachelor of Science in Biology**, Major in Molecular Biology, University of Basel, Switzerland
Focus on biochemistry, biophysics, microbiology and cell biology
Elective subject: business sciences

1997 – 2000 **School for medical laboratory technicians**, Kantonsspital Luzern, Switzerland

1990 – 1997 **Matura Typus C** (mathematics)
Kantonsschule Sursee, Switzerland

PROFESSIONAL EXPERIENCE

2008 **Mentor** of an undergraduate laboratory trainee from the Ecole Supérieure de Biotechnologie Strasbourg (ESBS), Biozentrum, University of Basel

2005 – 2008 **Teaching assistant** in undergraduate microbiology laboratory course of the Ecole Supérieure de Biotechnologie Strasbourg (ESBS), Biozentrum, University of Basel

2003 **Statistics tutor**, Assistant of Dr. E. Lüdin, statistic lecture for scientists, University of Basel

2001-2002 **Guide** for visitors of the Botanic Garden of the University of Basel

2001-2005 **Medical laboratory technician**, Bio-Analytica AG, Luzern (temporary)

2000-2001 **Medical laboratory technician**, Bio-Analytica AG, Luzern

1997-2000 **Medical laboratory technician**, Hygienisch mikrobiologisches Institut, Kantonsspital Luzern

POSTER AND PRESENTATIONS

2008 1th EMBO Conference on Centrosomes and Spindle Pole Bodies, EMBL Heidelberg, Germany
Poster: “The role of microtubule organizing centers in the multinucleated hyphae of *Ashbya gossypii”*

2008 Systems biology of a filamentous yeast, Biozentrum Basel, Switzerland
Presentation: “Microtubule organizers in multinucleated hyphae: News from EM studies”

2008 Research days, Stowers Institute of Medical Research, Kansas City, USA
Presentation: “The role of microtubule organizing centers in nuclear dynamics of the filamentous fungus *Ashbya gossypii*”

2008 1th German / French / European Meeting on Yeast and Filamentous Fungi, Université Louis Pasteur, France
Presentation: “The role of microtubule organizing centers in nuclear dynamics of *Ashbya gossypii*”

2007 8th VAAM-Symposium “Molecular Biology of Fungi”, University of Hamburg, Germany
Presentation: “The role of microtubule organizing centers in nuclear dynamics of *Ashbya gossypii*”

2007 24th Fungal Genetics Conference, Asilomar, USA
Poster: “Role of microtubule organizing centers in the distribution, oscillation, by-passing and division of nuclei in the filamentous fungus *Ashbya gossypii*”

2006 Swiss Yeast Meeting 2006, Basel, Switzerland
Poster: “The role of MTOCs in the distribution, oscillation, by-passing and division of nuclei in the filamentous fungus *Ashbya gossypii*”

2005 EMBO Workshop on Centrosomes and Spindle Pole Bodies, EMBL Heidelberg, Germany
Poster: “Functions of the SPB proteins Cnm67 and Spc72 in *S. cerevisiae* and the filamentous fungus *A. gossypii*”

2005 22th International Conference on Yeast Genetics, Bratislava, Slovakia
Poster: “Cellular functions of the SPB proteins Cnm67 and Spc72 in *Saccharomyces cerevisiae* and the filamentous fungus *Ashbya gossypii*”